

Electronic Supporting Information for
**Tuning the Aggregation Behaviour of BN-Coronene Diimides with
the Imide Substituents and their Performance in Devices (OLED,
OFET)**

Jonas Hoffmann,^{a,b,c} Bernard Geffroy,^d Emmanuel Jaques,^e Muriel Hissler,^{c,*} and Anne Staubitz^{a,b*}

*E-mail: muriel.hissler@univ-rennes1.fr, staubitz@uni-bremen.de

- a. University of Bremen, Institute for Organic and Analytic Chemistry, Leobener Straße 7, D-28359 Bremen, Germany
- b. University of Bremen, MAPEX Center for Materials and Processes, Bibliothekstraße 1, D-28359 Bremen, Germany
- c. Université Rennes 1, CNRS, ISCR-UMR 6226, 263 Av. Général Leclerc, F-35042 Rennes, France
- d. Université Paris-Saclay, CEA, CNRS, NIMBE, LICSEN, 91191, Gif-sur-Yvette, France
- e. Université Rennes 1, CNRS, IETR-UMR 6164, 263 Av. Général Leclerc, F-35042 Rennes, France

Table of Contents

List of Abbreviations	5
General Methods and Materials.....	7
Analyses	7
Chemicals and Solvents.....	8
Chromatography	9
Syntheses	10
<i>N,N'-Di(cyclohexyl)perylene-3,4,9,10-tetracabboxylic acid diimide (PDI^{Cy})</i>	11
<i>N,N'-(Diisopropylphenyl)-perylene-3,4,9,10-tetracabboxylic acid diimide (PDI^{Dip})</i>	11
<i>Perylene-3,4,9,10-tetra-n-butylester (PTBE)</i>	12
<i>1,7-Dibromoperylene-3,4,9,10-tetra-n-butylester (1,7-DB-PTBE)</i>	12
<i>1,7-Dibromoperylene-3,4,9,10-tetracabboxylic dianhydride (1,7-DB-PTCDA)</i>	13
<i>1,7-Dibromo-<i>N,N'</i>-di(cyclohexyl)perylene-3,4,9,10-tetracabboxylic acid di-imide (1,7-DB-PDI^{Cy})</i>	14
<i>1,7-Dibromo-<i>N,N'</i>-bis(diisopropylphenyl)-perylene-3,4,9,10-tetracabboxylic acid di-imide (1,7-DB-PDI^{Dip})</i>	14
<i>1,7-Di(<i>n</i>-hexylamino)-<i>N,N'</i>-di(cyclohexyl)perylene-3,4,9,10-tetracabboxylic acid di-imide (1,7-DHA-PDI^{Cy})</i>	15
<i>1,7-Di(<i>n</i>-hexylamino)-<i>N,N'</i>-bis(2,6-di(isopropyl)phenyl)perylene-3,4,9,10-tetracabboxylic acid di-imide (1,7-DHA-PDI^{Dip})</i>	16
<i>2-(Trimethylsilyl)thiophene (TphTMS)</i>	17
<i>Dichloro-2-thienyl borane (TphBCl₂)</i>	17
<i>1,7-Di(<i>n</i>-hexyl)-6,12-di(thiophen-2-yl)-1,12,6,7-di([1,2]azaborinine)-<i>N,N'</i>-di(cyclohexyl)perylene-3,4,9,10-tetracarboxylic acid di-imide (BNCDI^{Cy})</i>	18
<i>1,7-Di(<i>n</i>-hexyl)-6,12-di(thiophen-2-yl)-1,12,6,7-di([1,2]azaborinine)-<i>N,N'</i>-bis(2,6-di(isopropyl)phenyl)perylene-3,4,9,10-tetracarboxylic acid di-imide (BNCDI^{Dip})</i>	19
NMR Spectra	20

<i>N,N'</i> -Di(cyclohexyl)perylene-3,4,9,10-tetracaboxyclic acid diimide (PDI ^{Cy})	20
<i>N,N'</i> -(Diisopropylphenyl)-perylene-3,4,9,10-tetracaboxyclic acid diimide (PDI ^{Dip})	21
Perylene-3,4,9,10-tetra- <i>n</i> -butylester (PTBE)	22
1,7-Dibromoperylene-3,4,9,10-tetra- <i>n</i> -butylester (1,7-DB-PTBE)	23
1,7-Dibromoperylene-3,4,9,10-tetracaboxyclic dianhydride (1,7-DB-PTCDA)	24
1,7-Dibromo- <i>N,N'</i> -dicyclohexylperylene-3,4,9,10-tetracaboxyclic acid di-imide (1,7-DB-PDI ^{Cy}).....	26
1,7-Dibromo- <i>N,N'</i> -(Diisopropylphenyl)-perylene-3,4,9,10-tetracaboxyclic acid di-imide (1,7-DB-PDI ^{Dip})	27
1,7-Di(<i>n</i> -hexylamino)- <i>N,N'</i> -di(cyclohexyl)perylene-3,4,9,10-tetracaboxyclic acid di-imide (1,7-DHA-PDI ^{Cy})	28
1,7-Di(<i>n</i> -hexylamino)- <i>N,N'</i> -bis(2,6-diisopropylphenyl)perylene-3,4,9,10-tetracaboxyclic acid di-imide (1,7-DHA-PDI ^{Dip}).....	30
2-(Trimethylsilyl)thiophene (TphTMS)	31
Dichloro-2-thienyl borane (TphBCl ₂)	32
1,7-Di(<i>n</i> -hexyl)-6,12-di(thiophen-2-yl)-1,12,6,7-di([1,2]azaborinine)- <i>N,N'</i> -di(cyclohexyl)perylene-3,4,9,10-tetracarboxylic acid di-imide (BNCDI ^{Cy})	34
1,7-Di(<i>n</i> -hexyl)-6,12-di(thiophen-2-yl)-1,12,6,7-di([1,2]azaborinine)- <i>N,N'</i> -bis(2,6-diisopropylphenyl)perylene-3,4,9,10-tetracarboxylic acid di-imide (BNCDI ^{Dip})	37
UV/Vis Absorption, Fluorescence and Excitation Spectra	40
BNCDI ^{Cy}	40
BNCDI ^{Dip}	40
Studies of the Chromophores in PMMA	41
Luminescence at Low Temperature	42
Electrochemistry	44
BNCDI ^{Cy} Oxidation	44
BNCDI ^{Cy} Reduction	44

BNCDI^{Dip} Oxidation	45
BNCDI^{Dip} Reduction	45
BNCDI^{Dip} Reduction 2	46
Thermoanalysis (TGA and DSC)	46
Thermogravimetric analysis (TGA).....	46
Dynamics Scanning Calorimetry (DSC).....	47
Devices.....	48
OFET Fabrication and Characterization.....	48
OLED Fabrication.....	51
Quantum Chemical Calculations.....	53
Results	53
Nuclear independent chemical shift calcuations	53
BNCDI^{Cy}.....	54
CDI^{Cy}.....	57
BNCDI^{Dip}.....	60
CDI^{Dip}	64
Calculated Absorption Spectra	68
Literature	69

List of Abbreviations

APCI	Atmospheric pressure chemical ionization
ATR	Attenuated total reflection
aq.	Aqueous
br (IR)	Broad signal
br (NMR)	Broad signal
BBO	Broadband Observe
CDI	Coronene diimide
COSY	Correlation spectroscopy
Cy	Cyclohexyl (moiety)
d (NMR)	Double
Dip	2,6-Diisopropylphenyl (moiety)
DBU	1,8-Diazabicyclo[5.4.0]undec-7-ene
DCM	Dichloromethane
dd (NMR)	Double doublet
DFT	Density functional theory
DSS	4,4-Dimethyl-4-silapentane-1-sulfonic acid
EI	Electron ionization
HMBC	Heteronuclear multiple-bond correlation spectroscopy
HOMO	Highest occupied molecular orbital
HRMS	High resolution mass spectrometry
HSQS	Heteronuclear single-quantum correlation spectroscopy
IR	Infrared spectroscopy
LUMO	Lowest unoccupied molecular orbital
m (IR)	Medium intensity
m (NMR)	Multiplet
m_c (NMR)	Multiplet (centered)
Mp.	Melting point
NICS	Nucleus independent chemical shift
NMP	<i>N</i> -Methyl-2-pyrrolidone
NMR	Nuclear magnetic resonance
PDI	Perylene diimide
PMMA	Poly(methyl methacrylate)
PTCDA	Perylene tetracarboxylic dianhydride
qd (NMR)	Quartet of doublets

quin. (NMR)	Quintet
R_f	Retention factor
s (IR)	Strong intensity
s (NMR)	Singlet
sat.	Saturated
SCE	Standard calomel electrode
Sept. (NMR)	Septet
SPS	Solvent purification system
t (NMR)	Triplet
TEA	Triethylamine
TLC	Thin-layer chromatography
TMS	Trimethylsilyl
Tph	Thienyl
tt (NMR)	Triplet of triplets
w (IR)	Weak intensity

General Methods and Materials

All NMR tubes and glassware were dried in an oven at 200 °C overnight before use. If not stated otherwise, all reaction vessels were heated to minimum of 200 °C under a vacuum (1.3×10^{-2} mbar to 6.2×10^{-2} mbar) and purged with nitrogen or argon at least three times before adding the reagents. Syringes were purged with nitrogen or argon three times prior to use. Unless noted otherwise, a nitrogen filled glovebox from Inert, Innovative Technology, Inc. Company (< 0.1 ppm O₂ and < 0.1 ppm H₂O) was used for all reactions. All dry solvents were obtained from a solvent purification system (SPS, from Inert, Innovative Technology, Inc. Comp), degassed by three freeze-pump-thaw cycles and stored under a nitrogen atmosphere unless noted otherwise. In general, solvents were distilled prior to use except for HPLC grade solvents. For Kugelrohr distillation a Kugelrohr oven from Büchi was used.

Analyses

All NMR spectroscopic measurements were carried out at 300 K. ¹H NMR spectra were recorded on a Bruker DRX 500 (500 MHz), a Bruker Avance 600 (600 MHz), a Bruker Avance Neo (600 MHz) with a TXI probe head or a Bruker Avance Neo (600 MHz) with BBO probe head. ¹³C{¹H} NMR spectra were recorded on a DRX 500 (125 MHz), a Bruker Avance 600 (150 MHz), a Bruker Avance Neo (150 MHz) with a TXI probe head or a Bruker Avance Neo (150 MHz) with BBO probe head. ¹H and ¹³C{¹H} NMR spectra were referenced against the residual solvent signals. ¹H NMR spectra in D₂SO₄ were referenced against 20 µL of a solution containing 4,4-dimethyl-4-silapentane-1-sulfonic acid (DSS) in D₂O (1 mg/ µL). ¹¹B{¹H} NMR spectra were recorded on a Bruker DRX 500 (180 MHz) spectrometer. The reference of the ¹¹B{¹H} NMR spectra was BF₃·OEt₂ in CDCl₃. The ¹¹B{¹H} NMR spectra of the BNCDIs were performed using a quartz tube and a blank spectrum of CDCl₃ was subtracted to ensure that weak/broad signals could be detected without interference of the glass peak from residual boron in the probe head. ²⁹Si{¹H} NMR spectra were recorded on a Bruker Avance Neo (119 MHz) spectrometer with BBO probe head. The reference for ²⁹Si{¹H} NMR spectra was tetramethylsilane in CDCl₃. Where possible, NMR signals were assigned using ¹H COSY, ¹H/¹H NOESY, ¹H/¹³C{¹H} HSQC and ¹H/¹³C{¹H} HMBC experiments.

Tab. SI1: List of NMR solvents.

Solvent	Supplier	Purity	Comments
Benzene- <i>d</i> ₆	Deutero	99%	Dried over CaH ₂ , degassed and stored in a glovebox
Chloroform- <i>d</i> ₁	Deutero	99.9%	
Sulfuric acid- <i>d</i> ₂ in D ₂ O	Deutero	96-98%	
D ₂ O	Deutero	99.9%	

IR spectra were recorded on a Perkin Elmer Paragon 1000 FT-IR spectrometer with a A531-G Golden-Gate ATR-unit or a Nicolet Thermo iS10 scientific spectrometer with a diamond ATR unit.

Melting points were measured with a BÜCHI Melting Point M-560 instrument. If no melting point is given for a solid, no melting behavior was observed up to 300 °C.

Electron impact (EI) mass spectrometric experiments were measured using the direct inlet or indirect inlet methods on a MAT95 XL double-focusing mass spectrometer from Finnigan or a JEOL JMS-100 GCV (AccuTOFGCV) mass spectrometer. The ionization energy of the electron impact ionization was 70 eV. Atmospheric pressure chemical ionization (APCI) and electron spray ionization (ESI) experiments were performed on a Bruker Impact II from Bruker Daltonics.

UV/Vis spectra were recorded on a Perkin Elmer Lambda 14 or a Jasco V-770 spectrometer at 20 °C using a quartz cuvette with a length of 1 cm.

The UV-Vis emission and excitation spectra measurements were recorded on a FL 920 Edinburgh Instrument and corrected for the response of the photomultiplier. Quantum yields were calculated relative to fluorescein ($\Phi = 0.90$ in NaOH 0.1 N). Excitation was performed at 460 nm.

Chemicals and Solvents

Tabl. SI2: Overview of chemicals.

Chemical	Supplier	Purity	Comments
Acetic acid	Grüssing Inc.	99.5%	
Ammoniumchloride	Carl Roth	> 99.7%	
Boron trichloride solution	Sigma Aldrich		1 M in DCM
Bromine	Acros Organics	99%+	
1-Bromobutane	Merck	>98%	
2-Bromo thiophene	TCI	> 98%	
1-Butanol	Grüssing Inc.	99%	
<i>n</i> -Butyllithium	Sigma Aldrich		2.5 M in <i>n</i> -hexane
Calcium hydride	Acros Organics	90-95%	
Cyclohexylamine	Merck	> 99%	
2,6-Diisopropylaniline	Merck	> 99%	
DBU	Sigma Aldrich	98%	
DSS	Deutero	99%	
<i>n</i> -Hexylamine	Merck	99.9%	Distilled from CaH ₂ , degassed by the freeze-pump-thaw technique and stored in the glovebox.
Hydrochloric acid	Grüssing	37%	
Imidazole	Merck	99%	
Magnesium sulfate	Grüssing Inc.	99%	
Molecular sieves	Merck		3 Å
Perylene-3,4,10-11-tetracarboxylic acid dianhydride (PTCDA)	Merck	98%	
PMMA	Kunststoff- und Farben-Gesellschaft mbH		Mw = 100000 g/mol
Potassium carbonate	Grüssing Inc.	85%	
Potassium hydroxide	Grüssing Inc.	85%	
Sodium bisulfite	Sigma Aldrich		40% w/w
Sodium hydroxide	Grüssing Inc.	99%	
Sulfuric acid	Grüssing Inc.	95-97%	
Tetrabutylammonium hexafluorophosphate	Sigma Aldrich	> 99%	
<i>p</i> -Toluenesulfonic acid monohydrate	Riedel-de Haen	> 99%	
Trimethylsilylchloride	Sigma Aldrich	> 99%	

Tabl. SI3: List of the utilized solvents.

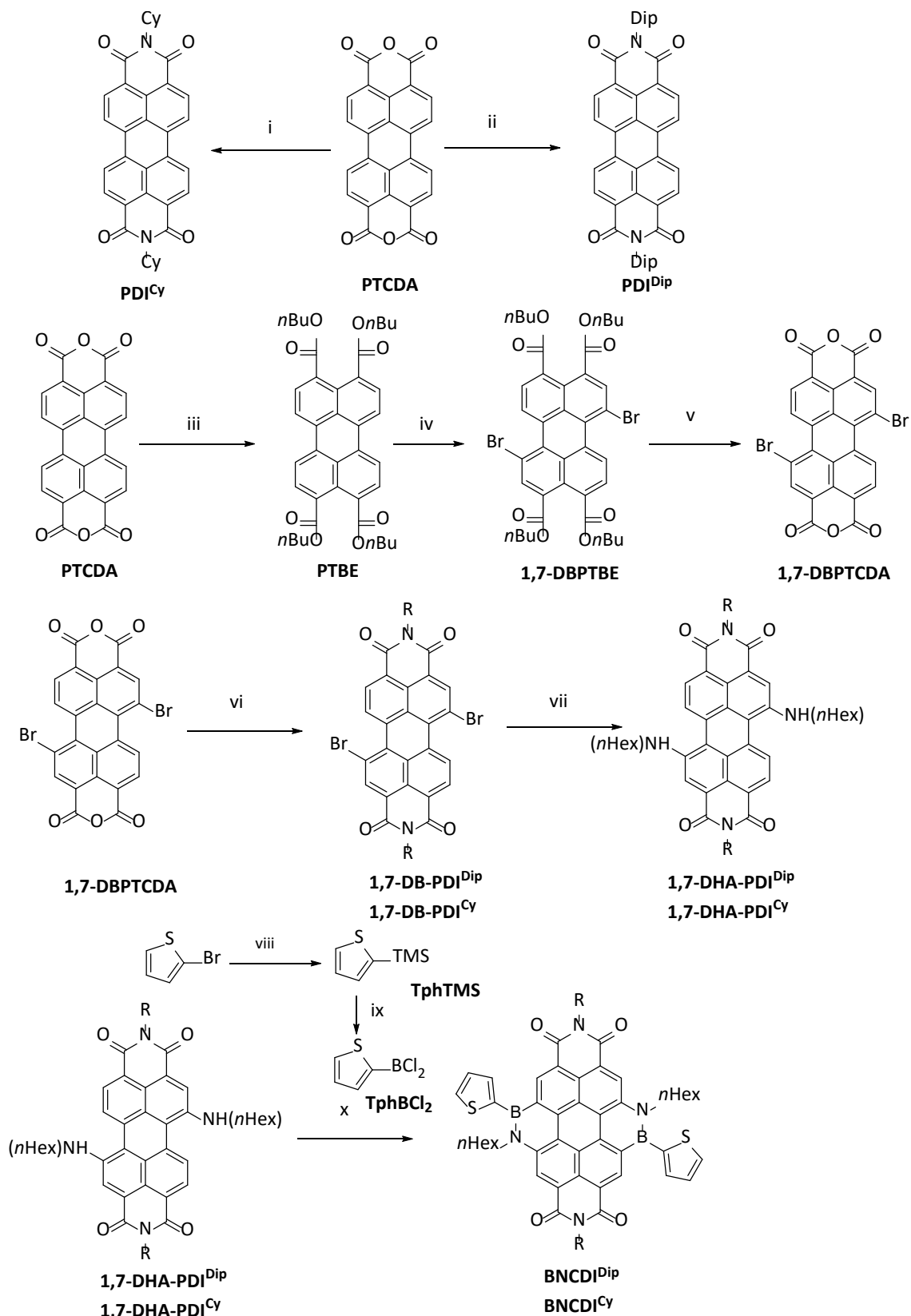
Solvent	Supplier	Purity	Comments
---------	----------	--------	----------

Acetonitrile	Sigma Aldrich	$\geq 99.5\%$	HPLC grade
Chloroform	Sigma Aldrich	$\geq 99.0\%$	
Dichloromethane	Fisher Scientific	99.8%	
Dichloromethane (dry)	Fisher Scientific	99.8%	Dried via solvent purification system, degassed by freeze-pump-thaw technique and stored in the glovebox
Diethyl ether (for SPS)	Riedel-de Haen	> 99.5%	Distilled, dried via solvent purification system, degassed by freeze-pump-thaw technique and stored in the glovebox.
Ethanol	Th. Geyer	99%	
Methanol	Fisher Scientific	99.9	HPLC grade
<i>N</i> -Methyl-2-pyrrolidinone	Acros Organics	99%	anhydrous
Petrol ether	Grüssing Inc	techn.	Bp. 60 -90 °C
Toluene	Sigma Aldrich	> 99.7%	
Toluene (dry)	Acros	$\geq 99.85\%$	Extra dry, stored over 3 Å molecular sieve, degassed by the freeze-pump-thaw technique and stored in the glovebox.
Triethylamine	ChemPur	99%	Dry, degassed by the freeze-pump-thaw technique and stored in the glovebox.

Chromatography

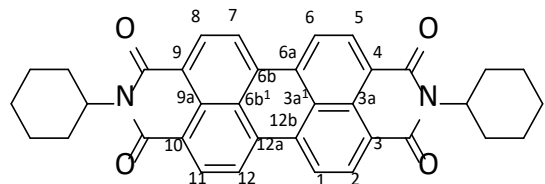
Unless stated otherwise chromatographic purifications were performed with silica gel (Merck, grain size 15-40 µm). Thin layer chromatography (TLC) was performed by using TLC Silicagel 60 F254 from MERCK on alumina plates. For the detection of the spots, a UV lamp ($\lambda = 254/366$ nm) was used.

Syntheses



Scheme 1: Conditions: i) cyclohexylamine, 130 °C, 24 h, 95% ii) 2,6-diisopropylaniline, imidazole, 140 °C, 4 h, 39% iii) 1-butanol, 1-bromobutane, DBU, MeCN, 85 °C, 24 h, 92% iv) Br₂, K₂CO₃, DCM, 25 °C, 24 h, 45% isomerically pure product v) p-TsOH H₂O, toluene, 100 °C, 30 h, 76% vi) NMP, AcOH a) cyclohexylamine 85 °C 4 h, 52% b) 2,6-diisopropylaniline, 120 °C, 24 h, 63% vii) n-hexylamine, 60 °C, 6 h, 50-51%, viii) nBuLi, -78 °C, Et₂O, 1 h then TMSCl, -78 °C to 25 °C, 78% ix) BCl₃, DCM, -50 °C, 72% x) TEA, toluene, 110 °C, 4-24 h, 83-97%.

N,N'-Di(cyclohexyl)perylene-3,4,9,10-tetracabboxylic acid diimide (**PDI^{Cy}**)



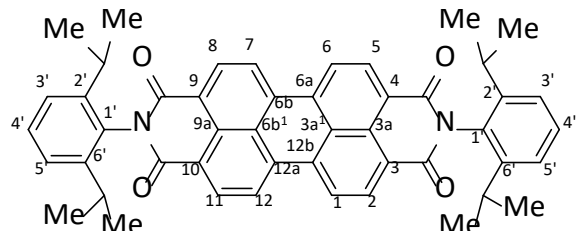
This synthetic procedure was adapted from literature.²

Under a nitrogen atmosphere a mixture of perylene-3,4,9,10-tetracarboxylic dianhydride (**PTCDA**, 5.00 g, 12.8 mmol) and cyclohexylamine (130 mL, 867 mmol) was heated to 130 °C for 24 h. After cooling to 25 °C, a purple precipitate formed, which was filtered, washed with aq. NaOH (150 mL, 5% w/w) and ethanol (50 mL). The solid was dried under reduced pressure and elevated temperature (2.1×10^{-2} mbar, 80 °C, 8 h) to give **PDI^{Cy}** (6.70 g, 12.2 mmol, 95%, lit.^[2]: 93%) as a dark red solid.

¹H NMR (600 MHz, CDCl₃): δ = 8.66 (d, ³J = 7.9 Hz, 4H, H-2,5,8,11), 8.60 (d, ³J = 7.9 Hz, 4H, H-1,6,7,12), 5.01 (tt, ³J = 12.1, 3.6 Hz, 2H, CH), 2.58 (qd, ³J = 12.4, 3.2 Hz, 4H, CH-CH_{ax}), 1.92 (m, 4H, CH-CH₂-CH_{ox}), 1.75 (m, 6H, CH-CH_{eq} and CH-(CH₂)₂-CH_{ax}), 1.46 (m, 4H, CH-CH₂-CH_{eq}), 1.36 (m, 2H, CH-(CH₂)₂-CH_{eq}) ppm. **¹³C{¹H} NMR** (151 MHz, CDCl₃): δ = 164.00 (C=O), 134.61 (C-6a,6b,12a,12b), 131.51 (C-2,5,8,11), 129.59 (C-3a,9a), 126.58 (C-3a¹,6b¹), 124.01 (C-3,4,10,11), 123.17 (C-1,6,7,12), 54.21 (CH), 29.30 (CH-CH₂), 26.72 (CH-CH₂-CH₂), 25.61 (CH-(CH₂)₂-CH₂) ppm. **HRMS** (EI): *m/z* [M]⁺ calcd. for C₃₆H₃₀N₂O₄ 554.22056; found 554.22139; 390.04 (100%). **IR** (ATR): $\tilde{\nu}$ = 2918 (m), 2853 (m), 1693 (s), 1647 (s), 1593 (s), 1575 (m), 1434 (w), 1404 (m), 1354 (m), 1337 (s), 1245 (m), 1260 (m), 1230 (m), 1180 (m), 1154 (w), 1117 (m), 978 (w), 962 (w), 807 (m), 744 (m), 651 (m) cm⁻¹.

The analytical data were in agreement with published values.²

N,N'-(Diisopropylphenyl)-perylene-3,4,9,10-tetracabboxylic acid diimide (**PDI^{Dip}**)

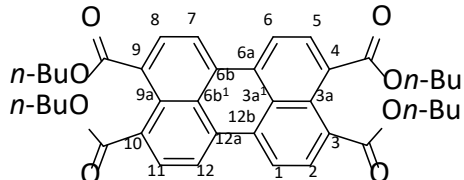


This synthetic procedure was combined from two methods^{3,4}: Under a nitrogen atmosphere a mixture of perylene-3,4,9,10-tetracarboxylic dianhydride (**PTCDA**, 1.00 g, 2.54 mmol), imidazole (30 g) and 2,6-diisopropylaniline (1.06 g, 6.00 mmol) was heated to 140 °C for 4 h. After cooling to 60 °C, ethanol (50 mL) was added to the reaction mixture. At 25 °C the reaction mixture was treated with aq. hydrochloric acid (2 M, 50 mL). The precipitate that formed was collected by vacuum filtration, washed with distilled water (300 mL), dried at 120 °C for 24 h, and purified by column chromatography (DCM, silica gel, R_f(DCM) = 0.68) to give the product (**PDI^{Dip}**, 704 mg, 0.99 mmol, 39%, lit.^[4]: 49%) as a red solid. **¹H NMR** (601 MHz, CDCl₃): δ = 8.80 (d, ³J = 7.9 Hz, 4H, H-2,5,8,11), 8.75 (d, ³J = 7.9 Hz, 4H, H-1,6,7,12), 7.51 (t, ³J = 7.8 Hz, 2H, Ph-H-4'), 7.36 (d, ³J = 7.8 Hz, 2H, Ph-H-3',5'), 2.76 (sept., ³J = 6.8 Hz, 4H, CH(CH₃)), 1.19 (d, ³J = 6.8 Hz, 24H, CH(CH₃)) ppm. **¹³C{¹H} NMR** (151 MHz, CDCl₃): δ = 163.61 (C(O)N), 145.77 (Ph-C-2',6'), 135.22 (C-6a,6b,12a,12b), 132.25 (C-2,5,8,11), 130.64 (Ph-C-1'), 130.33 (C-3a,9a), 129.86 (Ph-C-4'), 127.00 (C-3a¹,6b¹), 124.28 (Ph-C-3',5'), 123.57 (C-3,4,9,10), 123.48 (C-1,6,7,12), 29.37 (CH(CH₃)₂), 24.17 (CH₃) ppm. **HRMS** (EI): *m/z* [M]⁺ calcd. for C₄₈H₄₂N₂O₄ 710.31391; found 710.31455; 390.06 (100%). **IR** (ATR): $\tilde{\nu}$ = 3031 (w), 2959 (m), 2925 (m), 1771 (m), 1703(s), 1664

(s), 1592 (s), 1577 (s), 1382 (m), 1345 (s), 1301 (w), 1337 (s), 1248 (m), 1178 (m), 834 (m), 815 (m), 741 (m), 689 (w) cm⁻¹.

The analytical data were in agreement with reported values.⁴

Perylene-3,4,9,10-tetra-*n*-butylester (PTBE)



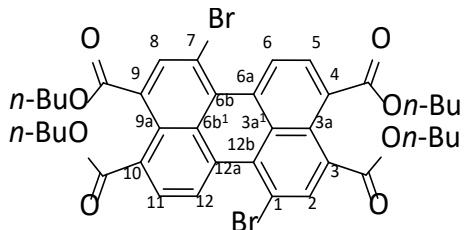
This synthetic procedure published for a similar compound and was adapted with changes from the literature⁵ and was not performed under inert conditions.

A mixture of perylene-3,4,9,10-tetracarboxylic dianhydride (**PTCDA**, 4.00 g, 10.2 mmol), DBU (6.40 mL, 40.8 mmol), *n*-butanol (25.6 mL, 81.6 mmol) in MeCN (150 mL) was stirred at 25 °C for 0.5 h. To this slightly orange mixture, 1-bromobutane (8.73 mL, 81.6 mmol) was added, followed by MeCN (30 mL). The mixture was stirred for 24 h at 85 °C. After cooling to 25 °C and additional stirring for 21 h, the beginning precipitation was completed by adding methanol (250 mL). The mixture was filtered to give the product as an orange solid without further purification (**PTBE**, 6.10 g, 9.40 mmol, 92%).

¹H NMR (500 MHz, CDCl₃) δ = 8.22 (d, ³J = 7.9 Hz, 4H, H-1,6,7,12), 8.00 (d, ³J = 7.9 Hz, 4H, H-2,5,8,11), 4.34 (t, ³J = 6.8 Hz, 8H, CH₂-C₃H₇), 1.84-1.75 (m, 8H, CH₂-CH₂-C₂H₅), 1.53-1.44 (m, 8H, C₂H₄-CH₂-CH₃), 1.00 (t, ³J = 7.4 Hz, 12H, CH₃) ppm. **¹³C{¹H} NMR** (125 MHz, CDCl₃): δ = 168.67 (COO-(C₄H₉)), 133.17 (C-3,4,9,10), 130.62 (C-6a,6b,12a,12b), 130.54 (C-2,5,8,11-), 129.13 (C-3a,9a), 128.95 (C-3a¹,6b¹), 121.51 (C-1,6,7,12), 65.49 (CH₂-C₃H₇), 30.80 (CH₂-CH₂-C₂H₅), 19.42 (C₂H₄-CH₂), 13.95 (CH₃) ppm. **HRMS** (EI): *m/z* calcd. for C₄₀H₄₄O₈ 652.30362 [M]⁺; found 652.30296 [M]⁺ (100%). **IR** (ATR): ν = 2958 (m), 2930 (w), 2870 (w), 1721 (s), 1705 (m), 1588 (m), 1472 (m), 1270 (s), 1267 (m), 1167 (s), 1131 (s), 1096 (m), 1004 (m, 939 (m), 842 (m), 805 (m), 746 (s) cm⁻¹. **Mp.**: 165 °C.

The analytical data were in agreement with previously published values.⁶

1,7-Dibromoperylene-3,4,9,10-tetra-*n*-butylester (1,7-DB-PTBE)



This synthetic procedure was adapted from the literature⁷ and was not performed under inert conditions.

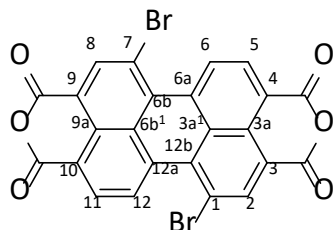
A mixture of perylene-3,4,9,10-tetra-*n*-butylester (**PTBE**, 5.00 g, 7.66 mmol) and K₂CO₃ (2.50 g, 18.1 mmol) in DCM (60 mL) was stirred at 25 °C. To this mixture, bromine (5.12 mL, 100 mmol) was added dropwise over a period of 2 h 5 min and the mixture was stirred for 24 h at 25 °C. Then a saturated aqueous solution of NaHSO₃ (35 mL, 40% w/w) was added dropwise over a period of 4 h. The organic layer was washed with water (100 mL), dried over MgSO₄, filtered, and after the removal of the solvent, the remaining orange material was dried (3.4 × 10⁻⁴ mbar, 60 °C, 24 h). An isomeric mixture of 1,6- and 1,7-isomers in a ratio of 1:4 as determined by ¹H NMR spectroscopy was obtained

(5.90 g, 7.28 mmol). The isomeric mixture (5.90 g) was dissolved in DCM (60 mL) and further MeCN (540 mL) was added to the solution. The flask was left open in the fume hood for 3 days and crystals were isolated (3.47 g). The second recrystallization using DCM (40 mL) and MeCN (370 mL) yielded the pure isomer (**1,7-DB-PTBE**, 2.81 g, 3.47 mmol, 45%, lit.^[7]: 62%).

¹H NMR (500 MHz, CDCl₃): δ = 8.91 (d, ³J = 7.9 Hz, 2H, H-6,12), 8.28 (s, 2H, H-2,8), 8.07 (d, ³J = 7.9 Hz, 2H, H-5,11), 4.35 (td, ³J = 6.8 Hz, ⁴J = 1.7 Hz, 8H, CH₂-C₃H₇), 1.84-1.73 (m, 8H, CH₂-CH₂-C₂H₅), 1.54-1.44 (m, 8H, C₂H₄-CH₂), 1.01 (t, ³J = 7.4 Hz, 12H, CH₃) ppm. **¹³C{¹H} NMR** (126 MHz, CDCl₃): δ = 168.13 (COO-(C₄H₉)-4,10), 167.26 (COO-(C₄H₉)-3,9), 136.80 (CH-2,8), 131.93 (C-6b,12b), 131.87 (C-6a,12a), 131.27 (C-3,9), 130.61 (C-(3a,9a or 3a¹,6b¹)), 130.60 (C-(3a,9a or 3a¹,6b¹)), 129.17 (CH-5,11), 127.77 (CH-6,12), 126.64 (C-4,10), 118.85 (C-1,7), 65.96 (CH₂-C₃H₇), 65.74 (CH₂-C₃H₇), 30.76 (CH₂-CH₂-C₂H₅), 30.73 (CH₂-CH₂-C₂H₅), 19.40 (C₂H₄-CH₂), 19.37 (C₂H₄-CH₂-CH₃), 13.93 (CH₃) ppm. **HRMS** (EI): *m/z* calcd. for C₄₀H₄₂⁸¹Br₂O₈ 810.10490 [M]⁺, found 810.10195 [M]⁺ (100). **IR** (ATR): $\tilde{\nu}$ = 2958 (m), 2932 (w), 2872 (w), 1717 (s), 1475 (m), 1397 (m), 1299 (s), 1267 (m), 1223 (m), 1194 (m), 1172 (s), 1058 (m), 1030 (m), 980 (m), 938 (m), 887 (m), 864 (m), 840 (m), 755 (m) cm⁻¹. **Mp.**: 125 °C.

The analytical data were in agreement with reported values.⁷

1,7-Dibromoperylene-3,4,9,10-tetracabboxylic dianhydride (1,7-DB-PTCDA)



This synthetic procedure was adapted from the literature⁷ and was not performed under inert conditions.

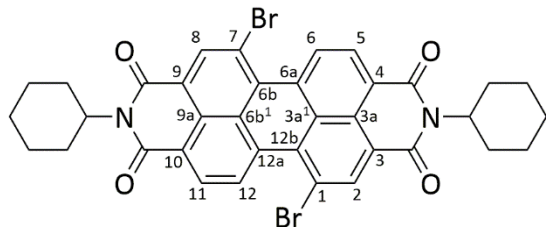
A mixture of 1,7-dibromoperylene-3,4,9,10-tetra-*n*-butylester (**1,7-DB-PTBE**, 2.50 g, 3.08 mmol) and *p*-TsOH·H₂O (2.50 g, 15.4 mmol) in toluene (90 mL) was stirred at 100 °C for 30 h. Subsequently, the reaction mixture was filtered and washed with methanol (250 mL) and water (150 mL). Then the precipitate was stirred with chloroform (200 mL) at 71 °C for 2 h. After having cooled to 23 °C, the precipitate was filtered and washed again with chloroform (400 mL). Drying (60 °C, 10 h, 1.6 × 10⁻³ mbar) afforded the product as a red solid (**1,7-DB-PTCDA**, 1.29 g, 2.34 mmol, 76%, lit.⁷: 95%).

¹H NMR (500 MHz, D₂SO₄): δ = 9.02 (d, ³J = 7.9 Hz, 2H, H-6,12), 8.35 (s, 2H, H-2,8), 8.13 ppm (d, ³J = 7.9 Hz, 2H, H-5,11) ppm. **¹H-¹³C{¹H} HSQC/HMBC NMR** (126 MHz, D₂SO₄): δ = 158.2 (COO-3,9), 157.3 (COO-4,10), 136.4 (C-2,8), 130.2 (C-6b,12b), 130.1 (C-6a,12a), 128.8 (C-5,11), 124.1 (C-6,12), 123.3 (C-(3a¹,6b¹)), 123.0 (C-(3a,9a)), 119.0 (C-1,7), 110.7 (C-4,10), 110.4 (C-3,9) ppm. **HRMS** (EI): *m/z* [M]⁺ calcd. for C₂₄H₆O₆⁷⁹Br₂ 547.85256; found 547.85214 (100%). **IR** (ATR): $\tilde{\nu}$ = 1773 (s), 1724 (s), 1593 (s), 1593 (s), 1376 (w), 1297 (m), 1285 (m), 1230 (m), 1213 (m), 1138 (m), 1057 (m), 1037 (m), 956 (w), 859 (w), 804 (w), 733(w), 693 (m) cm⁻¹.

The analytical data were in agreement with reported values.⁷

¹ Due to the low solubility only ¹H, ¹H-¹³C{¹H}-HSQC and ¹H, ¹³C{¹H}-HMBC NMR signals were used to identify and assign the signals.

1,7-Dibromo-N,N'-di(cyclohexyl)perylene-3,4,9,10-tetracabboxylic acid di-imide (1,7-DB-PDI^{Cy})



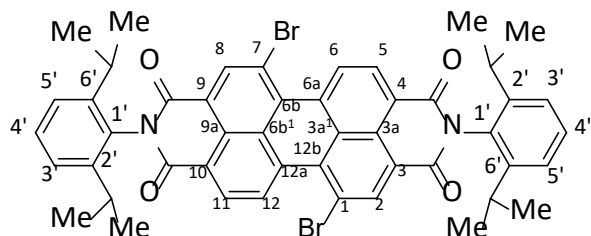
This synthetic procedure was adapted from the literature,⁸ where a similar molecule was described.

A mixture of 1,7-dibromoperylene-3,4,9,10-tetracabboxylic acid dianhydride (**1,7-DB-PTCDA**, 1.00 g, 1.82 mmol) and NMP (30 mL) was placed in an ultrasonic bath for 1 h. Then cyclohexylamine (0.630 mL, 5.45 mmol) and acetic acid (0.676 mL, 11.8 mmol) were added and the reaction mixture was heated to 85 °C under a nitrogen atmosphere for 7 h. After cooling to 25 °C, the reaction mixture was poured into methanol (150 mL) and cooled to -10 °C for 12 h. The solid was separated by filtration, washed with methanol (250 mL), dried (6.2 x 10⁻² mbar, 22 °C, 2 h) and was purified by column chromatography (silica, eluent: chloroform:petrol ether (3:1), R_f(CHCl₃) = 0.75). The product was obtained as a dark red solid (**1,7-DB-PDI^{Cy}**, 670 mg, 52%).

¹H NMR (500 MHz, CDCl₃) δ = 9.48 (d, ³J = 8.2 Hz, 2H, H-6,12), 8.89 (s, 2H, H-2,8), 8.68 (d, ³J = 8.2 Hz, 2H, H-5,11), 5.03 (tt, ³J = 12.4, 3.6 Hz, 2H, CH), 2.55 (qd, ³J = 12.4, 9.0 Hz, 4H, CH-CH_{ax}), 1.92 (d, ³J = 12.4 Hz, 4H, CH-CH₂-CH_{ax}), 1.81-1.76 (m, 6H, CH-CH_{eq} and CH-(CH₂)₂-CH_{ax}), 1.51-1.31 (m, 6H, CH₂, CH-CH₂-CH_{eq} and CH-(CH₂)₂-CH_{eq}) ppm. **¹³C{¹H} NMR** (125 MHz, CDCl₃): δ = 163.49 (COO-4,10), 162.94 (COO-3,9), 138.11 (CH-2,8), 132.99 (C-6b,12b), 132.83 (C-6a,12a), 130.13 (CH-5,11), 129.41 (C-3,9), 128.62 (CH-6,12), 127.19 (C-3a,9a), 123.87 (C-4,10), 123.46 (C-3a¹,6b¹), 120.86 (C-1,7), 54.41 (CH), 29.26 (CH-CH₂), 26.66 (CH-CH₂-CH₂), 25.55 (CH-(CH₂)₂-CH₂) ppm. **HRMS** (EI): *m/z* [M]⁺ calcd. for C₃₆H₂₆⁷⁹Br⁸¹BrN₂O₄ 710.02389; found 710.02443. calcd. for C₃₆H₂₆⁸¹Br₂N₂O₄ 712.02184; found 712.02315; 547.84 (100%). **IR** (ATR): $\tilde{\nu}$ = 2926 (w), 2852 (w), 1697 (m), 1655 (s), 1587 (m), 1575 (m), 1382 (m), 1326 (m), 1302 (w), 1257 (w), 1237 (s), 1187 (m), 1156 (m), 1143 (m), 979 (w), 859 (w), 824 (m), 808 (m), 745 (m), 690 (m), 683 (m), 657 (m) cm⁻¹.

The analytical data were in agreement with previously reported values.⁸

1,7-Dibromo-N,N'-bis(diisopropylphenyl)-perylene-3,4,9,10-tetracabboxylic acid di-imide (1,7-DB-PDI^{Dip})



This synthetic procedure was adapted from the literature.⁸

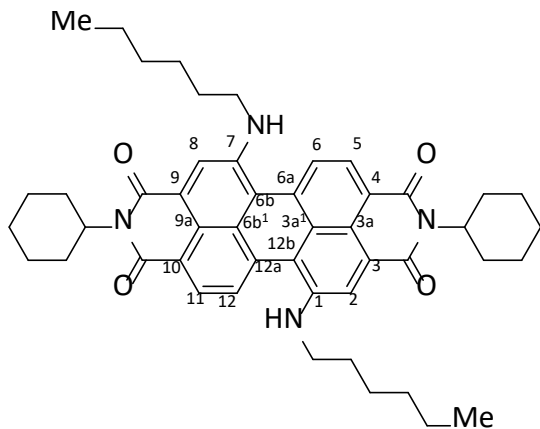
This synthetic procedure was adapted from the literature.⁷: Under nitrogen atmosphere, a mixture of 1,7-dibromoperylene-3,4,9,10-tetracabboxylic acid dianhydride (**1,7-DB-PTCDA**, 3.79 g, 6.89 mmol) and NMP (40 mL) was placed in an ultrasonic bath for 1 h. Then 2,6-diisopropylaniline (7.36 g, 41.5 mmol) and acetic acid (2.25 mL, 39.5 mmol) were added, and the reaction was heated to 120 °C for 4 d. After

cooling to 25 °C water (100 mL) was added. The precipitate was collected by vacuum filtration and washed with water (600 mL) and methanol (150 mL) and cooled to -10 °C for 12 h. The solid was collected by filtration and washed with cold methanol (50 mL). The resulting powder was dried (2.0 x 10⁻² mbar, 200 °C, 14 h) and was purified by column chromatography (silica, eluent: DCM, R_f(DCM) = 0.75). The product was obtained as a dark red solid (**1,7-DB-PDI^{Dip}**, 3.80 g, 4.37 mmol, 63%, lit.⁷: 66%).

¹H NMR (601 MHz, CDCl₃) δ = 9.57 (d, ³J = 8.2 Hz, 2H, H-6,12), 9.02 (s, 2H, H-2,8), 8.81 (d, ³J = 8.2 Hz, 2H, H-5,11), 7.52 (t, ³J = 7.8 Hz, 2H, Ph-H-4'), 7.37 (d, ³J = 7.8 Hz, 2H, Ph-H-3',5'), 2.74 (sept., ³J = 6.7 Hz, 4H, CH), 1.19 (dd, ³J = 6.7 Hz, ⁴J = 1.8 Hz, 24H, CH₃) ppm. **¹³C{¹H} NMR** (151 MHz, CDCl₃): δ = 163.15 ((C(O)N)-4,10), 162.65 ((C(O)N)-3,9), 145.75 (Ph-C-2',6'), 138.63 (C-2,8), 133.59 (C-6b,12b), 133.43 (C-6a,12a), 130.80 (C-5,11), 130.27 (Ph-C-1'), 130.05 (Ph-C-4'), 129.79 (C-3,9), 128.87 (C-6,12), 127.85 (C-3a,9a), 124.36 (Ph-C-3',5'), 123.35 (C-4,10), 123.02 (C-3a¹,6b¹), 121.22 (C-1,7), 29.45 (CH(CH₃)), 24.19 and 24.16 (CH₃) ppm. **HRMS** (EI): *m/z* [M]⁺ calcd. for C₄₈H₄₀N₂O₄⁷⁹Br₂ 866.13493; found 866.13370; 549.70 (100%). **IR** (ATR): ν = 2959 (m), 2925 (m), 1707 (s), 1668 (s), 1589 (s), 1383 (m), 1336 (s), 1248 (m), 1178 (m), 834 (m), 809 (m), 746 (m), 692 (w) cm⁻¹.

The analytical data were in agreement with previously reported values.⁷

1,7-Di(*n*-hexylamino)-*N,N'*-di(cyclohexyl)perylene-3,4,9,10-tetracarboxylic acid di-imide (1,7-DHA-PDI^{Cy})

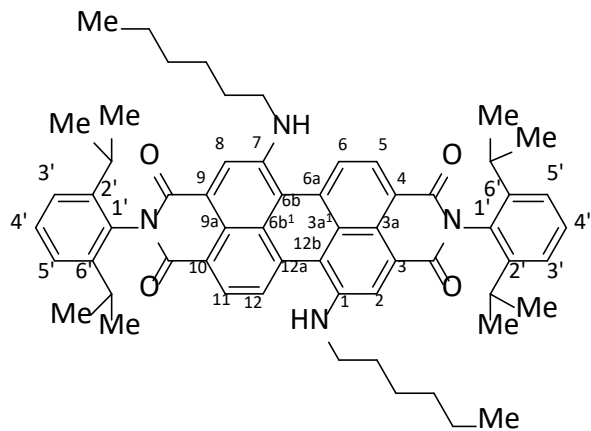


Under an argon atmosphere, 1,7-dibromo-*N,N'*-di(cyclohexyl)perylene-3,4,9,10-tetracarboxylic acid di-imide (**1,7-DB-PDI^{Cy}**, 100 mg, 140 µmol) and *n*-hexylamine (10.0 mL, 76.0 mmol) were mixed. The mixture was stirred at 60 °C for 3 d. Subsequently, the excess of *n*-hexylamine was removed with a rotary evaporator (80 °C, 10 mbar). The crude product was purified by column chromatography (silica, eluent: DCM, R_f(DCM) = 0.68) to yield the product as a green solid (**1,7-DHA-PDI^{Cy}**, 53 mg, 70.4 µmol, 50%).

¹H NMR (600 MHz, CDCl₃): δ = 8.60 (d, ³J = 8.1 Hz, 2H, H-6,12), 8.16 (d, ³J = 8.1 Hz, 2H, H-5,11), 7.96 (s, 2H, H-2,8), 5.59 (t, ³J = 4.6 Hz, 2H, NH), 5.01 (tt, ³J = 12.1, 3.6 Hz, 2H, CH), 3.19 (q, ³J = 6.8 Hz, 4H, NH-CH₂), 2.57 (qd, ³J = 12.1, 3.0 Hz, 4H, CH-CH_{ax}), 1.93 (d, ³J = 12.6 Hz, 4H, CH-CH₂-CH_{ax}), 1.83 - 1.71 (m, 6H, CH-CH_{eq} and CH-(CH₂)₂-CH_{ax}), 1.66 (quin., ³J = 7.1 Hz, 4H, NH-(CH₂)-CH₂), 1.51 - 1.21 (m, 18H, CH-CH₂-CH_{eq}, CH-(CH₂)₂-CH_{eq} and NH-(CH₂)₂-(CH₂)₃), 0.93 (t, ³J = 7.1 Hz, 6H, CH₃) ppm. **¹³C{¹H} NMR** (150 MHz, CDCl₃): δ = 164.36 ((C(O)N)-3,9), 163.91 ((C(O)N)-4,10), 145.89 (C-1,7), 133.86 (C-6a,12a), 129.89 (C-

4,10), 126.97 (C-5,11), 123.17 (C-3,9), 122.45 (C-3a,9a), 121.46 (C-6,12), 120.66 (C-3a¹,6b¹), 117.94 (C-2,8), 116.73 (C-6b,12b), 54.00 (CH), 44.75 (NH-CH₂), 31.64 (NH-CH₂-CH₂), 29.44 (CH-CH₂), 29.27 (NH-(CH₂)₂-CH₂), 27.09 (NH-(CH₂)₃-CH₂), 26.76 (CH-CH₂-CH₂), 25.68 (CH-(CH₂)₂-CH₂), 22.74 (NH-(CH₂)₄-CH₂), 14.15 (CH₃) ppm. **HRMS** (APCI): *m/z* [M+H]⁺ calcd. for C₄₈H₅₇N₄O₄ 753.43743; found 753.43686. **IR** (ATR): ν = 3314 (w), 2924 (m), 2851 (m), 1687 (s), 1641 (s), 1584 (s), 1568 (s), 1512 (w), 1452 (w), 1421 (m), 1330 (s), 1280 (m), 1257 (m), 1190 (m), 1124 (w), 1102 (w), 984 (m), 895 (w), 866 (w), 805 (m), 750 (m), 653 (m), 643 (m) cm⁻¹.

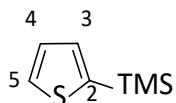
1,7-Di(*n*-hexylamino)-*N,N'*-bis(2,6-di(isopropyl)phenyl)perylene-3,4,9,10-tetracaboxylic acid di-imide (1,7-DHA-PDI^{Dip}**)**



Under an argon atmosphere, 1,7-dibromo-*N,N'*-bis(diisopropylphenyl)perylene-3,4,9,10-tetracarboxylic acid di-imide (**1,7-DB-PDI^{Dip}**, 100 mg, 117 μ mol) and *n*-hexylamine (10.0 mL, 76.0 mmol) were mixed. The mixture was stirred at 60 °C for 3 d. Subsequently, the excess of *n*-hexylamine was removed at a rotary evaporator (80 °C, 10 mbar). The crude product was purified by column chromatography (silica, eluent: DCM, R_f(DCM) = 0.74) to yield the product as a green solid (**1,7-DHA-PDI^{Dip}**, 54 mg, 59.3 μ mol, 51%).

¹H NMR (600 MHz, CDCl₃): δ = 8.91 (d, ³J = 8.1 Hz, 2H, H-6,12), 8.46 (d, ³J = 8.1 Hz, 2H, H-5,11), 8.30 (s, 2H, H-2,8), 7.49 (t, ³J = 7.8 Hz, 2H, Ph-H-4'), 7.35 (d, ³J = 7.8 Hz, 4H, Ph-H-3',5'), 5.81 (t, ³J = 7.8 Hz, 2H, NH), 3.48 (q, ³J = 7.1 Hz, 4H, NH-CH₂), 3.33-3.27 (m, 4H, NH-CH₂), 2.77 (sept., ³J = 6.6 Hz, 4H, Ph-(CH)-(CH₃)₂), 1.79 (quin., ³J = 7.1 Hz, 4H, NH-(CH₂)-CH₂), 1.43 - 1.32 (m, 8H, NH-(CH₂)₂-(CH₂)₃), 1.22 - 1.16 (m, 24H, Ph-(CH)-(CH₃)₂), 0.91 (t, ³J = 7.0 Hz, 6H, CH₃) ppm. **¹³C{¹H} NMR** (150 MHz, CDCl₃): δ = 163.84 ((C(O)N)-3,9), 163.75 ((C(O)N)-4,10), 146.19 (C-1,7), 145.67 (Ph-C-2',6'), 134.40 (C-6a,12a), 130.94 (Ph-C-1'), 130.54 (C-4,10), 129.51 (Ph-C-4'), 127.54 (C-5,11), 124.03 (Ph-C-3',5'), 123.24 (C-3,9), 123.00 (C-3a¹,6b¹), 121.78 (C-6,12), 120.42 (C-3a,9a), 118.85 (C-2,8), 117.21 (C-6b,12b), 44.90 (NH-CH₂), 31.46 (NH-CH₂-CH₂), 29.71 (NH-(CH₂)₂-CH₂), 29.51 (Ph-(CH)-(CH₃)₂), 26.90 (NH-(CH₂)₃-CH₂), 24.05 and 24.03 (Ph-(CH)-(CH₃)₂), 22.56 (NH-(CH₂)₄-CH₂), 14.00 (CH₃) ppm. **HRMS** (ESI): *m/z* [M+H]⁺ calcd. for C₆₀H₆₉N₄O₄ 909.53152; found 909.53133. **IR** (ATR): ν = 3338 (w), 2956 (m), 2925 (m), 2855 (m), 1690 (s), 1653 (m), 1583 (m), 1568 (m), 1507 (m), 1456 (m), 1421 (m), 1338 (s), 1276 (s), 1197 (m), 1125 (m), 866 (m), 840 (m), 805 (m), 764 (m), 750 (s), 737 (m), 691 (m) cm⁻¹.

2-(Trimethylsilyl)thiophene (**TphTMS**)

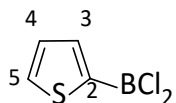


In a Schlenk tube, 2-bromothiophene (10.0 g, 61.3 mmol) was dissolved in diethyl ether (100 mL) and cooled to -78 °C. To this solution, *n*-butyllithium (27.0 mL, 67.5 mmol, 2.5 M in *n*-hexane) was added over a period of 5 min and the reaction mixture was stirred for 1 h. Subsequently, trimethylsilyl chloride (8.10 mL, 67.4 mmol) was added in one portion and the reaction mixture was stirred for 18 h. The reaction mixture was added to a sat. aq. ammonium chloride solution (150 mL). The organic phase was separated, washed with water (2 x 150 mL), dried over magnesium sulfate, filtered, and after careful removal of the solvent using a rotary evaporator (b.p. (**TphTMS**) = 70 °C (20 mbar)), the product was obtained as a colorless oil (7.52 g, 48.1 mmol, 78%).

¹H NMR (600 MHz, CDCl₃) δ = 7.61 (dd, ³J = 4.6 Hz, ⁴J = 0.9 Hz, 1H, H-5), 7.28 (dd, ³J = 3.3 Hz, ⁴J = 0.9 Hz, 1H, H-3), 6.60 (dd, ³J = 4.6 Hz, ³J = 3.3 Hz, 1H, H-4), 0.34 (s, 9H, CH₃) ppm. **¹³C{¹H} NMR** (151 MHz, CDCl₃) δ = 140.21 (C-2), 134.08 (C-3), 130.51 (C-5), 128.22 (C-4), 0.16 (CH₃) ppm. **²⁹Si{¹H} NMR** (119 MHz, CDCl₃) δ = -6.54 (s) ppm. **HRMS (EI)**: *m/z* [M]⁺ calcd. for C₇H₁₂SSi 156.04235; found 156.04191; 141.10 (100%). **IR (ATR)**: υ = 2956 (w), 1406 (m), 1325 (w), 1248 (s), 1213 (m), 1082 (m), 991 (m), 857 (m), 825 (s), 754 (s), 701 (s) cm⁻¹.

The analytical data were in accordance to previously reported values.⁹

Dichloro-2-thienyl borane (**TphBCl₂**)

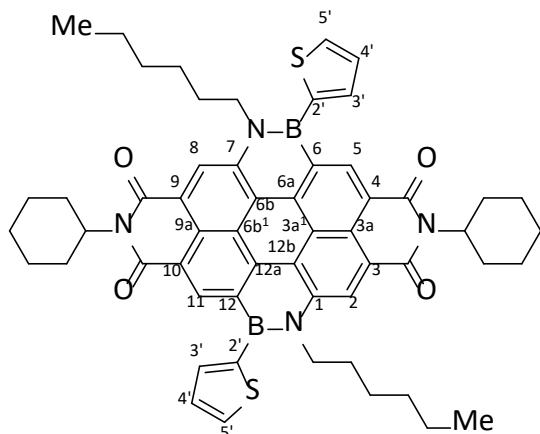


Under a argon atmosphere, 2-(trimethylsilyl)thiophene (**TphTMS**, 5.96 g, 38.1 mmol) was added to a solution of boron trichloride (60.0 mL, 60.0 mmol, 1 M in DCM) within 10 min at -50 °C. The reaction mixture was slowly warmed to 22 °C over the course of 14 h. After the solvent was removed *in vacuo*, the crude product was purified by inert Kugelrohr distillation (70 °C, 17 mbar) to give the product as a colorless oil (**TphBCl₂**, 4.66 g, 27.6 mmol, 72%). This very corrosive product was stored in the glovebox freezer (-25 °C).

¹H NMR (500 MHz, C₆D₆) δ = 7.64 (dd, ³J = 3.7 Hz, ⁴J = 1.0 Hz, 1H, H-5), 7.10 (dd, ³J = 4.6 Hz, ⁴J = 1.0 Hz, 1H, H-3), 6.60 (dd, ³J = 4.6 Hz, ³J = 3.7 Hz, 1H, H-4) ppm. **¹³C{¹H} NMR** (126 MHz, C₆D₆) δ = 143.46 (C-3), 140.48 (C-5), 139.0 (C-2, only HMBC), 129.75 (C-4) ppm. **¹¹B{¹H} NMR** (160 MHz, C₆D₆) δ = 48.88 (s) ppm. Due to the corrosive nature of this molecule mass spectrometry data were not obtained.

The analytical data are in accordance with literature.¹⁰

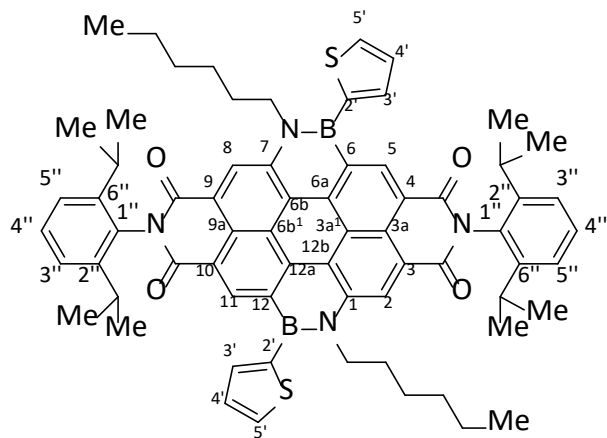
1,7-Di(*n*-hexyl)-6,12-di(thiophen-2-yl)-1,12,6,7-di([1,2]azaborinine)-*N,N'*-di(cyclohexyl)perylene-3,4,9,10-tetracarboxylic acid di-imide (BNCDI^{Cy}**)**



In a nitrogen filled glovebox, a vial was charged with 1,7-di(*n*-hexylamino)-*N,N'*-di(cyclohexyl)perylene-3,4,9,10-tetracaboxylic acid di-imide (**1,7-DHA-PDI^{Cy}**, 19.0 mg, 25.2 μ mol), toluene (5.0 mL), triethylamine (0.5 mL) and dichloro-2-thienyl borane (**TphBCl₂**, 175 mg, 403 μ mol). The sealed vial was heated 24 h at 110 °C. After cooling to 25 °C, all volatiles were removed *in vacuo* and the red product was dried (9.7 x 10⁻² mbar, 70 °C, 2 h). The residue was dissolved in DCM (30 mL), washed with brine (3 x 50 mL), 1 M NaOH (3 x 50 mL) and water (3 x 50 mL). After drying over magnesium sulfate, filtration, removal of the solvent, the product was subjected to column chromatography (silica, eluent: gradient petrol ether to DCM, R_f(DCM) = 0.65) to give the product (**BNCDI^{Cy}**, 23 mg, 24.5 μ mol, 97%) as a red-violet solid.

¹H NMR (500 MHz, CDCl₃): δ = 9.56 (s, 2H, H-2,8), 9.54 (s, 2H, H-5,11), 7.87 (dd, ³J = 4.8 Hz, ⁴J = 0.8 Hz, 22H, Tph-H-3'), 7.61 (dd, ³J = 3.2 Hz, ⁴J = 0.8 Hz, 2H, Tph-H-5'), 6.60 (dd, ³J = 4.8 Hz, ³J = 3.2 Hz, 2H, Tph-H-4'), 5.23 (tt, ³J = 12.0, 3.8 Hz, 2H, CH), 4.79 (t, ³J = 7.8 Hz, 4H, N-CH₂), 2.70 (qd, ³J = 12.0, 3.0 Hz, 4H, CH-CH_{ax}), 2.12 (quin., ³J = 7.8 Hz, 4H, N-(CH₂)-CH₂), 1.98 (d, ³J = 13.5 Hz, 4H, CH-CH₂-CH_{ox}), 1.91 (d, ³J = 12.0 Hz, 4H, CH-CH_{eq}), 1.79 (d, ³J = 13.0 Hz, 2H, CH-(CH₂)₂-CH_{ax}), 1.59 - 1.26 (m, 18H, CH-CH₂-CH_{eq}, CH-(CH₂)₂-CH_{eq} and N-(CH₂)₂-(CH₂)₃), 0.90 (t, ³J = 7.0 Hz, 6H, CH₃) ppm. **¹³C{¹H} NMR** (126 MHz, CDCl₃): δ = 165.06 ((C(O)N)-4,10), 165.04 ((C(O)N)-3,9), 138.79 (C-1,7), 137.33 (C-5,11), 136.68 (Tph-C-2', only HMBC), 134.22 (Tph-C-5'), 133.85 (C-6a,12a), 132.51 (C-6,12, only HMBC), 130.03 (Tph-C-3'), 128.55 (Tph-C-4'), 123.70 (C-3,9 or C-4,10), 123.54 (C-3,9 or C-4,10), 123.15 (C-3a¹,6b¹), 122.67 (C-3a,9a), 12089 (C-2,8), 120.46 (C-6b,12b), 54.56 (CH), 50.70 (N-CH₂), 31.81 (N-CH₂-CH₂), 31.48 (CH-CH₂), 29.53 (N-(CH₂)₂-CH₂), 26.85 (N-(CH₂)₃-CH₂), 26.85 (CH-CH₂-CH₂), 25.70 (CH-(CH₂)₂-CH₂), 22.74 (N-(CH₂)₄-CH₂), 14.13 (CH₃) ppm. **¹¹B{¹H} NMR** (160 MHz, CDCl₃): δ = 38.70 (br) ppm. **HRMS (EI)**: *m/z* [M]⁺ calcd. for C₅₆H₅₈N₄O₄¹¹B₂S₂ 936.41460; found 936.41893 (100%). **IR (ATR)**: ν = 2921 (m), 2852 (m), 1698 (s), 1654 (s), 1599 (s), 1566 (m), 1450 (s), 1416 (m), 1404 (m), 1343 (w), 1302(s), 1280 (m), 1245 (s), 1202 (m), 1087 (w), 1020 (w), 897 (w), 847 (w), 812 (m), 706 (m), 651 (m), 599 (w) cm⁻¹.

1,7-Di(*n*-hexyl)-6,12-di(thiophen-2-yl)-1,12,6,7-di([1,2]azaborinine)-*N,N'*-bis(2,6-di(isopropyl)phenyl)perylene-3,4,9,10-tetracarboxylic acid di-imide (BNCDI^{Dip})

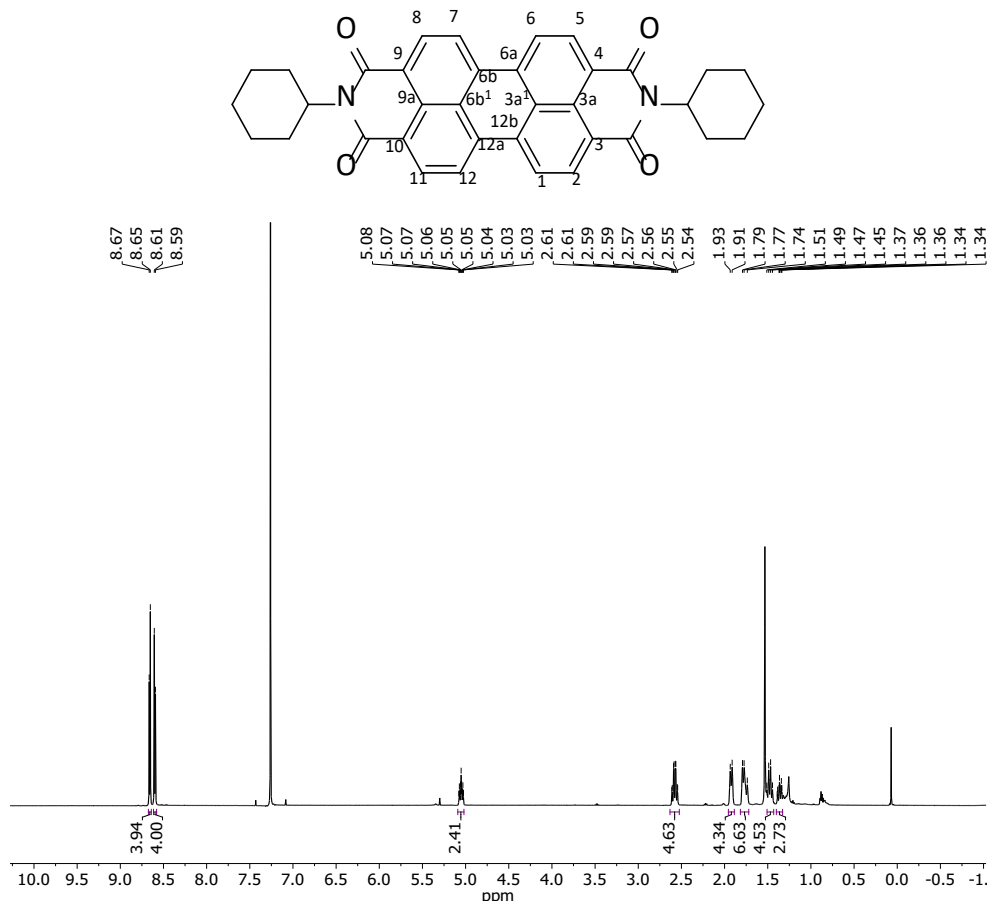


In a nitrogen filled glovebox, a pressure tube (50 mL) was charged with 1,7-di(*n*-hexylamino)-*N,N'*-bis(diisopropylphenyl)perylene-3,4,9,10-tetracaboxylic acid di-imide (**1,7-DHA-PDI^{Dip}**, 120 mg, 132 µmol), toluene (4.8 mL), triethylamine (200 µL) and dichloro-2-thienyl borane (100 mg, 607 µmol). The sealed tube was heated for 10 h at 110 °C. After cooling to 25 °C, the reaction mixture was dissolved in DCM (30 mL), washed with brine (3 x 50 mL), 1 M NaOH (3 x 50 mL) and water (3 x 50 mL). After drying over magnesium sulfate, filtration, and removal of the solvent *in vacuo*, the crude product was purified by column chromatography (silica, eluent: DCM, R_f(DCM) = 0.81) to give the red/violet product (**BNCDI^{Dip}**, 120 mg, 110 µmol, 83%).

¹H NMR (500 MHz, CDCl₃): δ = 9.75 (s, 2H, H-5,11), 9.74 (s, 2H, H-2,8), 7.86 (dd, ³J = 4.8 Hz, ⁴J = 0.8 Hz, 2H, Tph-H-3'), 7.67 (dd, ³J = 3.3 Hz, ⁴J = 0.8 Hz, 2H, Tph-H-5'), 7.53 (t, ³J = 7.9 Hz, 2H, Ph-H-4''), 7.50 (dd, ³J = 4.8 Hz, ³J = 3.3 Hz, 2H, Tph-H-4'), 7.40 (d, ³J = 7.9 Hz, 4H, Ph-H-3'',5''), 4.79 (m, 4H, N-CH₂), 2.91 (m, 4H, Ph-(CH)-(CH₃)₂), 2.20 (m, 4H, NH-CH₂), 1.54 (m, 4H, N-(CH₂)-CH₂), 1.51 - 1.21 (m, 8H, NH-(CH₂)₂-(CH₂)₃), 1.22 (t, ³J = 6.8 Hz, 24H, Ph-(CH)-(CH₃)₂), 0.87 (t, ³J = 7.0 Hz, 6H, CH₃) ppm. **¹³C{¹H} NMR** (126 MHz, CDCl₃): δ = 164.69 ((C(O)N)-4,10), 164.49 ((C(O)N)-3,9), 145.84 (Ph-C-2'',6''), 139.16 (C-1,7), 138.02 (C-2,8), 136.60 (Tph-C-2'), 134.59 (C-6a,12a), 134.42 (Tph-C-5'), 132.71 (C-6,12, only HMBC), 131.06 (Ph-C-1''), 130.13 (Tph-C-3'), 129.71 (Ph-C-4''), 128.62 (Tph-C-4'), 124.20 (Ph-C-3'',5''), 123.92 (C-3a₁,6b₁), 123.24 (C-3,4/9,10), 121.63 (C-3a,9a), 121.14 (C-5,11), 120.61 (C-6b,12b), 50.92 (NH-CH₂), 31.90 (NH-CH₂-CH₂), 31.42 (NH-(CH₂)₂-CH₂), 29.42 (Ph-(CH)-(CH₃)₂), 26.75 (NH-(CH₂)₃-CH₂), 24.25 and 24.23 (Ph-(CH)-(CH₃)₂), 22.58 (NH-(CH₂)₄-CH₂), 14.08 (CH₃) ppm. **¹¹B{¹H} NMR** (160 MHz, CDCl₃): δ = 38.21 (br) ppm. **HRMS** (APCI, MeOH/toluene, positive mode): *m/z* [M+H]⁺ calcd. For C₆₈H₇₁¹¹B₂N₄O₄S₂ 1093.51179; found 1093.51256. **HRMS** (APCI, MeOH/toluene, negative mode): *m/z* [M]⁻ Calcd. for C₆₈H₇₀¹¹B₂N₄O₄S₂ 1092.50507; found 1092.50602. **IR** (ATR): υ = 2956 (w), 2921 (w), 2851 (w), 1707 (m), 1669 (m), 1600 (m), 1562 (m), 1436 (m), 1311 (s), 1280 (m), 1245 (s) 1207 (m), 1192 (m), 1053 (m), 847 (m), 813 (m), 792 (m), 759 (m), 753 (m), 720 (m), 700 (s) cm⁻¹.

NMR Spectra

N,N'-Di(cyclohexyl)perylene-3,4,9,10-tetracabboxylic acid diimide (**PDI^{Cy}**)



***N,N'*-(Diisopropylphenyl)-perylene-3,4,9,10-tetracabboxylic acid diimide (PDI^{Dip})**

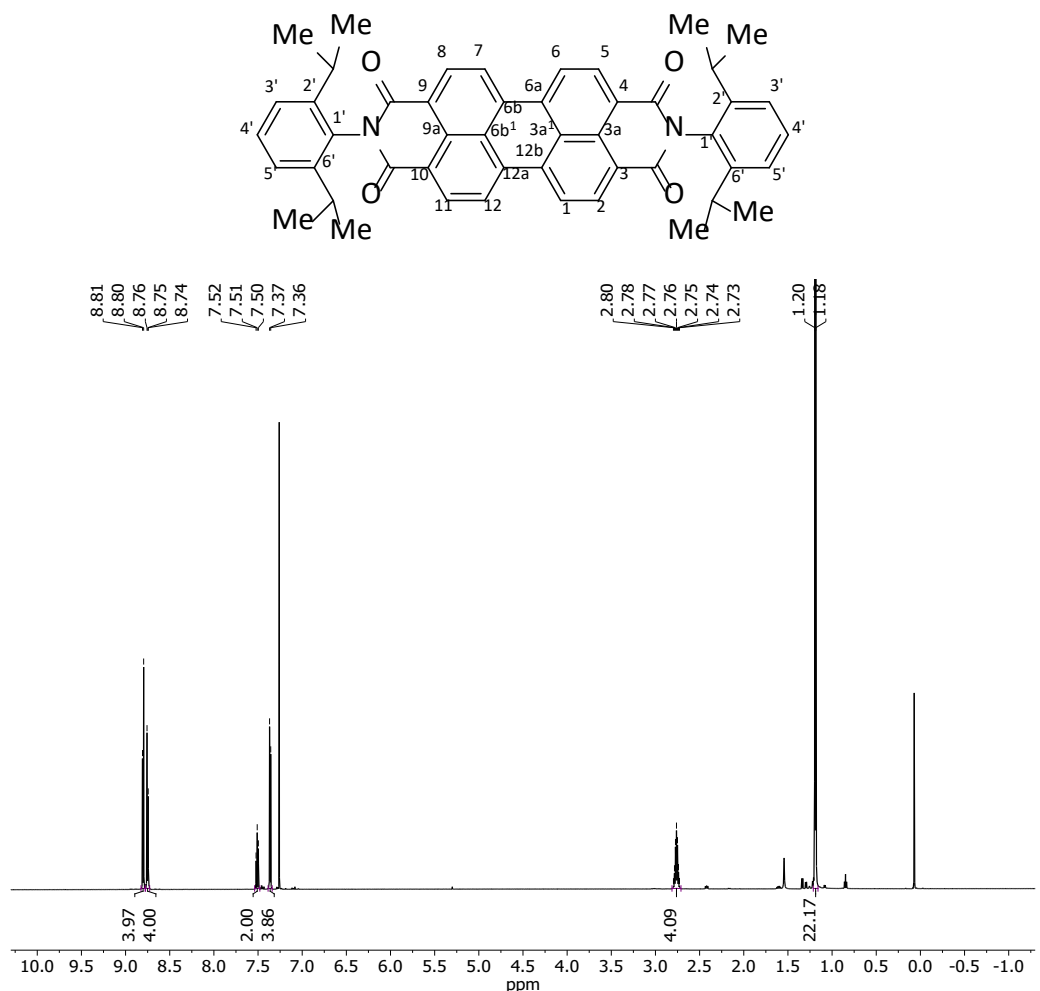


Fig. SI3: ¹H NMR (600 MHz, CDCl₃) spectrum of PDI^{Dip}.

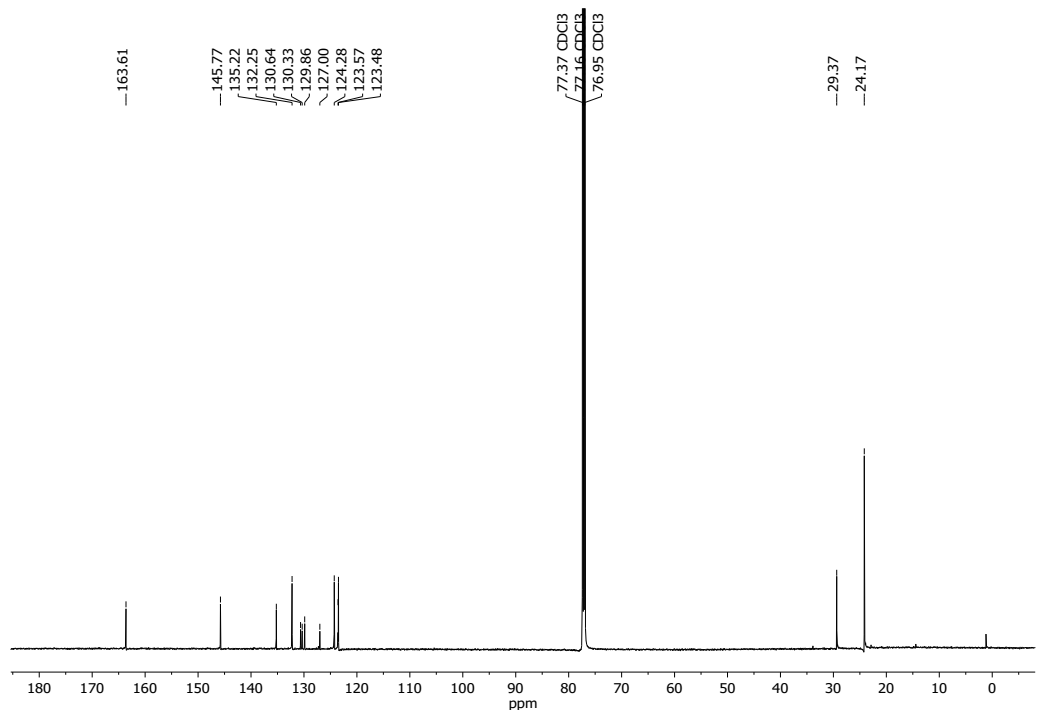


Fig. SI4: ¹³C{¹H} NMR (151 MHz, CDCl₃) spectrum of PDI^{Dip}.

Perylene-3,4,9,10-tetra-*n*-butylester (PTBE)

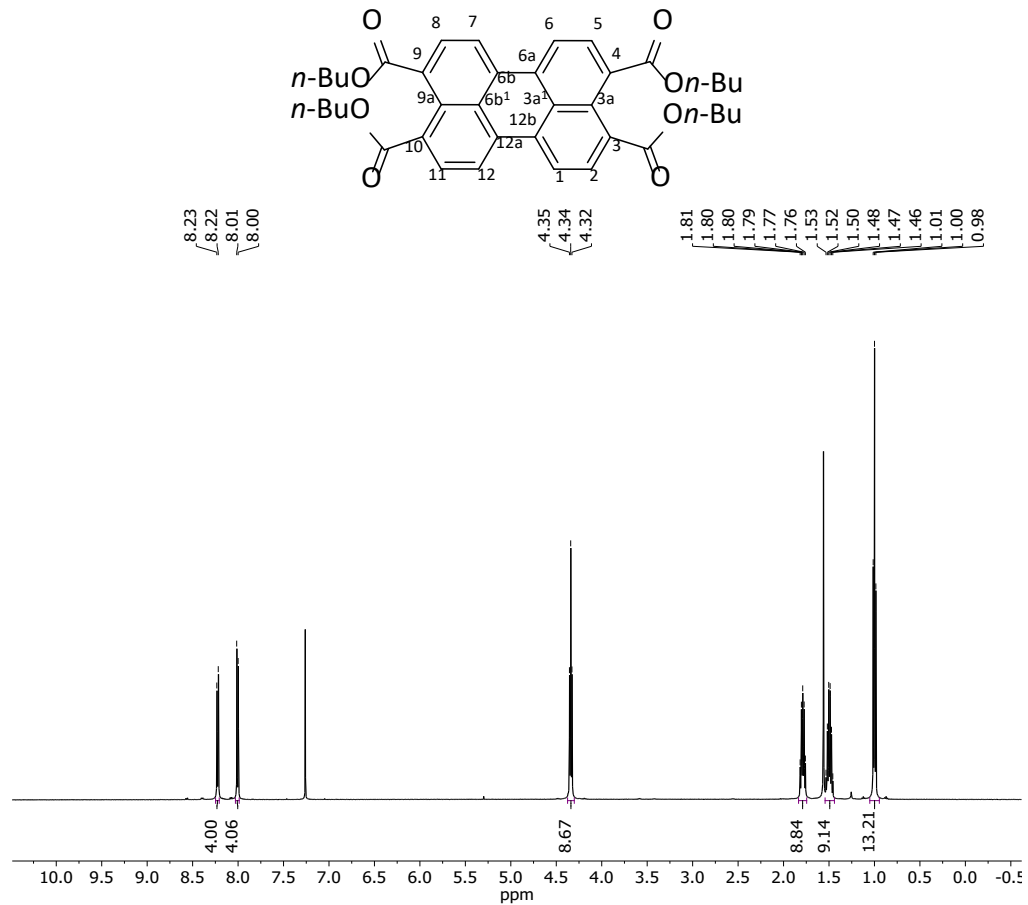


Fig. S15: ^1H NMR (500 MHz, CDCl_3) spectrum of **PTBE**.

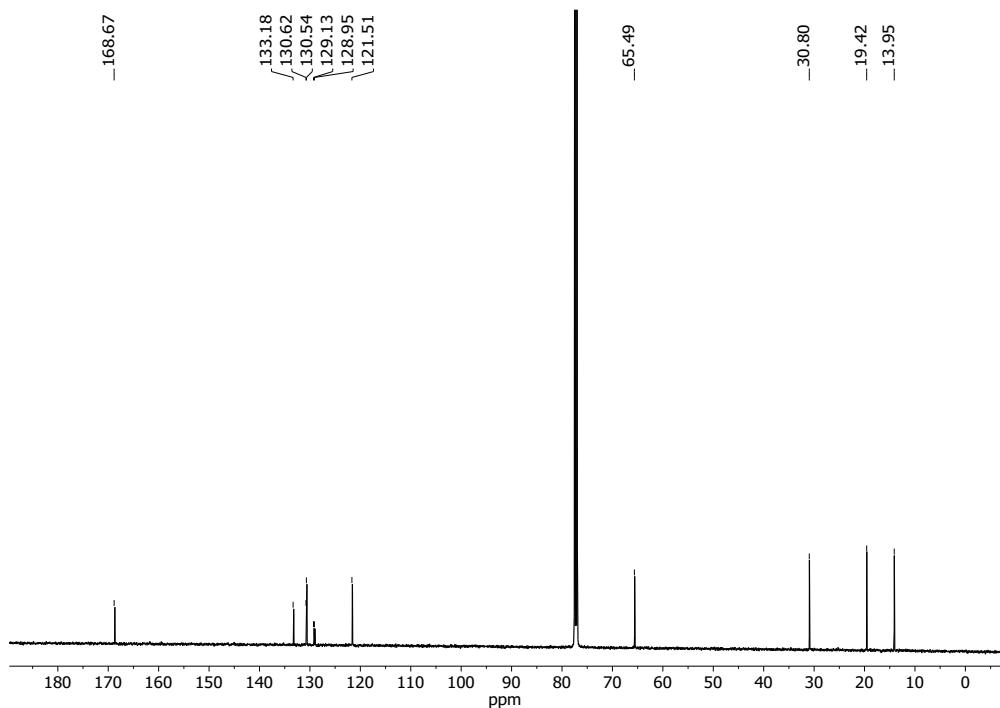


Fig. S16: $^{13}\text{C}\{\text{H}\}$ NMR (125 MHz, CDCl_3) spectrum of PTBE.

1,7-Dibromoperylene-3,4,9,10-tetra-*n*-butylester (1,7-DB-PTBE)

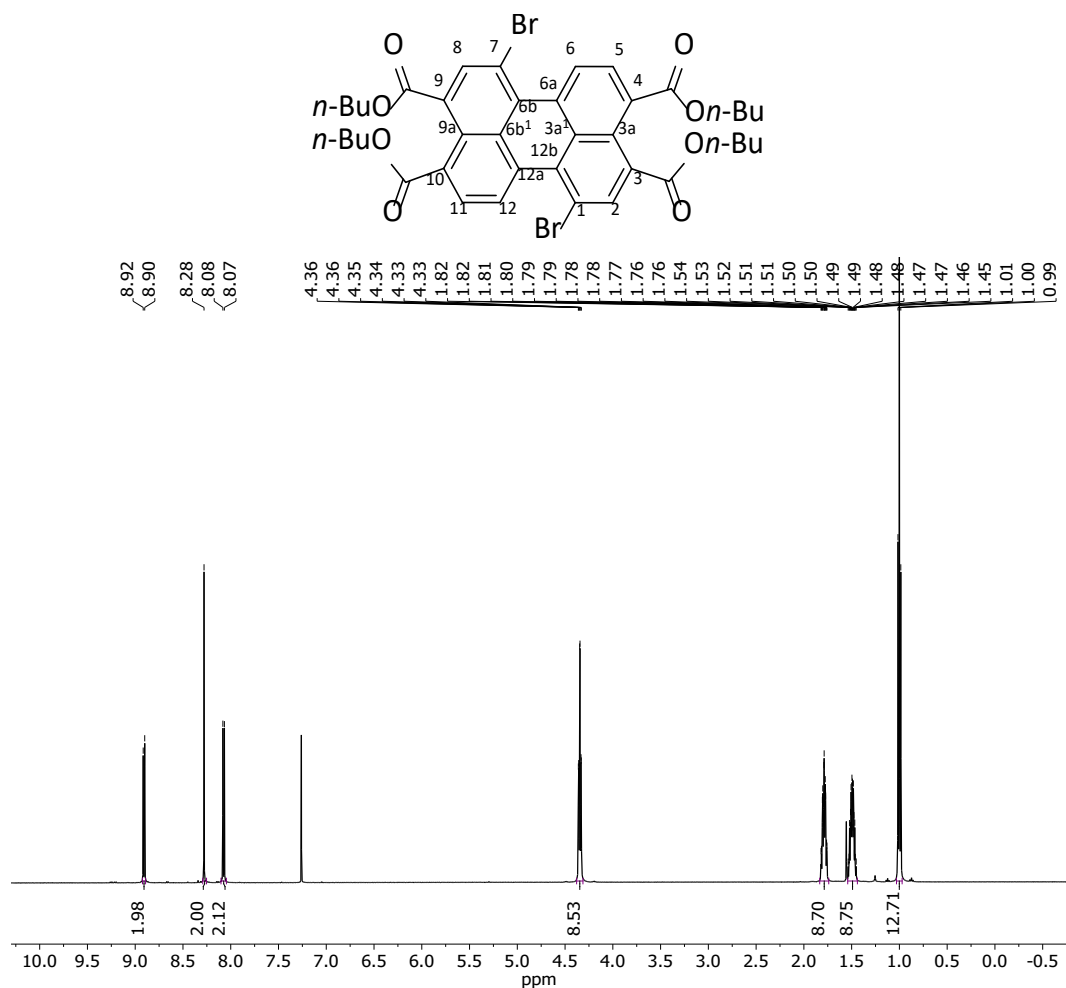


Fig. SI7: ^1H NMR (500 MHz, CDCl_3) spectrum of **1,7-DB-PTBE**.

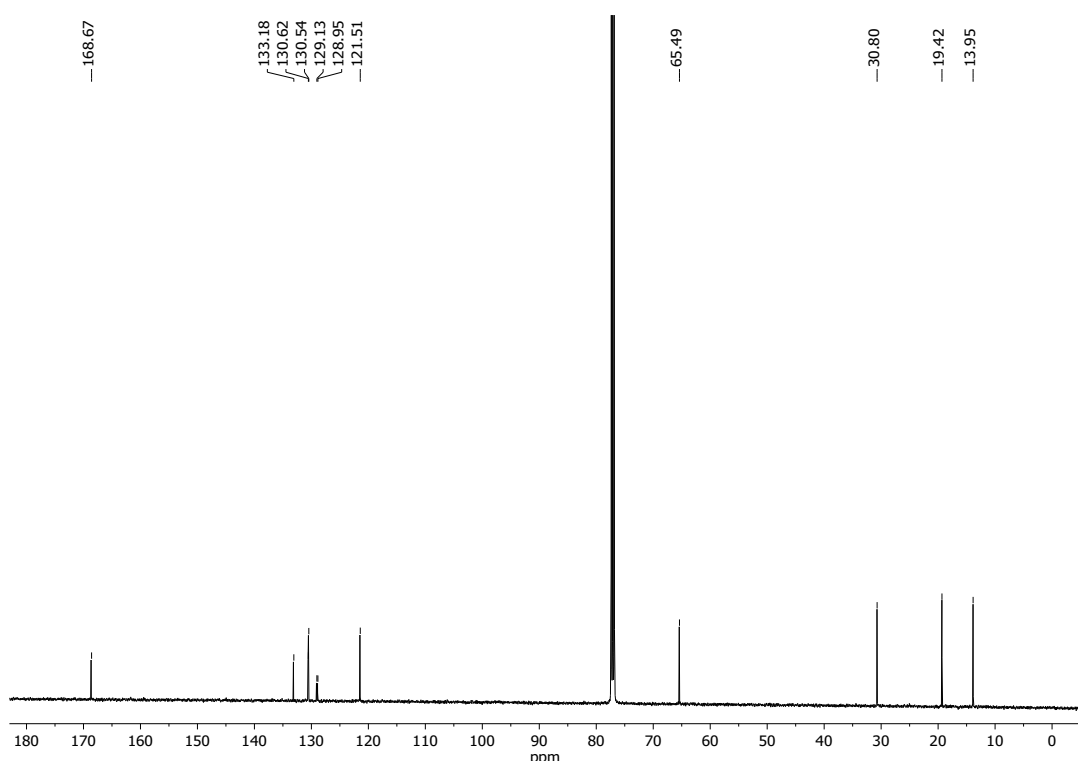


Fig. S18: $^{13}\text{C}\{^1\text{H}\}$ NMR (125 MHz, CDCl_3) spectrum of **1,7-DB-PTBE**.

1,7-Dibromoperylene-3,4,9,10-tetracabboxylic dianhydride (1,7-DB-PTCDA)

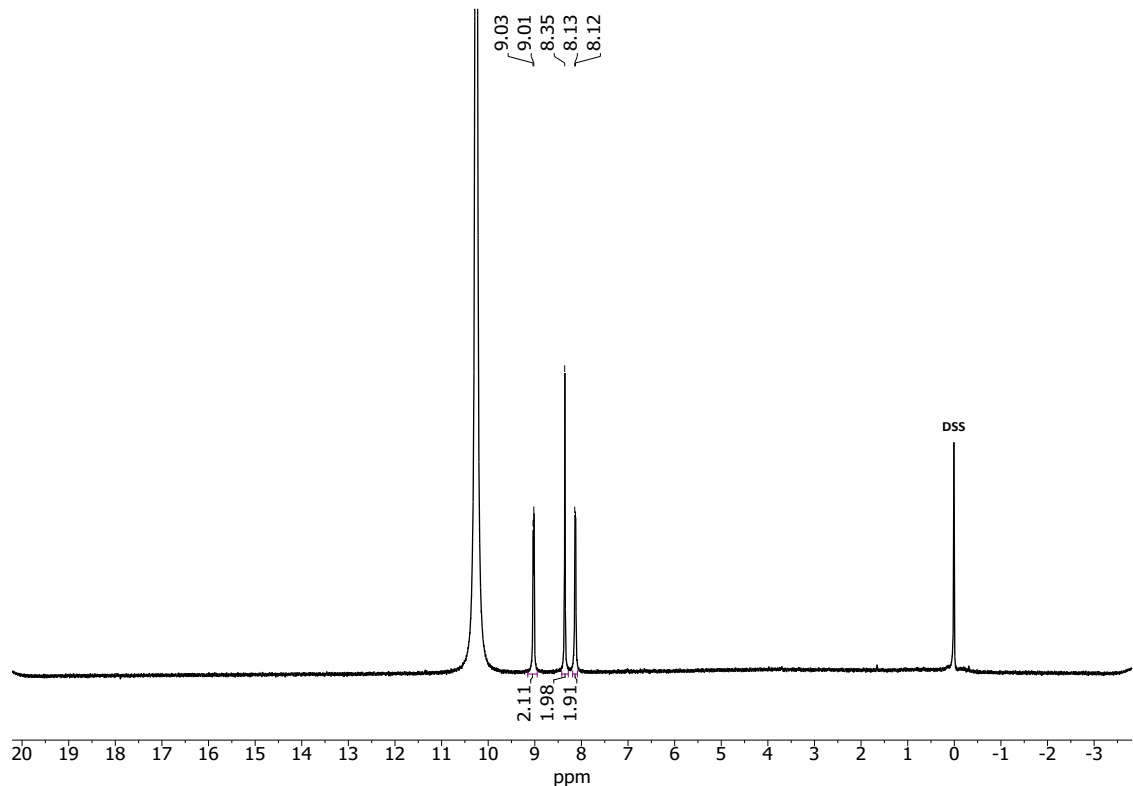
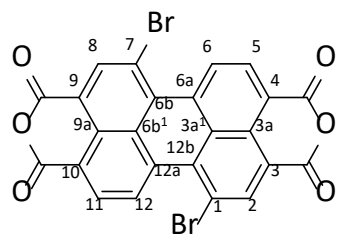


Fig. S19: ^1H NMR (500 MHz, D_2SO_4 +DSS) spectrum of **1,7-DB-PTCDA**.

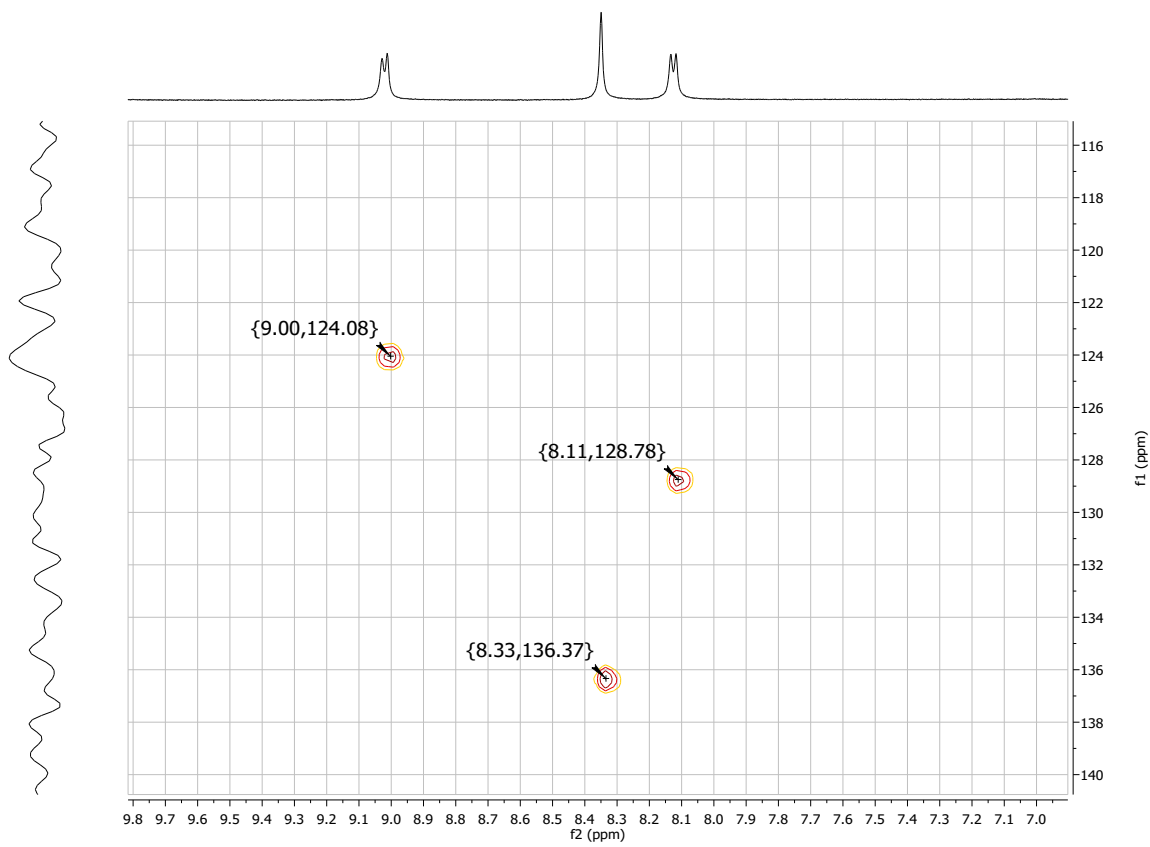


Fig. SI10: ^1H - ^{13}C { ^1H } HSQC spectrum of 1,7-DB-PTCDA.

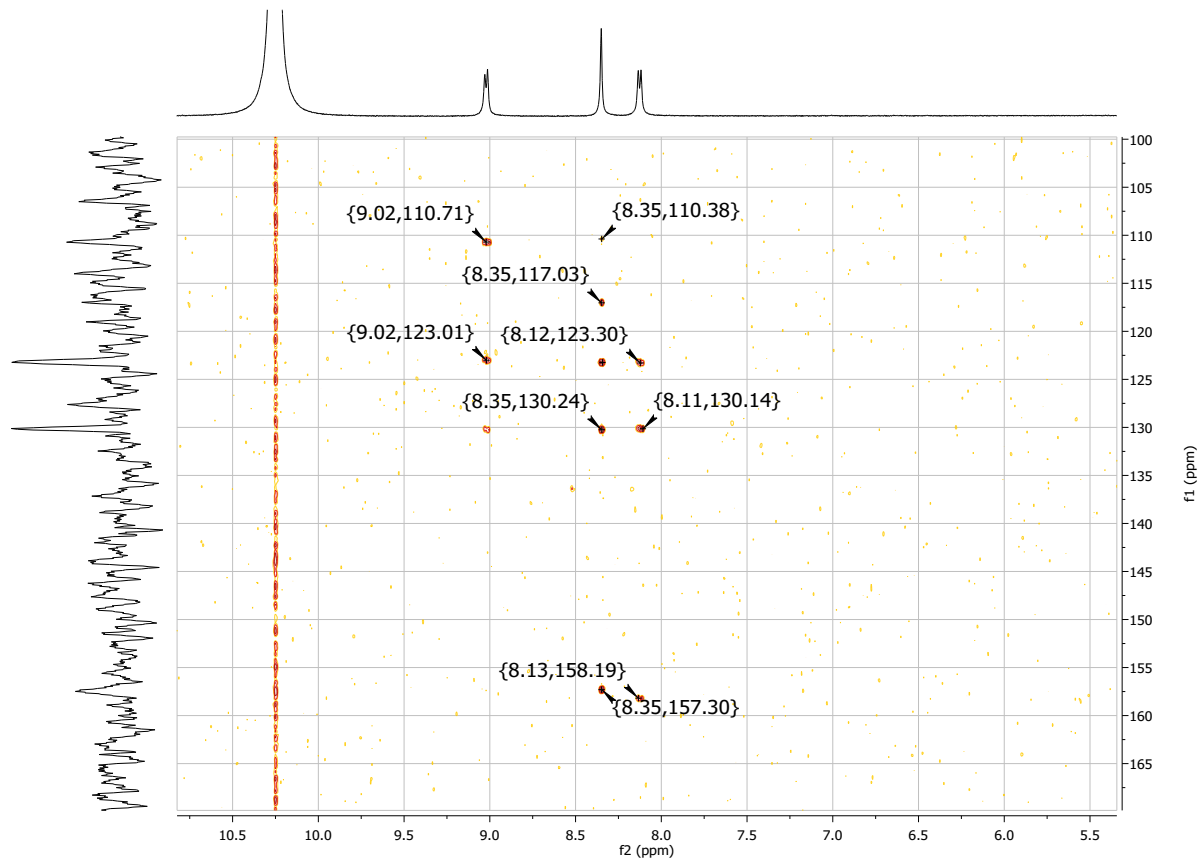


Fig. SI11: ^1H - ^{13}C { ^1H } HMBC spectrum of 1,7-DB-PTCDA.

1,7-Dibromo-N,N'-dicyclohexylperylene-3,4,9,10-tetracaboxylic acid di-imide (1,7-DB-PDI^{Cy})

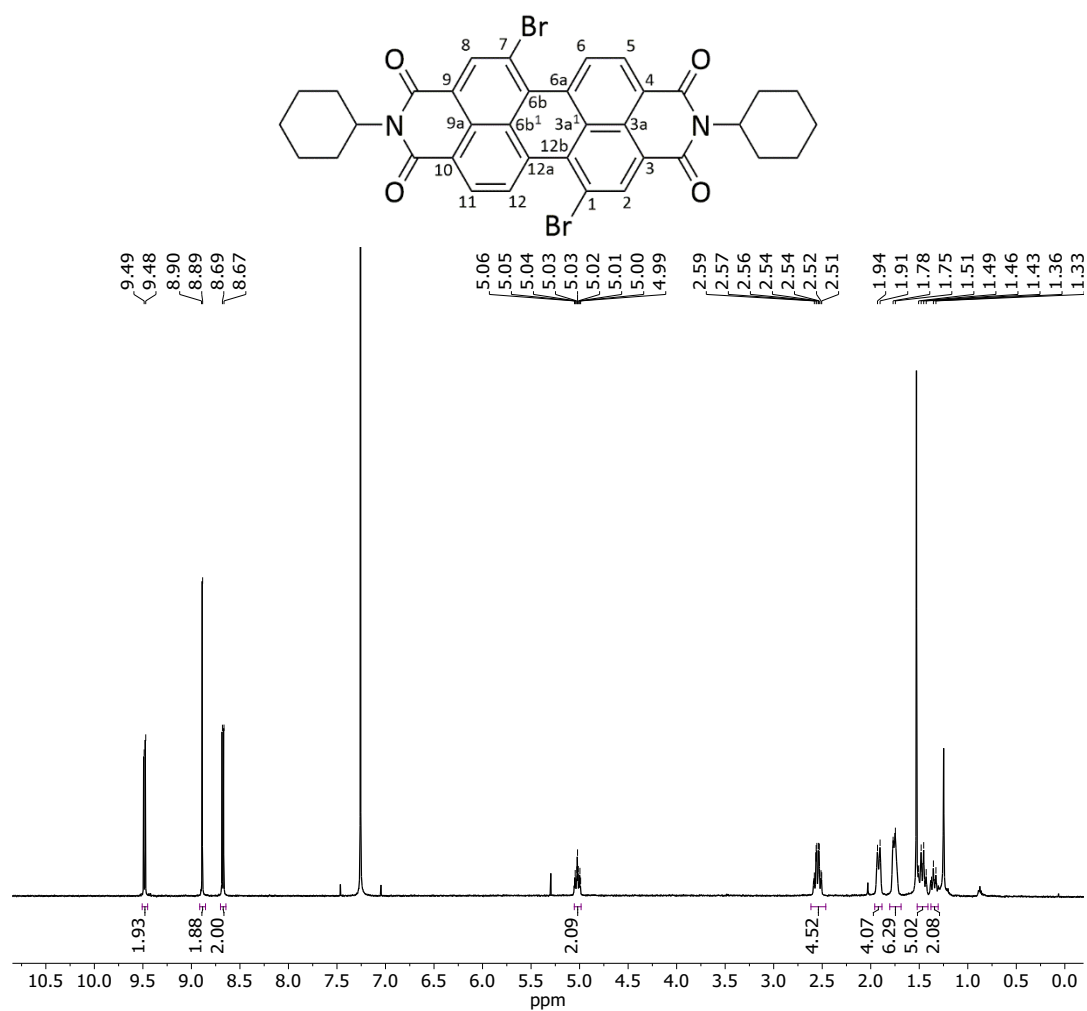


Fig. SI12: ¹H NMR (500 MHz, CDCl₃) spectrum of 1,7-DB-PDI^{Cy}.

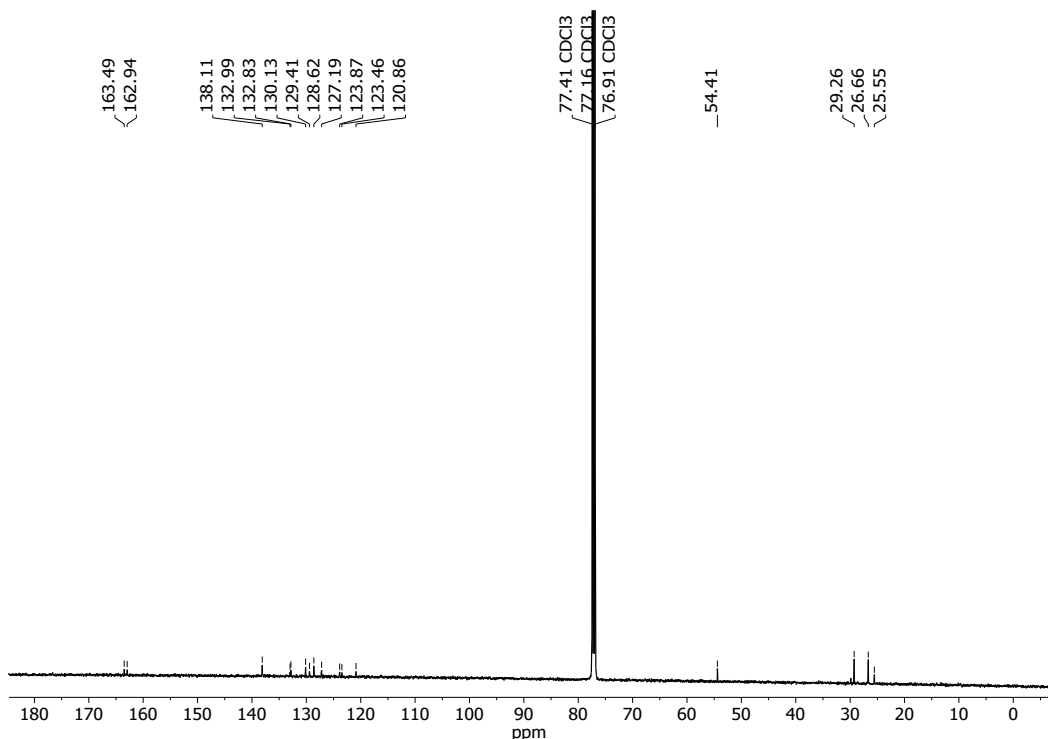


Fig. SI13: $^{13}\text{C}\{^1\text{H}\}$ NMR (125 MHz, CDCl_3) spectrum of **1,7-DB-PDI^{Dip}**.

1,7-Dibromo-N,N'-(Diisopropylphenyl)-perylene-3,4,9,10-tetracabboxylic acid di-imide (1,7-DB-PDI^{Dip})

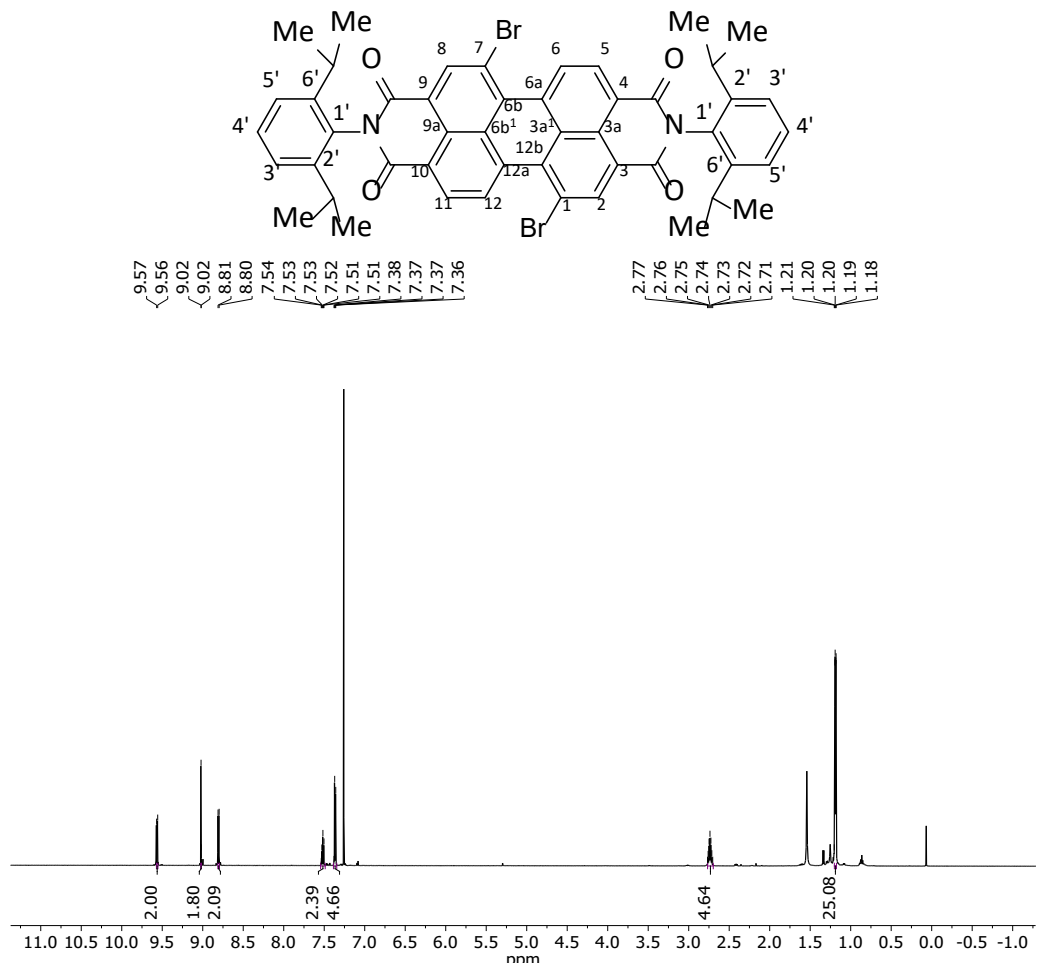


Fig. SI14: ^1H NMR (601 MHz, CDCl_3) spectrum of **1,7-DB-PDI^{Dip}**.

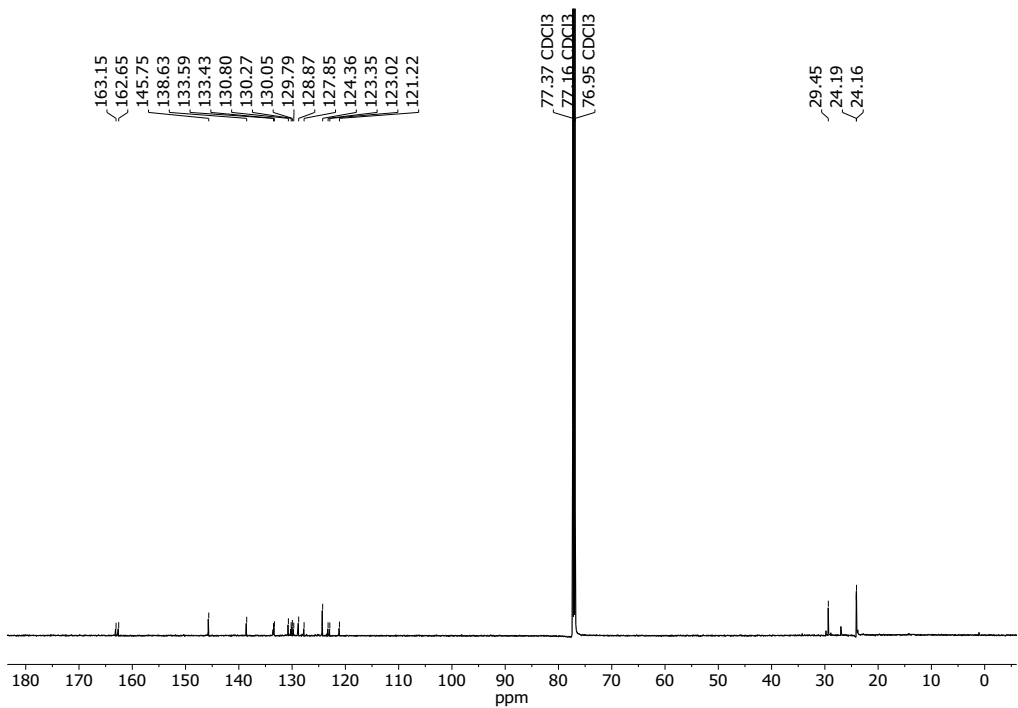


Fig. SI15: $^{13}\text{C}\{^1\text{H}\}$ NMR (151 MHz, CDCl_3) spectrum of **1,7-DB-PDI**^{Dip}.

1,7-Di(*n*-hexylamino)-*N,N'*-di(cyclohexyl)perylene-3,4,9,10-tetracabboxylic acid di-imide (1,7-DHA-PDI^{Cy})

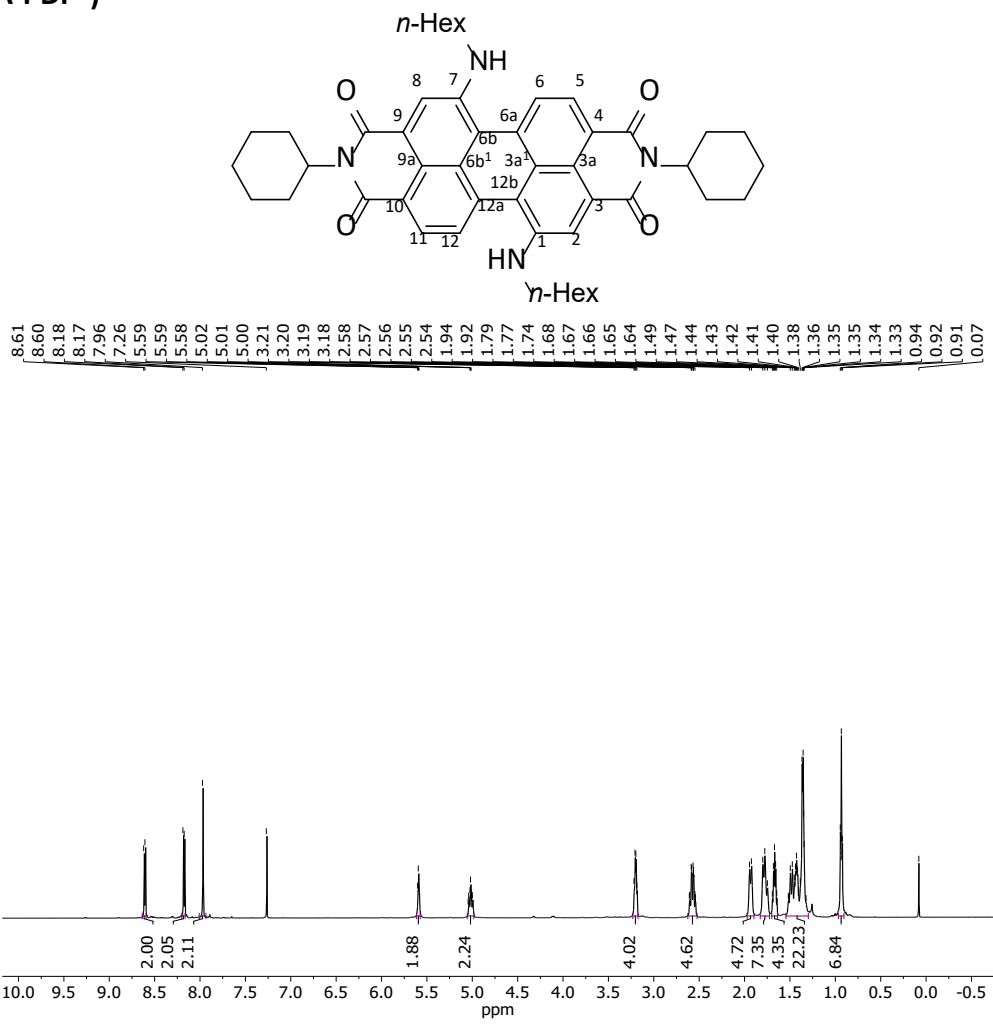


Fig. SI16: ^1H NMR (600 MHz, CDCl_3) spectrum of **1,7-DHA-PDI**^{Cy}.

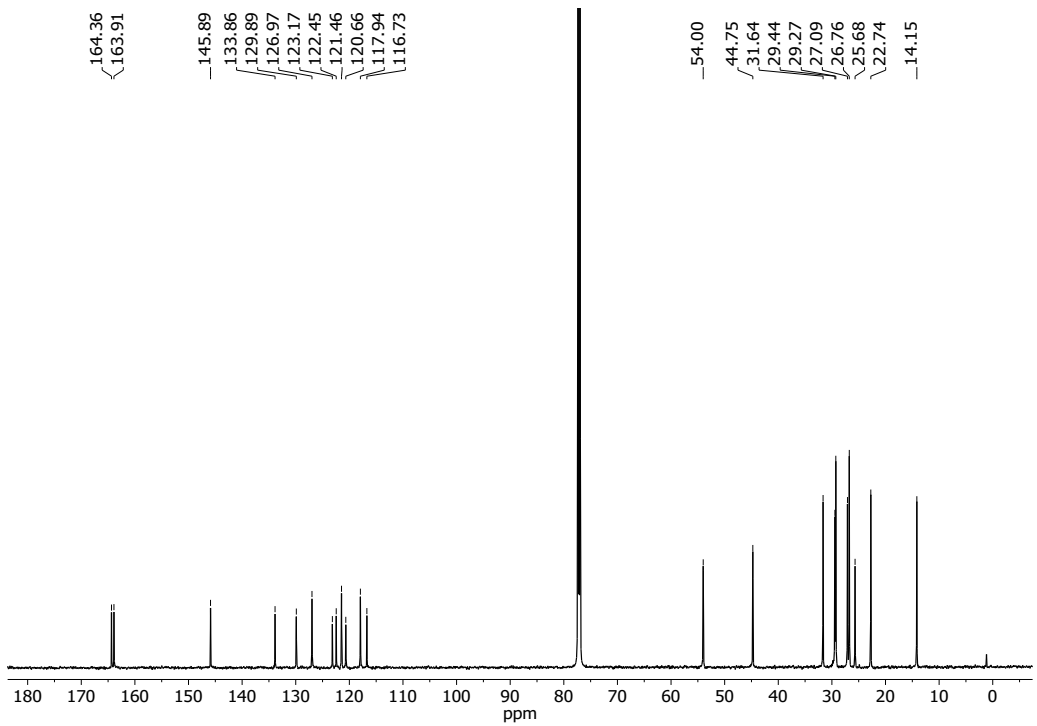


Fig. SI17: $^{13}\text{C}\{^1\text{H}\}$ NMR (150 MHz, CDCl_3) spectrum of **1,7-DHA-PDI^{Cy}**.

1,7-Di(*n*-hexylamino)-*N,N'*-bis(2,6-diisopropylphenyl)perylene-3,4,9,10-tetracabboxylic acid di-imide (1,7-DHA-PDI^{Dip})

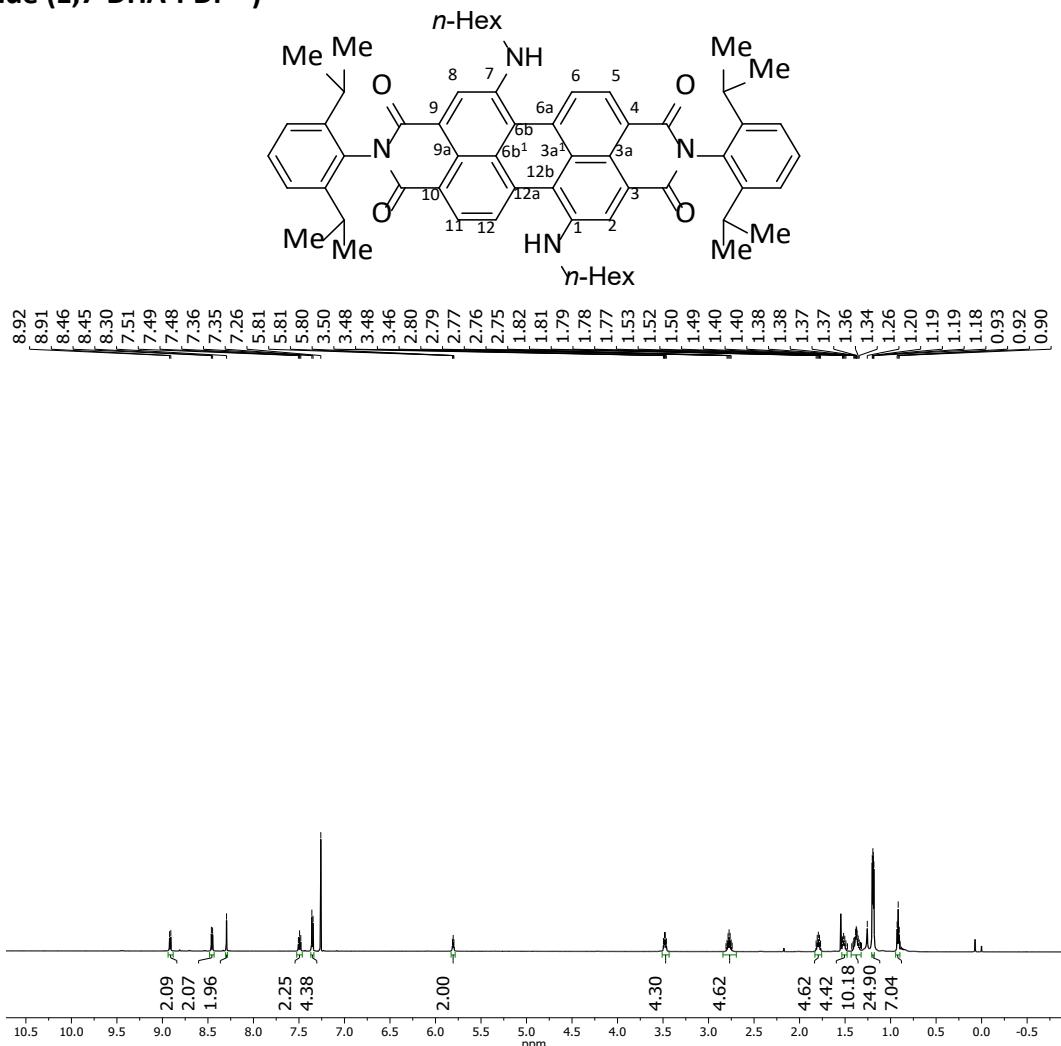


Fig. SI18: ¹H NMR (600 MHz, CDCl₃) spectrum of 1,7-DHA-PDI^{Dip}.

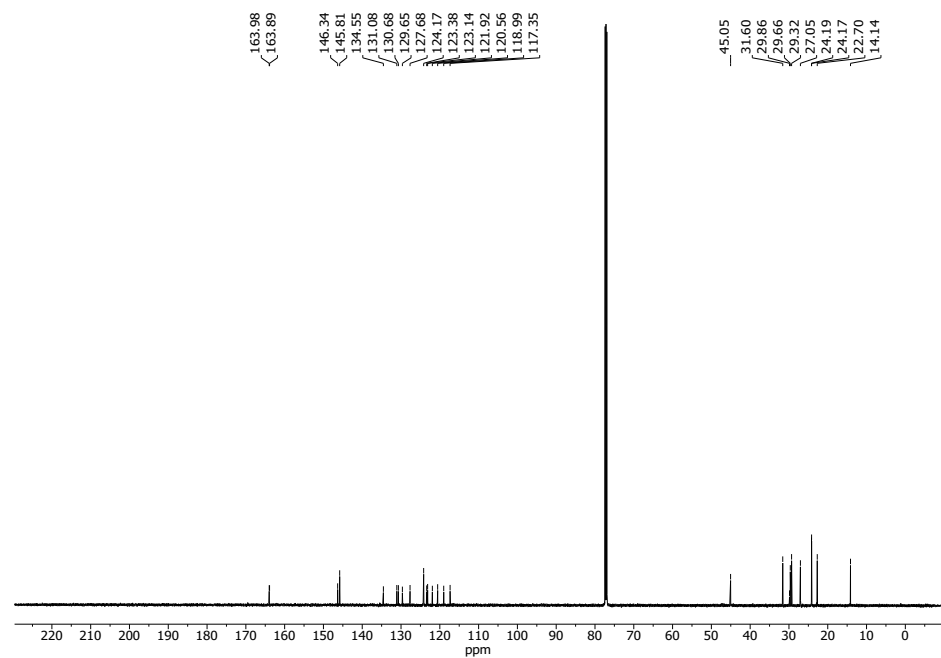


Fig. SI19: ¹³C{¹H} NMR (150 MHz, CDCl₃) spectrum of 1,7-DHA-PDI^{Dip}.

2-(Trimethylsilyl)thiophene (TpHtMS)

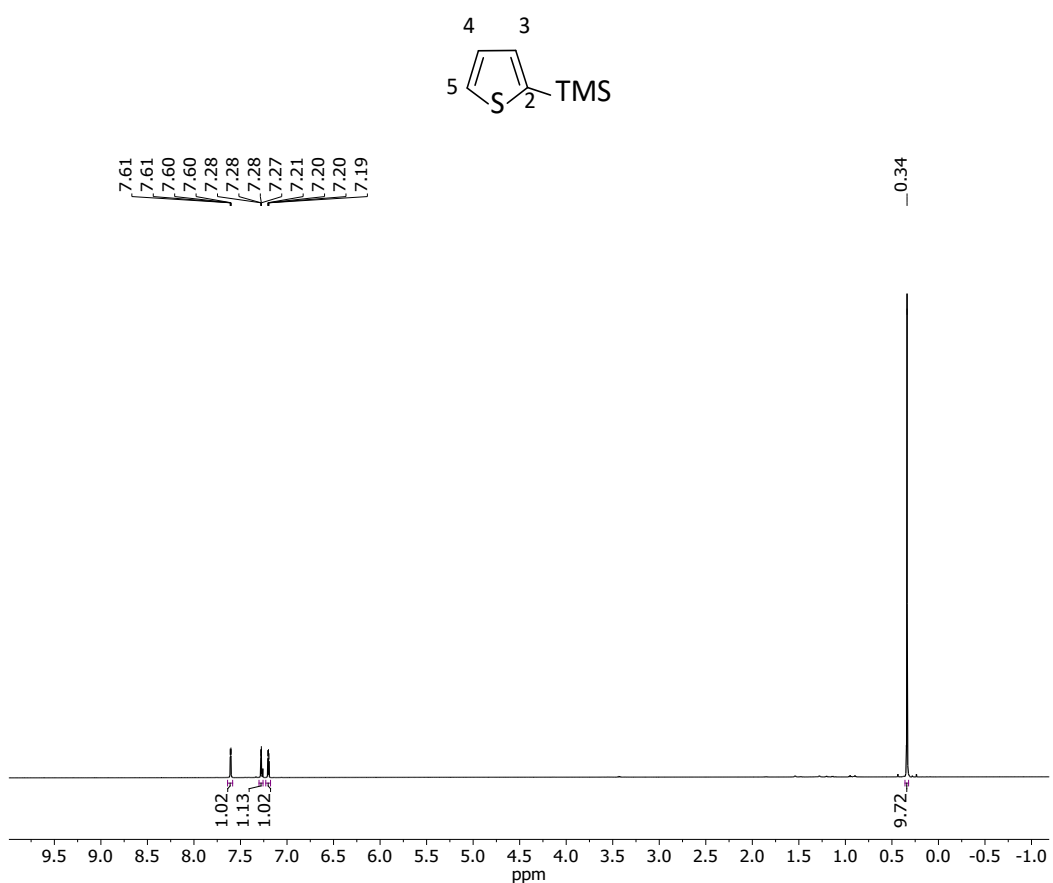


Fig. SI20: ¹H NMR (600 MHz, CDCl₃) spectrum of TpHtMS.

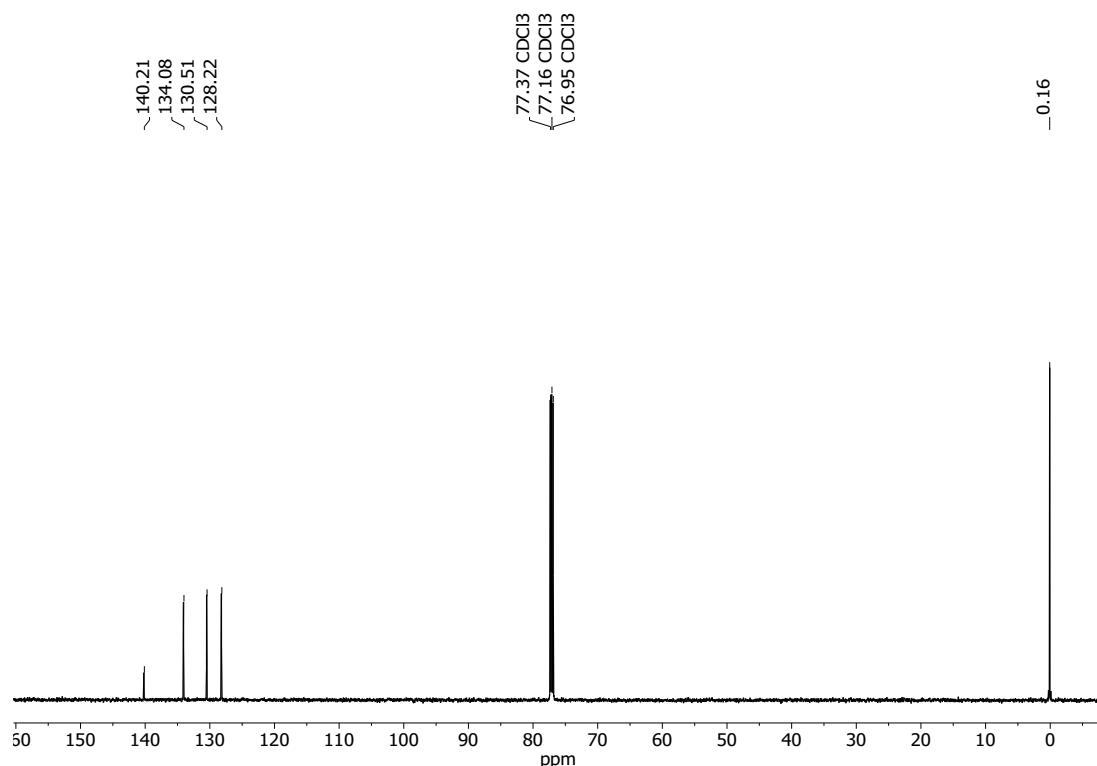


Fig. SI21: ¹³C{¹H} NMR (151 MHz, CDCl₃) spectrum of TpHtMS.

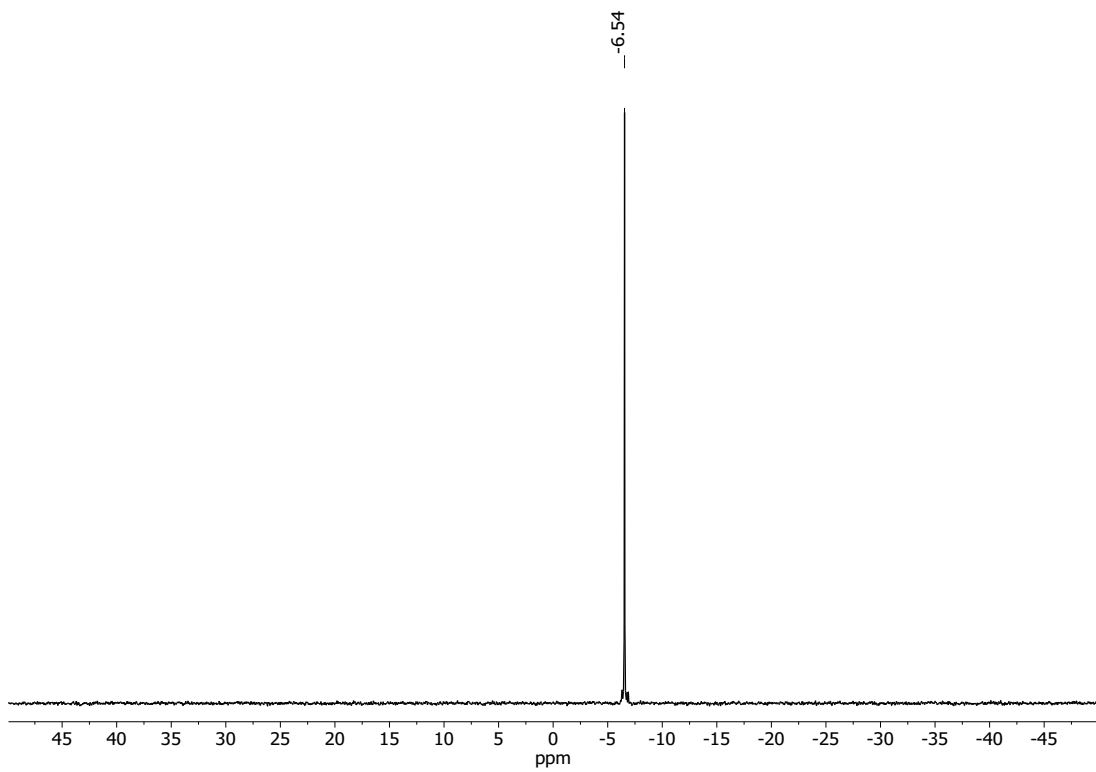


Fig. SI22: ²⁹Si{¹H} NMR (119 MHz, CDCl₃) spectrum of **TphTMS**.

Dichloro-2-thienyl borane (**TphBCl₂**)

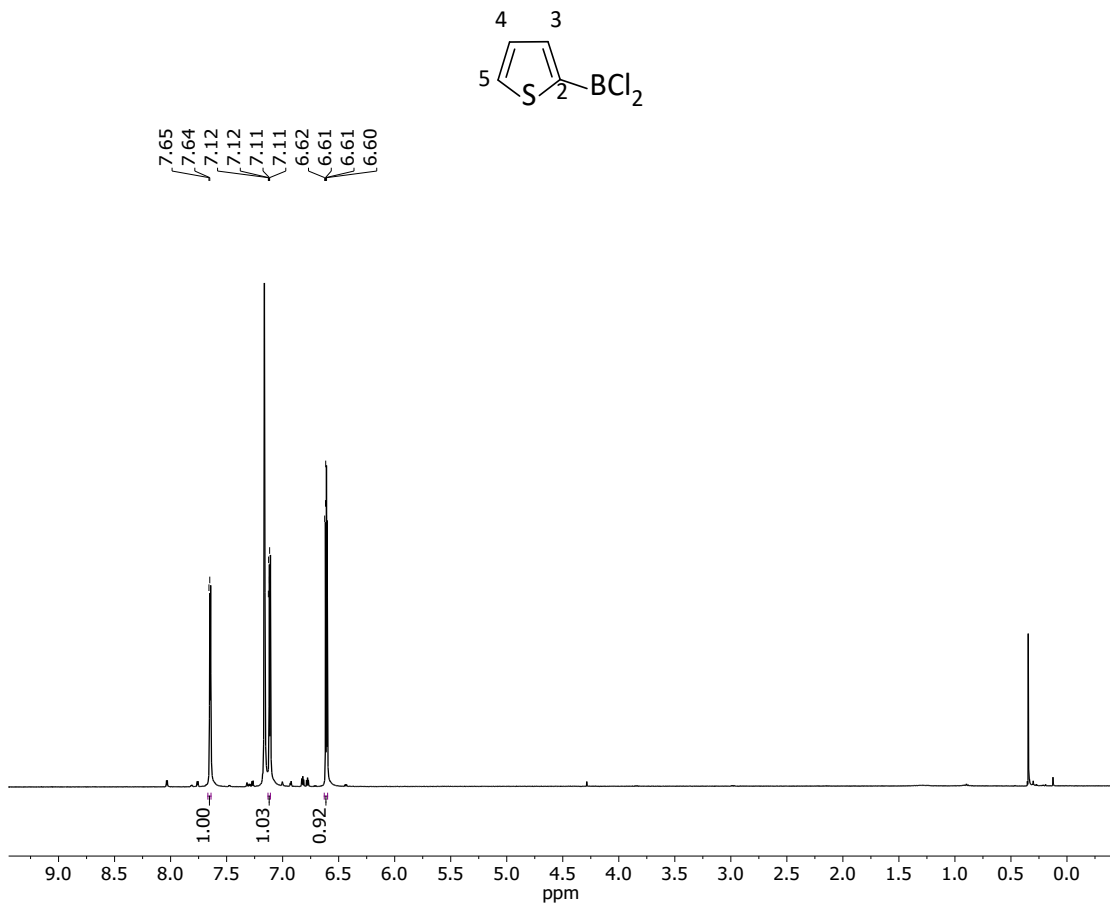


Fig. SI23: ¹H NMR (500 MHz, C₆D₆) spectrum of **TphBCl₂**.

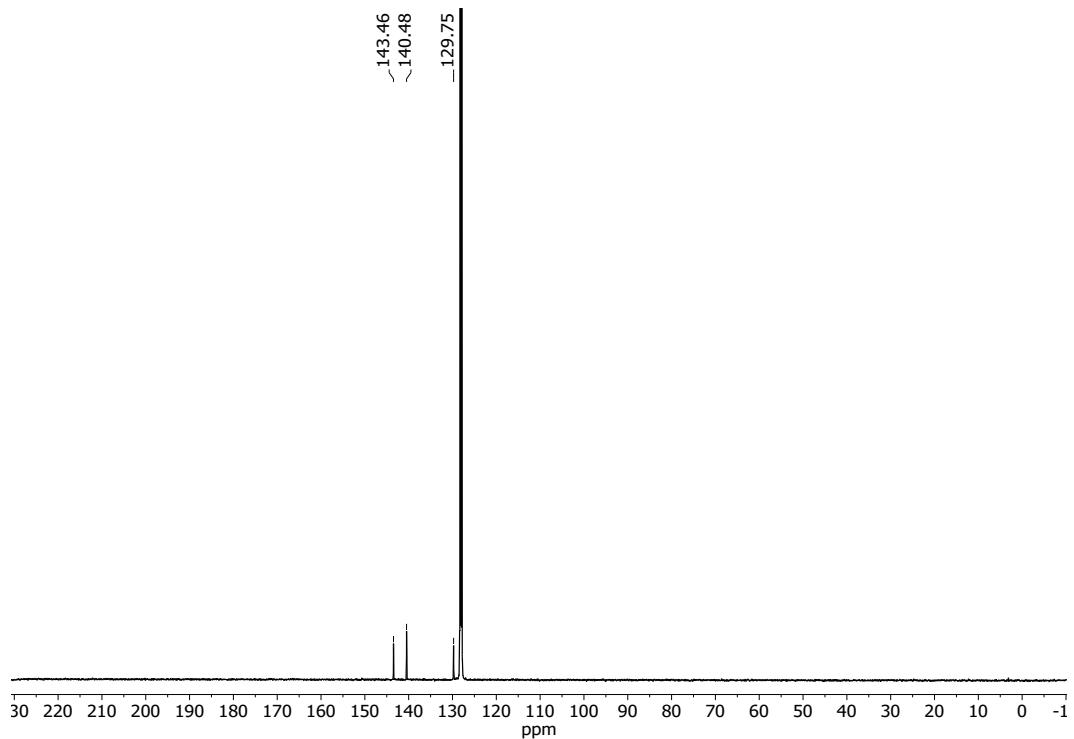


Fig. SI24: $^{13}\text{C}\{^1\text{H}\}$ NMR (126 MHz, C_6D_6) spectrum of TphBCl_2 .

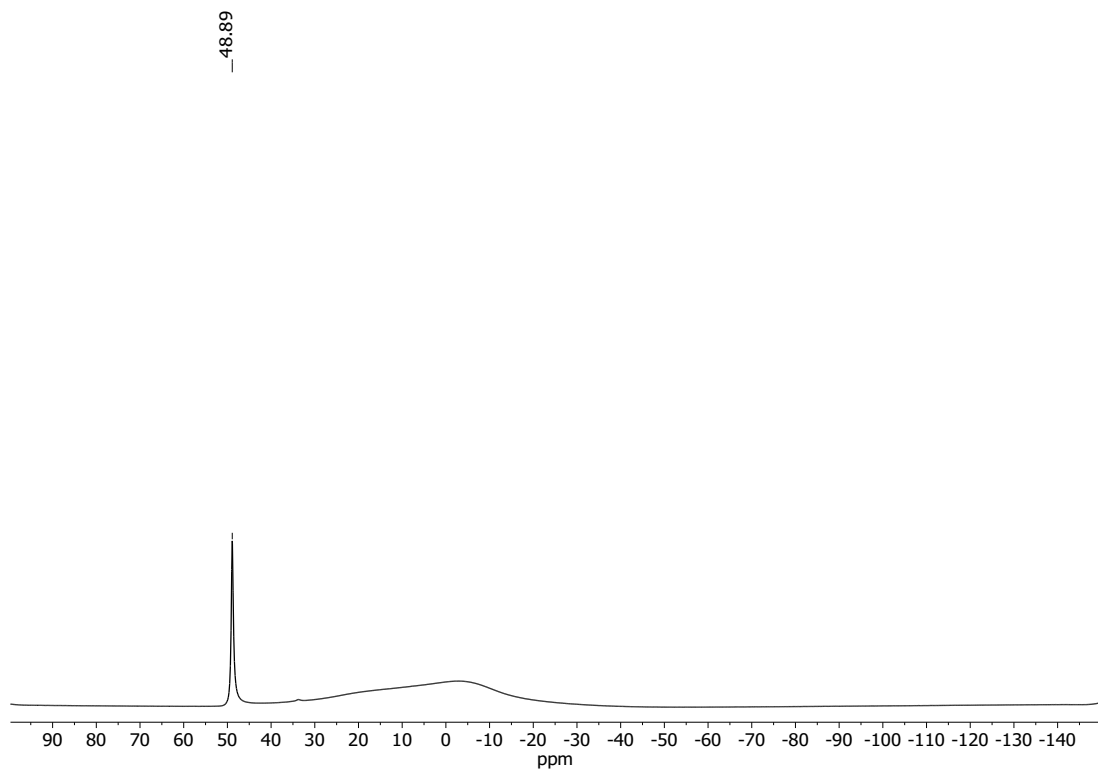


Fig. SI25: $^{11}\text{B}\{^1\text{H}\}$ NMR (160 MHz, C_6D_6) spectrum of TphBCl_2 .

1,7-Di(*n*-hexyl)-6,12-di(thiophen-2-yl)-1,12,6,7-di([1,2]azaborinine)-*N,N'*-di(cyclohexyl)perylene-3,4,9,10-tetracarboxylic acid di-imide (BNCDI^{Cy})

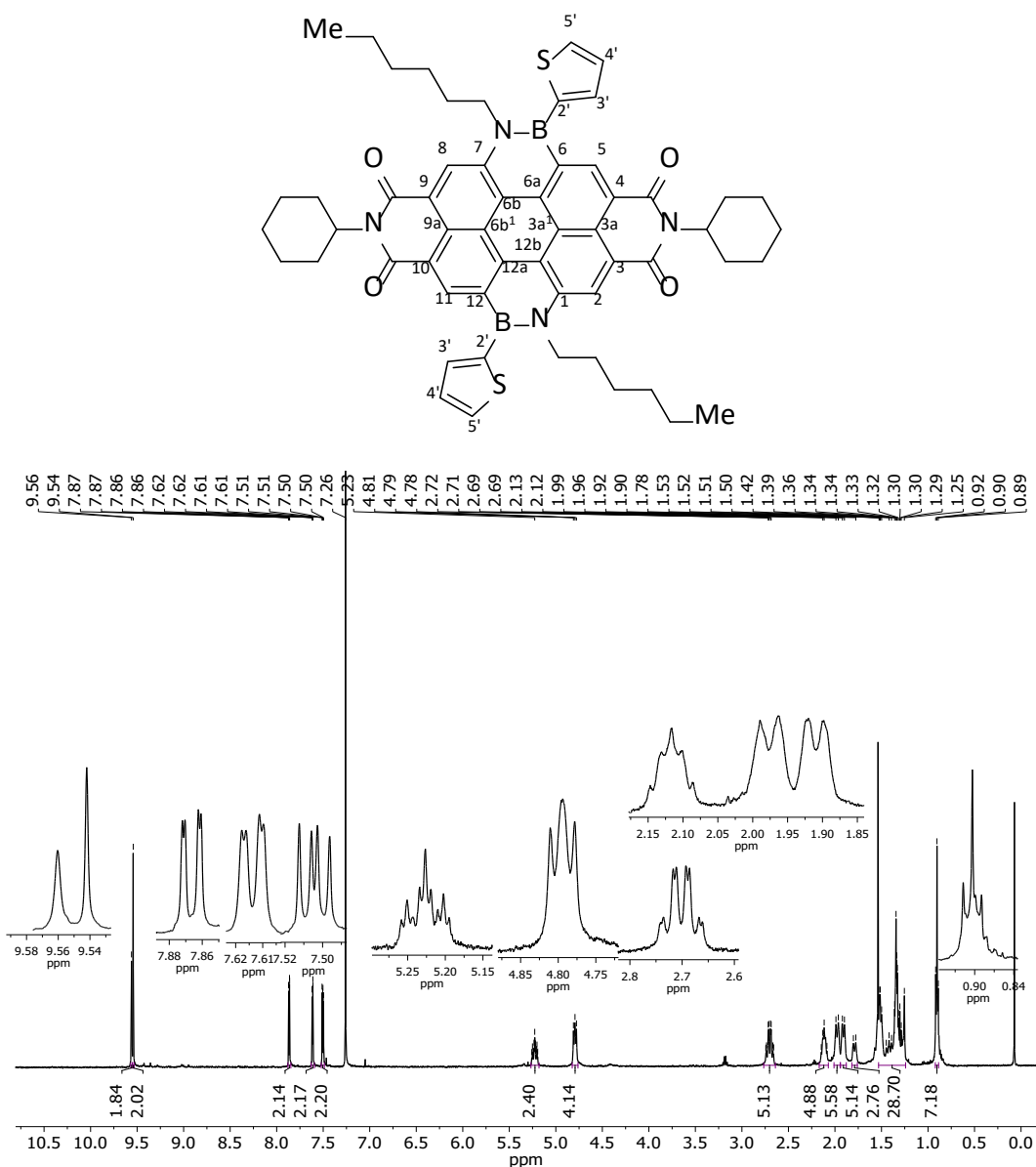


Fig. SI26: ¹H NMR (500 MHz, CDCl₃) spectrum of BNCDI^{Cy}.

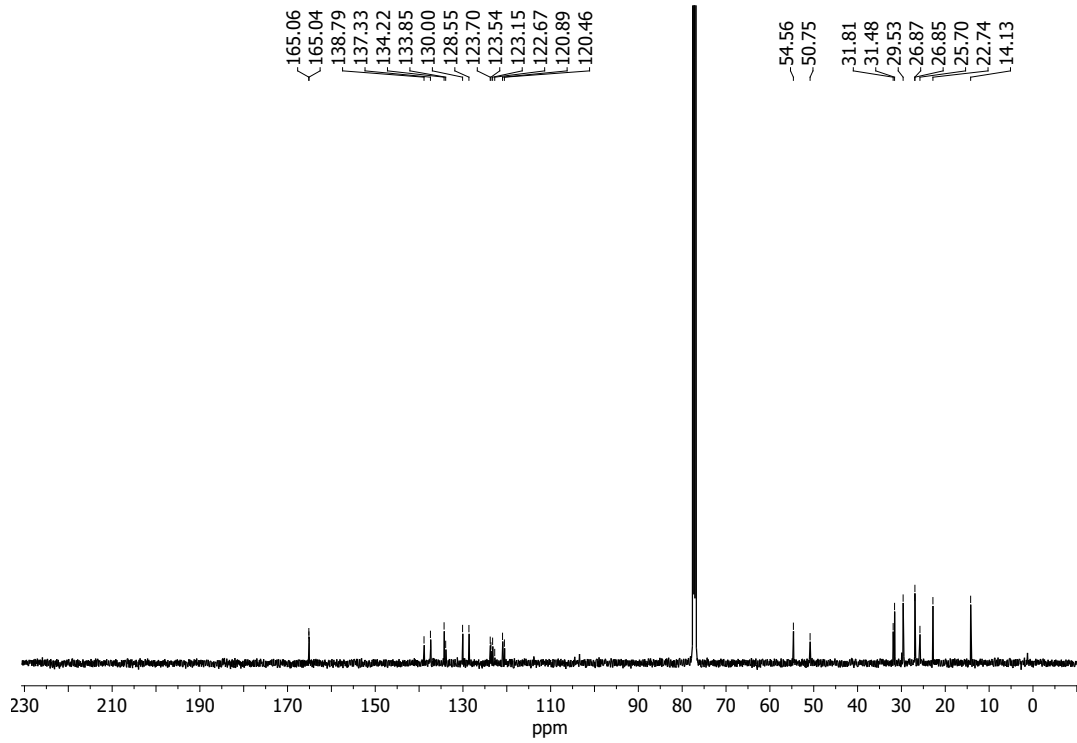


Fig. SI27: $^{13}\text{C}\{^1\text{H}\}$ NMR (126 MHz, CDCl_3) spectrum of **BNCDI** $^\gamma$.

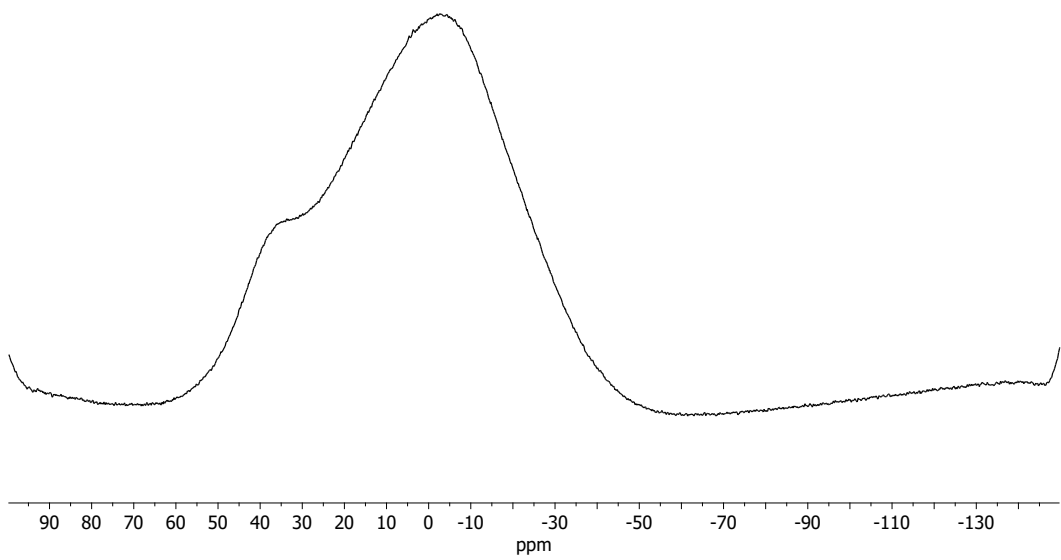


Fig. SI28: $^{11}\text{B}\{^1\text{H}\}$ NMR (160 MHz, CDCl_3) spectrum of **BNCDI** $^\gamma$.

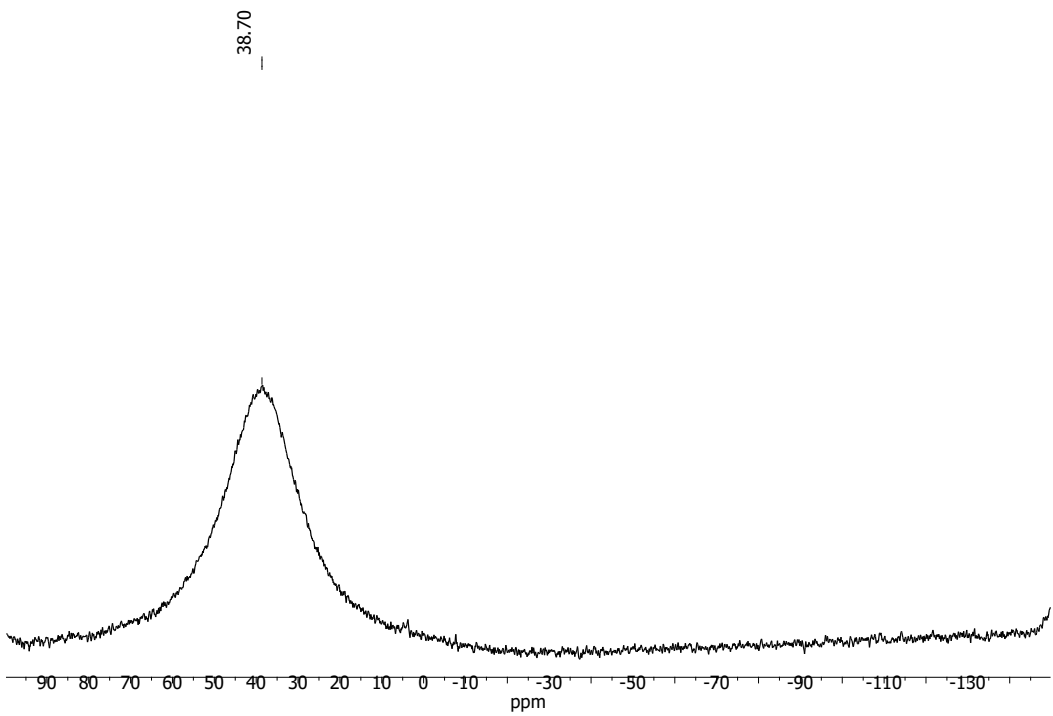


Fig. SI29: $^{11}\text{B}\{^1\text{H}\}$ NMR (160 MHz, CDCl_3) differential spectrum of CDCl_3 and **BNCDI^{CY}**.

1,7-Di(*n*-hexyl)-6,12-di(thiophen-2-yl)-1,12,6,7-di([1,2]azaborinine)-*N,N'*-bis(2,6-diisopropylphenyl)perylene-3,4,9,10-tetracarboxylic acid di-imide (BNCDI^{Dip})

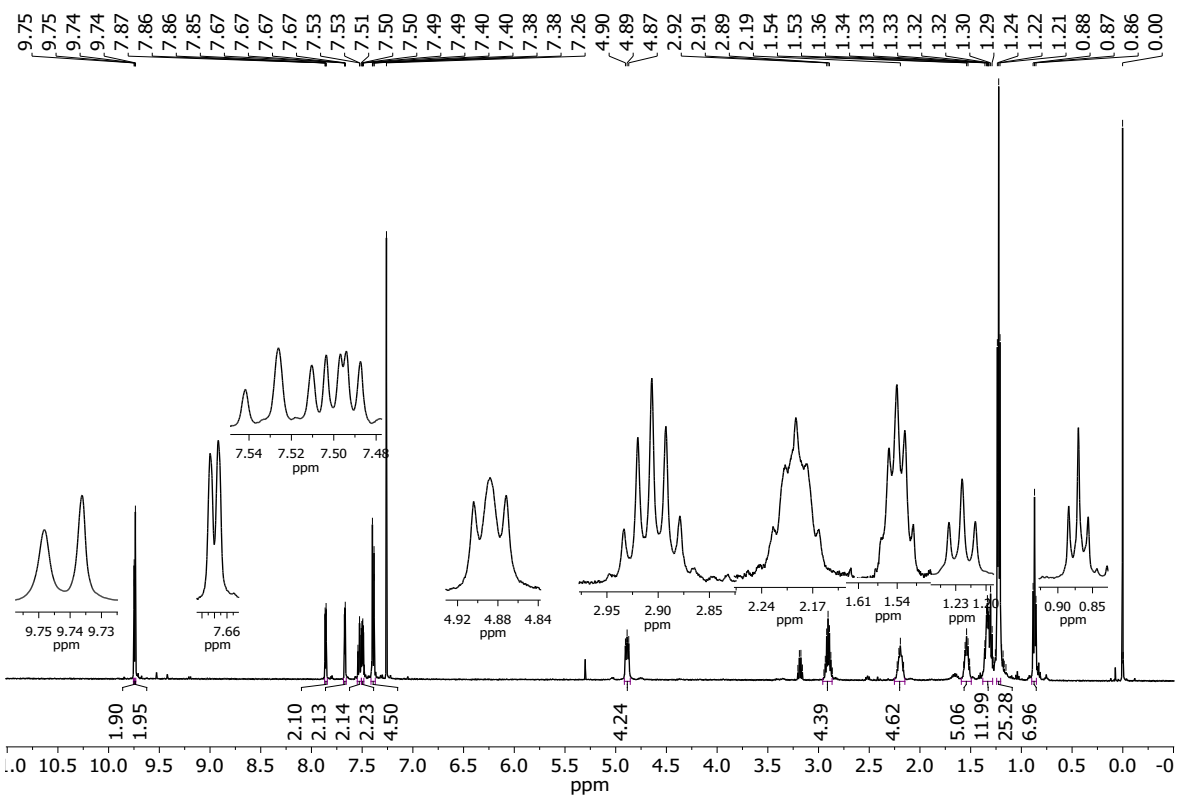
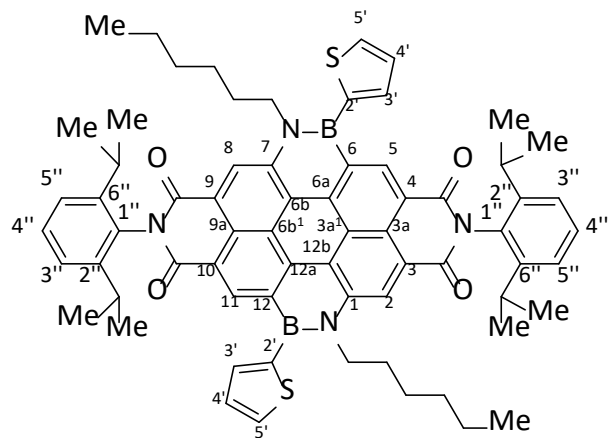


Fig. SI30: ^1H NMR (500 MHz, CDCl_3) spectrum of **BNCDI**^{Dip}.

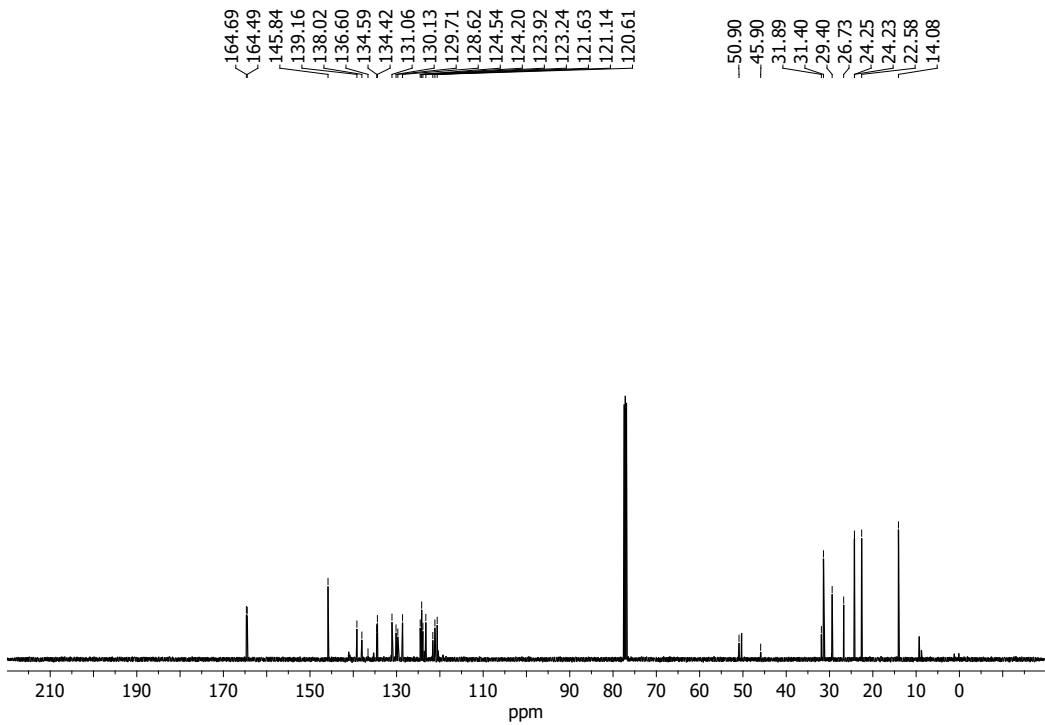


Fig. SI31: $^{13}\text{C}\{^1\text{H}\}$ NMR (126 MHz, CDCl_3) spectrum of $\text{BNCDI}^{\text{Dip}}$.

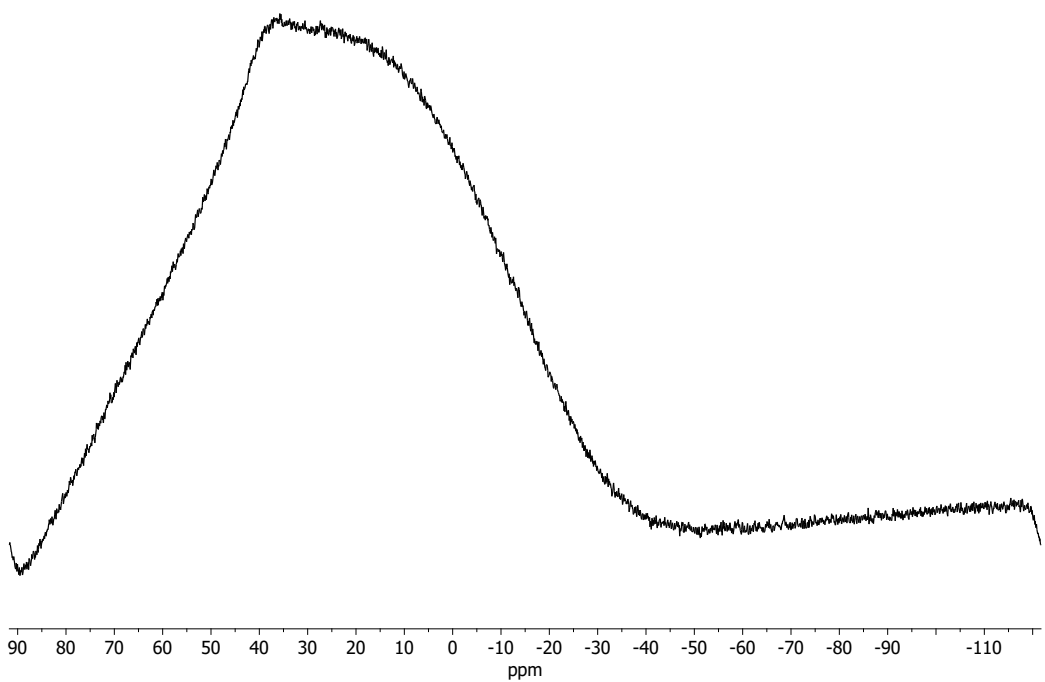


Fig. SI32: $^{11}\text{B}\{^1\text{H}\}$ NMR (160 MHz, CDCl_3) spectrum of $\text{BNCDI}^{\text{Dip}}$.

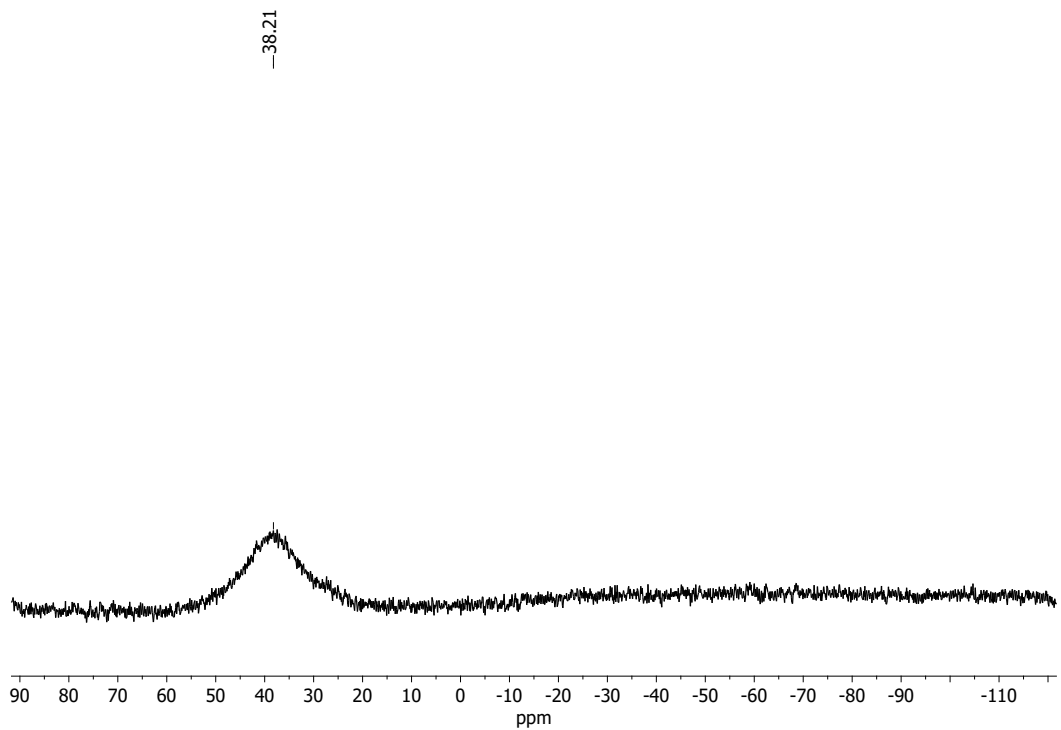


Fig. SI33: $^{11}\text{B}\{^1\text{H}\}$ NMR (160 MHz, CDCl_3) differential spectrum of CDCl_3 and $\text{BNCDI}^{\text{Dip}}$.

UV/Vis Absorption, Fluorescence and Excitation Spectra

UV/Vis spectra were recorded on a Perkin Elmer Lambda 14 spectrometer at 20 °C using a quartz cuvette with a length of 1 cm.

The UV-Vis emission and excitation spectra measurements were recorded on a FL 920 Edinburgh Instrument and they were corrected for the response of the photomultiplier. Quantum yields were calculated relative to fluorescein ($\phi = 0.90$ in NaOH 0.1 N). The excitation wavelength was 460 nm in all cases.

BNCDI^{Cy}

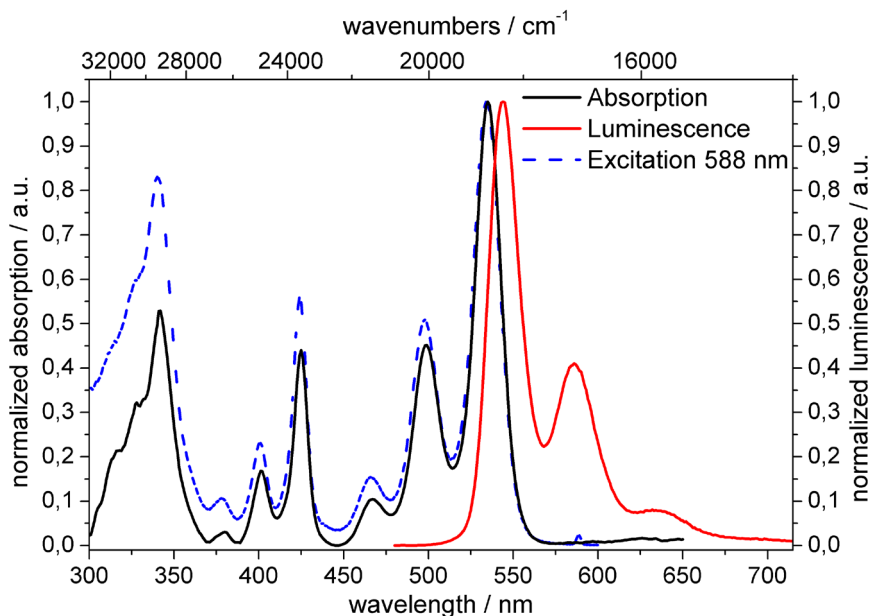


Fig. SI34: Absorption/Emission/Excitation spectra of BNCDI^{Cy} in dichloromethane (10^{-6} M).

BNCDI^{Dip}

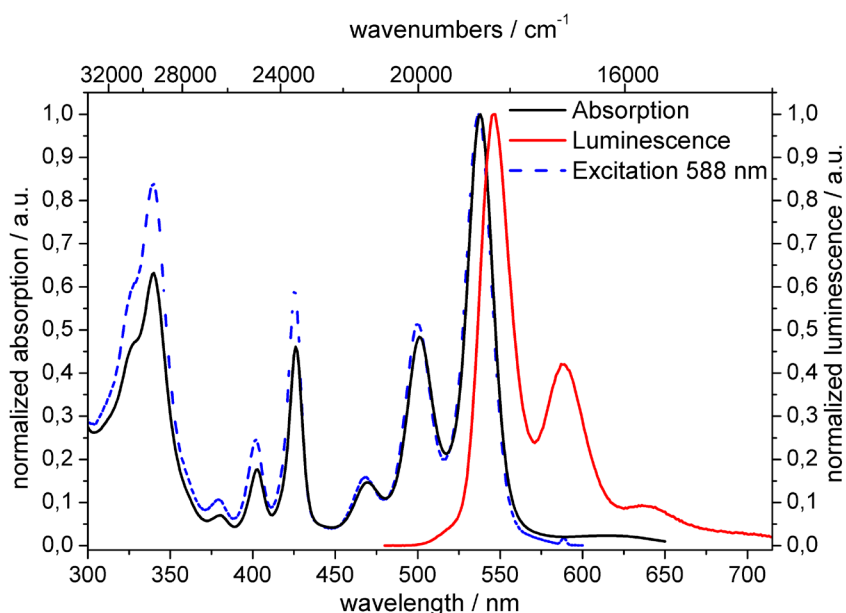


Fig. SI35: Absorption/Emission/Excitation spectra of BNCDI^{Dip} in dichloromethane (10^{-6} M).

Studies of the Chromophores in PMMA

Microscopic images von PMMA/**BNCDI** blends were obtained with a Zeiss Axio Imager 2 with LD/ED Epiplan – NEOFLUAR 50 x and LD Epiolan 20x. Both **BNCDIs** were dissolved with PMMA in dichloromethane and drop casted on a glass substrate.

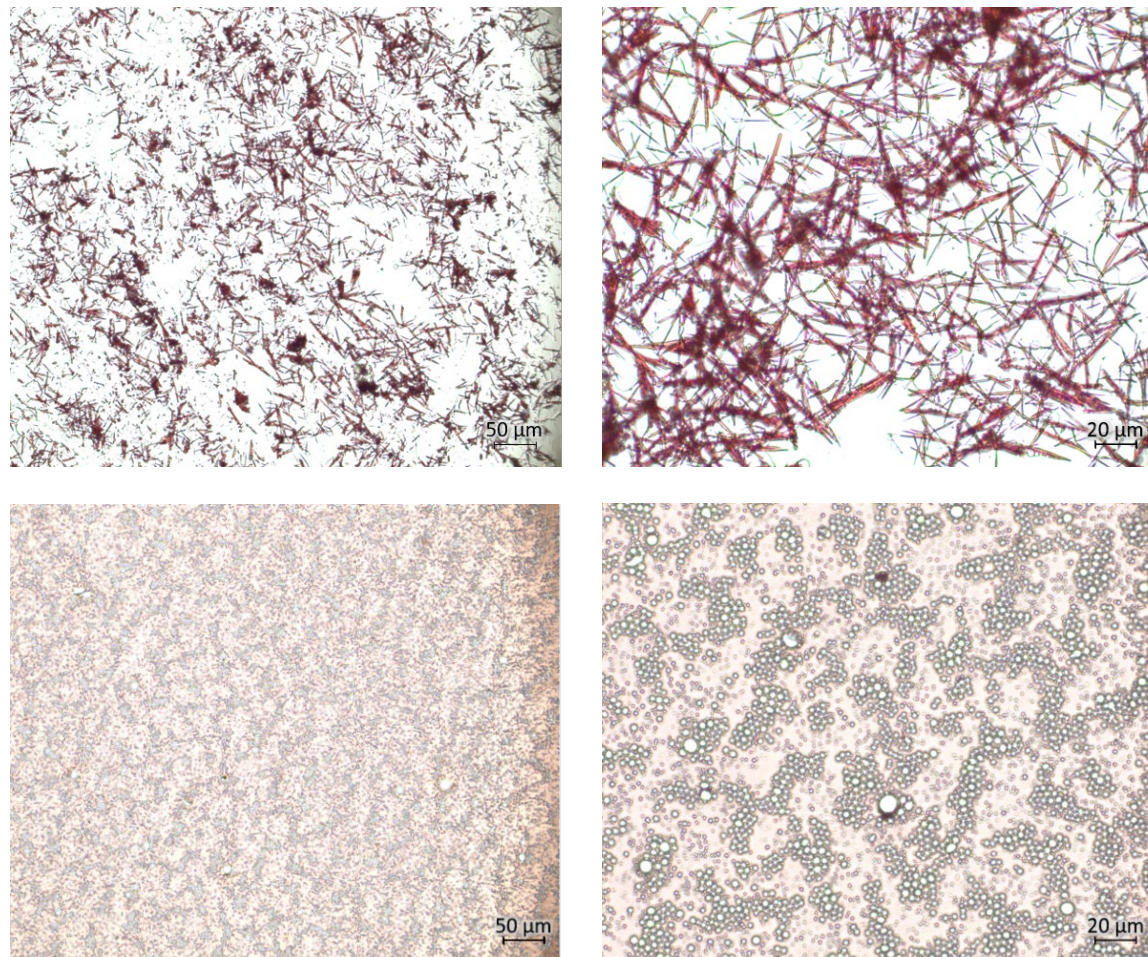


Fig. SI36: Microscopic images of **BNCDI**^{Cy} (upper row) and **BNCDI**^{Dip} (bottom row) in a PMMA blend (50%) with different magnifications. Some bubbles may arise from the evaporation of DCM as they were clearly visible by the high profile of the measured samples. They could not be removed by drying in a vacuum chamber.

Luminescence at Low Temperature

Low temperature measurements were performed with a cryostat (Oxford Instruments) set-up using *isopentane* as a solvent and the same luminescence machine as mentioned above. Solutions of the respective compound were prepared in *isopentane* (Acros Organics, reagent grade), filled in a one-piece Quartz cuvette (1 cm) and capped with a septum. The sample was cooled to 77 K and warmed by a controlled heating system.

To investigate the temperature-dependent emission behavior of the novel **BNCDIs**, they were analyzed in *isopentane* which forms a glassy state when frozen (113 K). The luminescence of both **BNCDIs** was completely quenched at 150 K, where *isopentane* was still in the liquid state (Fig. SI37).

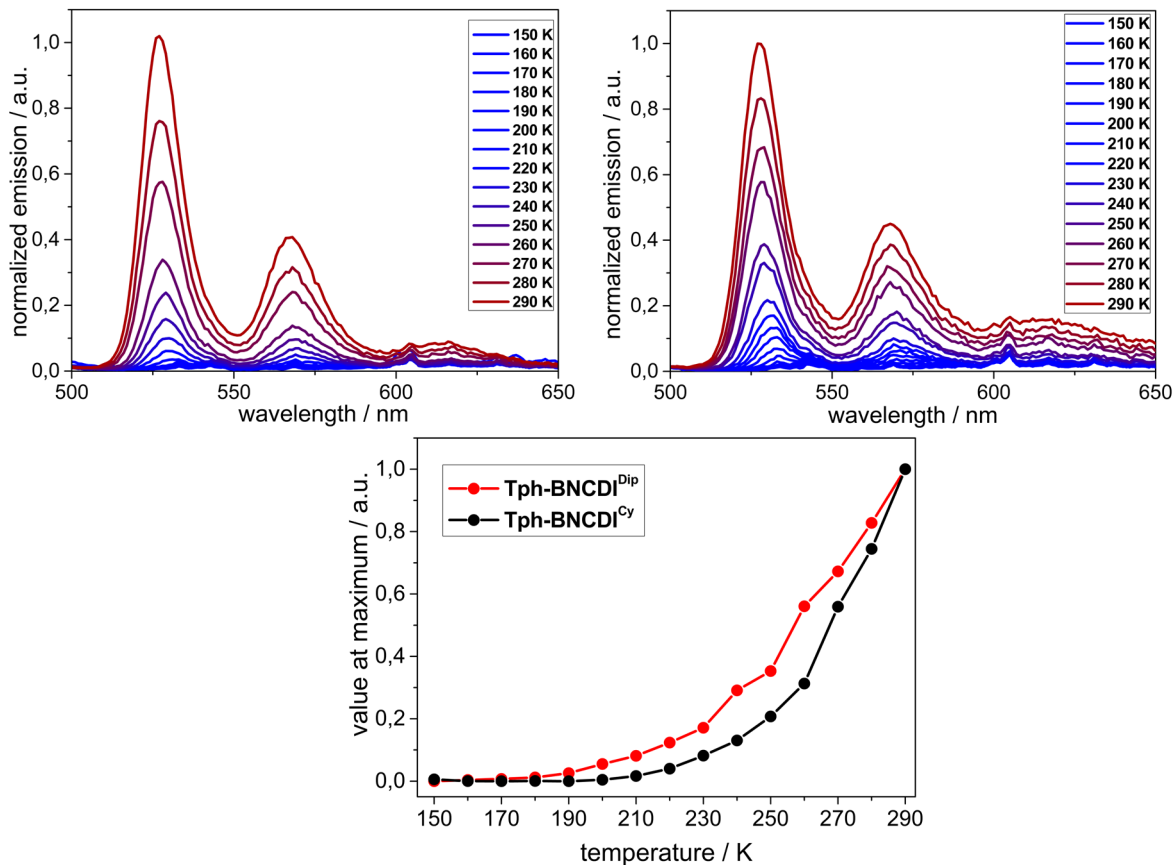


Fig. SI37: Emission spectra of **BNCDI^{Cy}** (top, left) and **BNCDI^{Dip}** (top, right) in *isopentane* (5.3×10^{-6} M) upon heating from 150 K to 290 K. Comparison luminescence maxima of **BNCDI^{Cy}** (black) and **BNCDI^{Dip}** (red).

In the same experimental settings, the respective PDI^s were investigated (Fig. SI38).

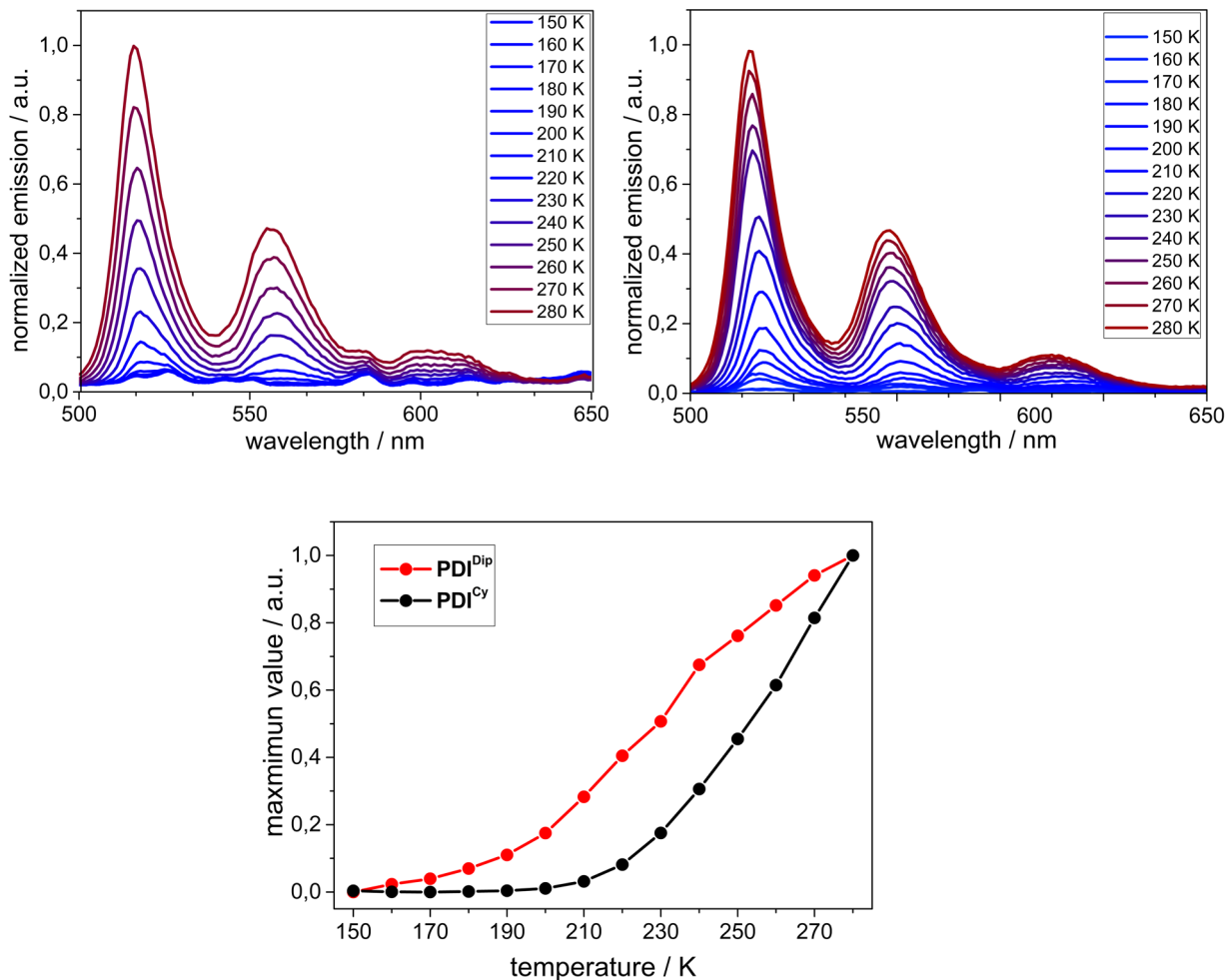


Fig. SI38: Emission spectra of PDI^{Cy} (top, left) and PDI^{Dip} (top, right) in isopentane (5.3×10^{-6} M) upon heating from 150 K to 280 K. Comparison luminescence maxima of PDI^{Cy} (black) and PDI^{Dip} (red).

Electrochemistry

The electrochemical studies were carried out under argon using an Eco Chemie Autolab PGSTAT 30 potentiostat for cyclic voltammetry. A three-electrode configuration was used: the working electrode was a platinum disk, the reference electrode was a saturated calomel electrode and the counter-electrode a platinum wire. All potentials were internally referenced to the ferrocene/ferrocenium couple. For the measurements, concentrations of 10^{-3} M of the electroactive species were used in a 0.2 M solution of tetrabutylammonium hexafluorophosphate in degassed DCM. The scanning rate was 200 mV/s. Non-reversible waves were corrected against Fc/Fc^+ potential, whereas reversible reduction waves were corrected against $E_{1/2p}$ from ferrocene. Absolute HOMO/LUMO levels were calculated according to $E_{\text{LUMO}} = -4.8 \text{ eV} - E_{\text{red}}$ and $E_{\text{HOMO}} = -4.8 \text{ eV} - E_{\text{ox}}.$ ¹¹

BNCDI^{Cy} Oxidation

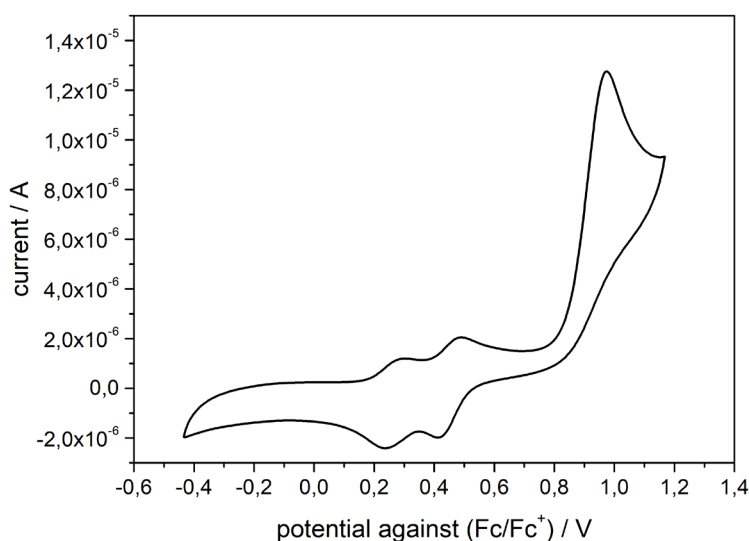


Fig. SI39: Oxidation of BNCDI^{Cy} corrected against ferrocene/ferrocenium.

BNCDI^{Cy} Reduction

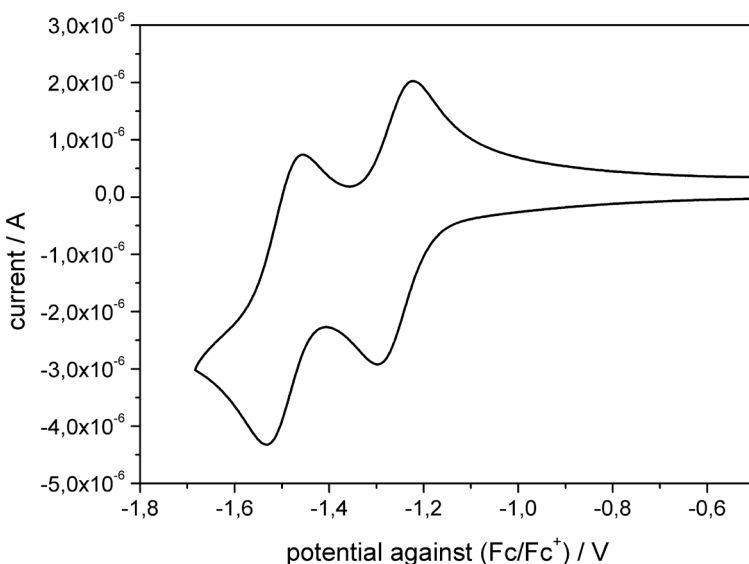


Fig. SI40: Reduction of BNCDI^{Cy} corrected against ferrocene/ferrocenium.

BNCDI^{Dip} Oxidation

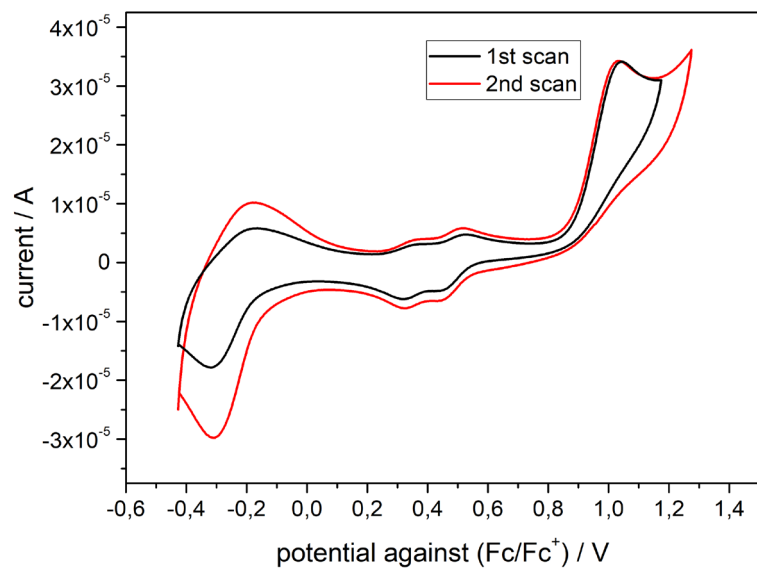


Fig. SI41: Oxidation of BNCDI^{Dip} corrected against ferrocene/ferrocenium.

BNCDI^{Dip} Reduction

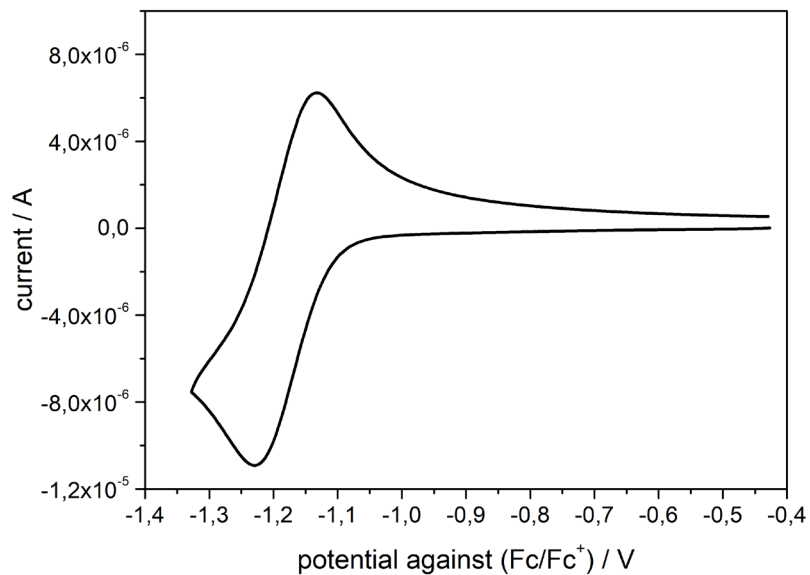


Fig. SI42: Reduction of BNCDI^{Dip} corrected against ferrocene/ferrocenium.

BNCDI^{Dip} Reduction 2

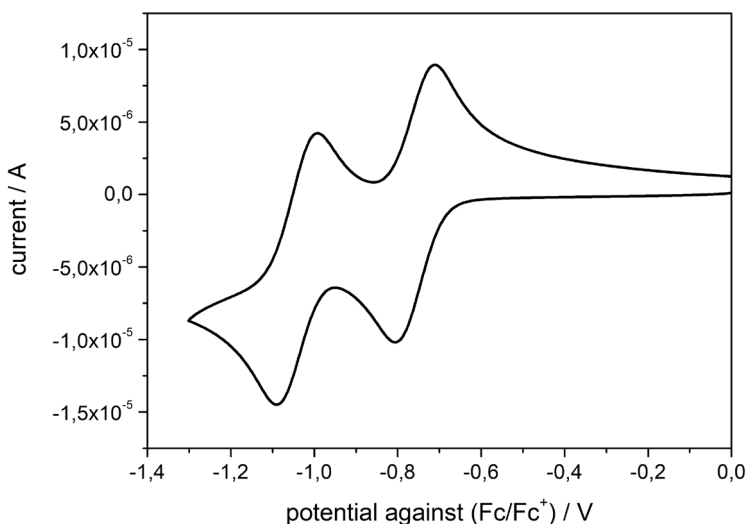


Fig. SI43: Reduction of **BNCDI^{Dip}** corrected against ferrocene/ferrocenium.

Thermoanalysis (TGA and DSC)

For thermal analysis, a Mettler Toledo DSC 3+ and a DSC/TGA 3+ with 40 µL aluminum crucibles were used. For TGA experiments, no lids were used, whereas in DSC experiments pierced lids were used. TGA was performed with a nitrogen flow of 20 mL/min and a heating rate of 10 K/min. The DSC was performed with the same settings.

Thermogravimetric analysis (TGA)

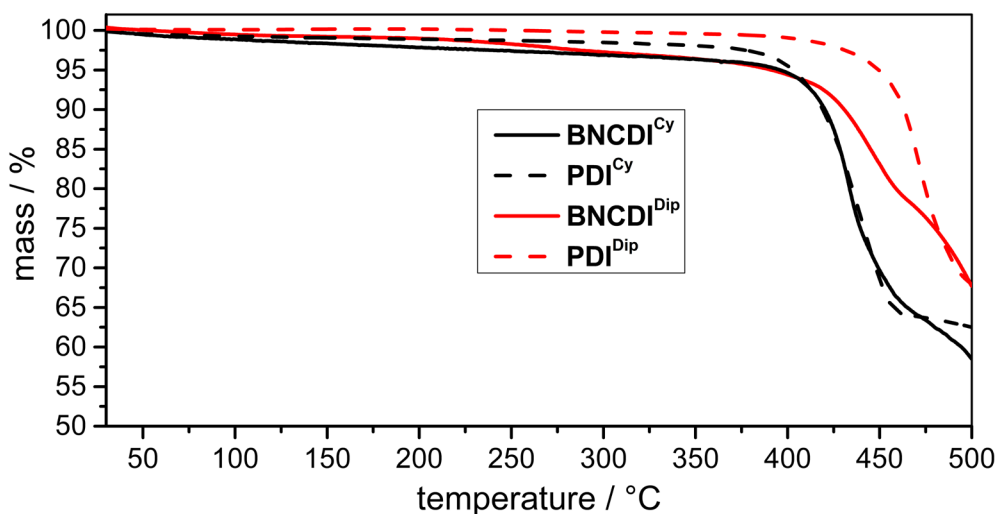


Fig. SI44: Thermogravimetric analysis of compounds **PDI^{Cy}**, **BNCDI^{Cy}**, **PDI^{Dip}** and **BNCDI^{Dip}** at 10 K/min with 20 mL/min nitrogen gas flow.

Dynamics Scanning Calorimetry (DSC)

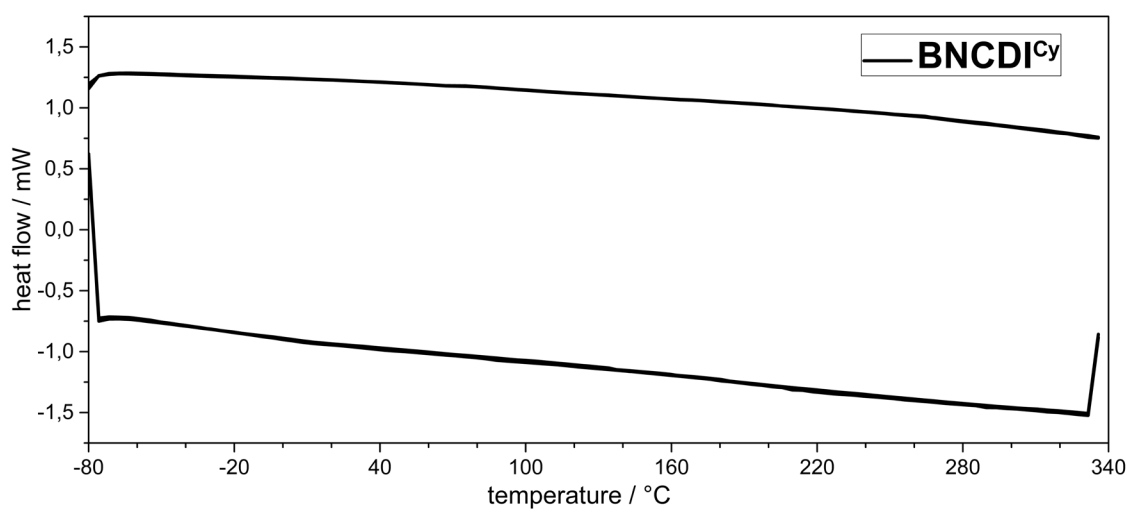


Fig. SI45: Dynamic scanning analysis of BNCDI^{Cy} at 10 K/min with 20 mL/min nitrogen gas flow.

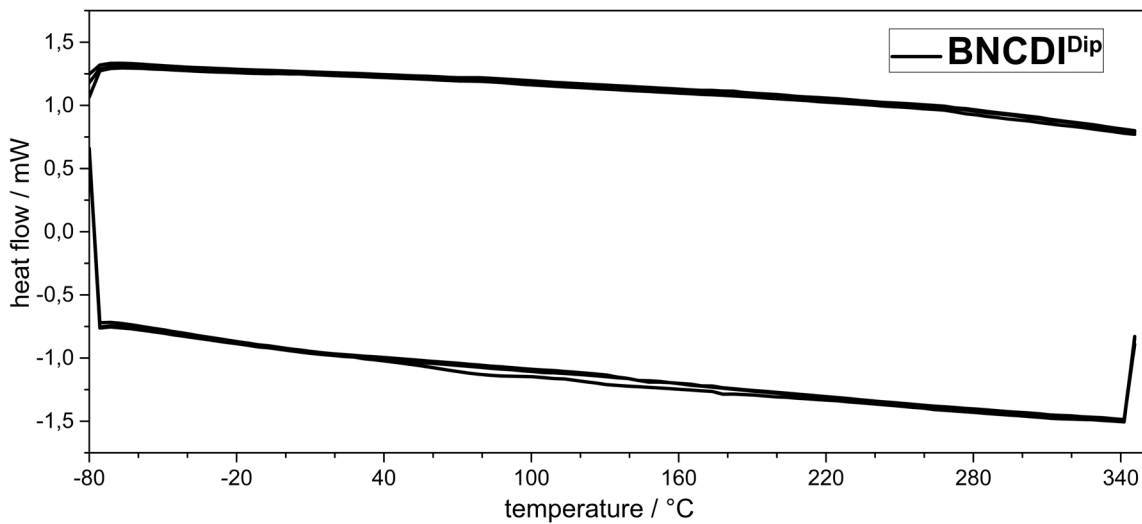


Fig. SI46: Dynamic scanning analysis of BNCDI^{Dip} at 10 K/min with 20 mL/min nitrogen gas flow.

Devices

OFET Fabrication and Characterization

Initially, glass substrates were cleaned with acetone and rinsed with ethanol. A 150 nm thick layer of aluminum was then deposited by thermal evaporation. This layer was wet etched to define gate electrodes. A 420 nm thick layer of SU-8 photoresist (from Microchem) was spin-coated and then exposed to UV light to define gate insulating layer (see MicroChem Su-8 2000 Permanent Epoxy Negative Photoresist Processing Guidelines for Su-8 2000.5, Su-8 2002, So-8 2005, Su-8 2007, Su-8 2010 and Su-8 2015- http://www.microchem.com/pdf/SU-82000DataSheet2000_5thru2015Ver4.pdf). Next, a 40 nm thick gold film was thermally evaporated and then wet etched to form source and drain electrodes. Finally, the active layer was deposited by thermal evaporation under a high vacuum of 2×10^{-7} mbar. The substrate temperature was kept constant ($T_{\text{sub}} = 30^\circ\text{C}$), deposition rate and layer thickness were fixed to 0.1 Å/s and 30 nm respectively.

The devices were stored and characterized in a glove box under nitrogen ambient. All electrical characterizations were performed using Keithley 2636A. Transfer characteristics I_D - V_{GS} were plotted at room temperature. All the measurements were made in the same conditions, the gate source voltage V_{GS} is varied from 40 V to -10 V with a 0.5 V step, at constant drain-source voltage V_{DS} . As usual, equations for MOSFETs have been used in linear regime. The drain current I_D in linear regime ($V_{DS} \ll V_{GS}-V_{TH}$) is given by:

$$I_D = \frac{W}{L} \mu_{FE} C_{ins} (V_{GS} - V_{TH}) V_{DS} \quad (\text{Eq. 1})$$

Here W and L are width and length of the channel (in μm), μ_{FE} is the field effect mobility (in cm²/Vs), C_{ins} is the capacitance of the gate insulator per area unit (in F/cm²), V_{TH} is the threshold voltage (in V) and V_{DS} is the drain source voltage (in V).

The threshold voltage V_{TH} can be determined by a linear extrapolation on the gate voltage axis of the transfer characteristic IDS-VGS at constant V_{DS} . The field effect mobility can be calculated from the slope $W \mu C_{ins} V_{DS} / L$ of this linear extrapolation. The switch from the off to the on state is quantified by the subthreshold swing S that is the inverse of the maximum slope of the transfer characteristics plotted in semi-logarithmic plot.

BNCDI^{Cy} has been incorporated into OFET structure as semiconducting layer in a Bottom-Gate Bottom-Contact Structure. Transfer characteristics have been measured in linear and saturated regime (i.e. $V_{DS} = 20$ V and $V_{DS} = 50$ V) and are shown (Fig. SI47).

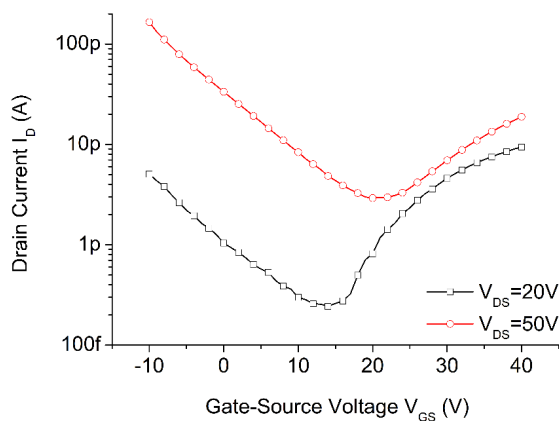


Fig. SI47: Transfer characteristics in linear and saturated regime of n-type OFET based on **BNCDI^{Cy}**.

Linear field effect mobility has been extracted and estimated to $\mu_{FE_lin}=1.02 \times 10^{-8} \text{ cm}^2/\text{V.s}$. The classical electrical parameters of OFET have been evaluated as following: threshold voltage $V_{TH} = 20.6 \text{ V}$, $I_{ON}/I_{OFF} = 36$ and Subthreshold slope $SS = 8.4 \text{ V/dec}$ for $V_{DS} = 20 \text{ V}$. In saturated regime, field effect mobility has been estimated to $\mu_{FE_sat} = 4.34 \times 10^{-8} \text{ cm}^2/\text{V s}$. The OFET has been measured as an n-type OFET with an electron accumulation behaviour in the channel for $V_{GS} > 0 \text{ V}$ and $V_{DS} > 0 \text{ V}$. No free holes accumulation has been observed for $V_{GS} < 0 \text{ V}$ and $V_{DS} < 0 \text{ V}$. On the transfer characteristics, an increase of the leakage current $I_{D OFF}$ is observed for negative gate-source voltage (Fig. SI48). As no hole accumulation has been detected in P-type configuration, this current behaviour comes from fixed traps into the semiconductor structure.

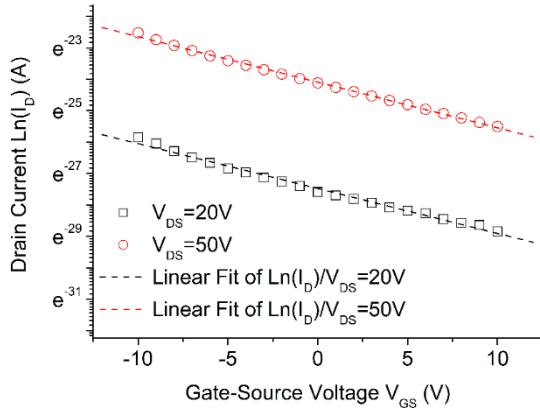


Fig. SI48: Leakage drain current according to Drain-Source voltage and Gate-Source voltage.

The leakage current $I_{D OFF}$ is V_{DS} dependant. This statement is obvious because Drain-Source voltage V_{DS} control the charges injection from source to drain. This current is also Gate-source voltage dependant. In the case of fixed traps, the energy provided by the gate electric field allows the charges to be emitted from these traps and then evacuated to the drain. The Fig. SI49 shows the leakage drain current dependence with Gate-Source voltage. The linear fit indicates clearly that the average energy needed for electron to be emitted from these traps are similar for $V_{DS} = 20 \text{ V}$ ad $V_{DS} = 50\text{V}$. This average energy has been estimated to $E_t = 0.143 \text{ eV}$.

The devices were annealed at different temperatures to reorganize semiconducting layer. Electrical performances were improved until an optimized baking temperature of 150°C . When this temperature was increased, electrical performances degraded. At 200°C , **BNCDI^{CY}** lost its semiconducting properties and no current modulation was observed. For the optimized temperature of 150°C , linear field effect mobility is $\mu_{FE_lin}=2.68 \times 10^{-8} \text{ cm/V.s}$. Comparison of transfer characteristics with and without annealing is shown in Fig. SI49a.

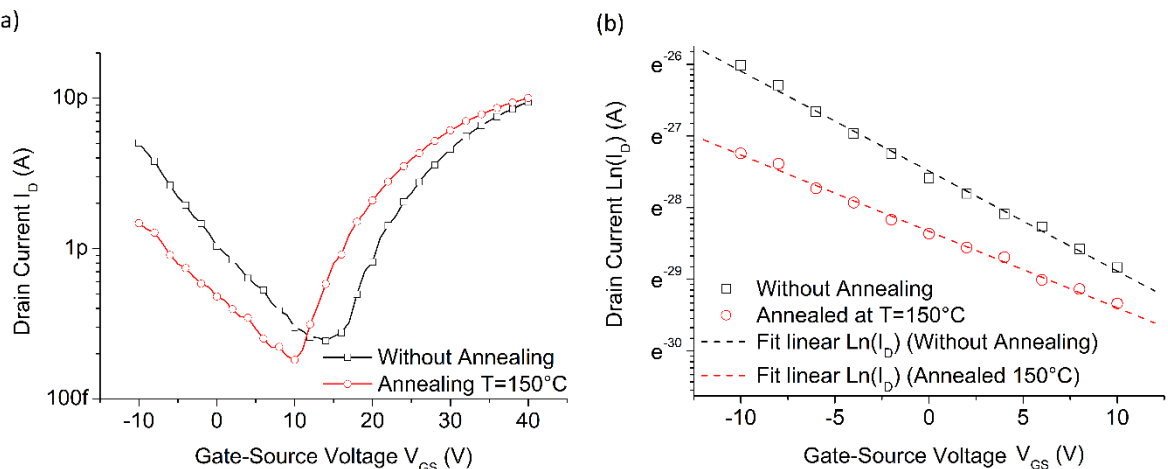


Fig. SI49: (a) Transfer characteristics with and without annealing for $V_{DS}=20\text{V}$. (b) Drain leakage current in \ln representation according to Gate-Source voltage V_{GS} .

In Fig. SI49b, we represent the drain leakage current. It can be seen that the baking treatment improves the structural organization of **BNCDI^{CY}** when analysing the Gate-Source voltage dependence of this leakage current. The drain leakage current is still activated with the Gate-Source electric field with an average energy estimated to be 0.102 eV. The reorganization of semiconducting layer decreases the defect density leading to an increase of linear field effect mobility, a decrease of threshold voltage V_{TH} , a decrease of I_{DOFF} current but without any effect on subthreshold slope. This latter observation indicates no change in the interface insulator/semiconductor. The threshold voltage shift of 5 V indicates an easier formation of the electron channel. Thus, temperature has an effect on the structural organization of **BNCDI^{CY}**.

The electrical conductivity σ of the film without gate electric field was measured to evaluate charges transport mechanisms of **BNCDI^{CY}** (Fig. SI50a). Using the Mott-Gurney relationship for SCLC charges transport, the carrier mobility (electron only) is $\mu_e = 3.42 \times 10^{-6} \text{ cm}^2/\text{V s}$ and free electron density was $n = 1.75 \times 10^{13} \text{ cm}^{-3}$. Both the low carrier mobility and low free electron density could explain the low field effect mobility observed in OFET structure. The carrier mobility using SCLC model does not take account of defect density because mobility is extracted in the free-defect regime ($J \propto V^2$). Moreover, the low free carrier density limits strongly the creation of conductive channel in an OFET structure.

Without the gate electric field, the conductivity of the film is not constant. Organic semiconductors are known as disordered semiconductors. Then Poole-Frenkel effect has been identified to explain the voltage dependence of conductivity. When the conductivity is plotted according to the square root of electric field between the two electrodes, the barrier lowering effect known as Poole-Frenkel effect is detected. Structural defects in molecule lead to energetic traps that limit the electrical conduction and induce the Gate-Source dependence seen in OFET characteristics. In Fig. SI50b, a linear dependence of $\ln(J/E)$ with $E^{1/2}$ was observed. Thus, the injection of electron through the semiconductor is electric field dependant according to lowering barrier effect known as Poole-Frenkel Effect. This barrier energy has been estimated to $\beta = 7.62 \times 10^{-3} \text{ eV}$. Thus, electrical conductivity $\sigma_0 = 9.4 \times 10^{-12} \text{ S cm}^{-1}$ has been calculated. Knowing the estimated free electron density and the elementary charge, carrier mobility using Poole-Frenkel model is $\mu_e = 3.41 \times 10^{-6} \text{ cm}^2/\text{V*s}$. This value is similar to the one obtained with SCLC

model.

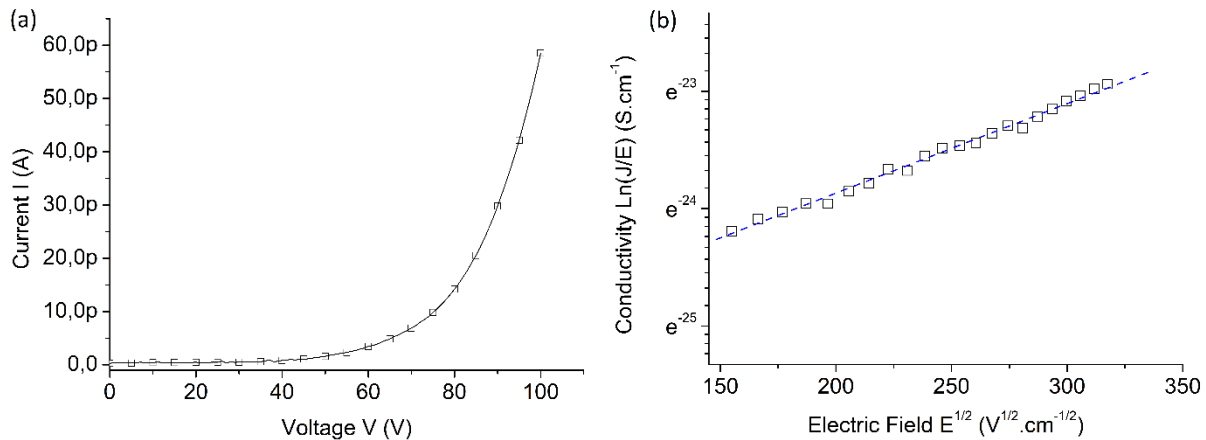


Fig. SI50: (a) Current-Voltage characteristics of **BNCDI^{CY}**. (b) Linear dependence of $\ln(J/E)$ with $E^{1/2}$.

OLED Fabrication

Multilayered electroluminescent (EL) devices have been fabricated onto patterned ITO coated glass substrates from Xin Yang Technology (90 nm thick and sheet resistance below $20 \Omega/\text{sq}$). Prior to organic layer deposition, the ITO substrates were carefully cleaned by common techniques. The organic materials (from Aldrich and Syntec) are deposited onto the ITO anode by sublimation under high vacuum ($1\text{-}5 \times 10^{-7} \text{ mbar}$) (at a rate of $0.2\text{--}0.3 \text{ nm/s}$). All devices share following basic structure: copper phthalocyanine (CuPc) is used as the hole injection layer (HIL), N,N' -diphenyl-N,N'-bis(1-naphthylphenyl)-1,10 -biphenyl-4,40 -diamine (α -NPB) and Tris(4-carbazoyl-9-ylphenyl)amine (TcTa) as hole transporting layers (HTL) and 1,3,5-tris(N-phenylbenzimidazole-2-yl)benzene (TPBi) as the electron transport layer (ETL). Specifically, the devices set-up is as the following: 10 nm of CuPc/40 nm of α -NPB/ 10 nm of TcTa/ 20 nm of emitting layer/50 nm of TPBi/1.2 nm of LiF and 100 nm of aluminum as the cathode. The emitting layer is a guest/host system with the compounds used as a dopant in 4,4'-bis(N-carbozyl)-1,1'biphenyl (CBP) (devices **A-B**) or 4,4'-bis(2,2-diphenylethenyl)-1,1'biphenyl (DPVBi) matrix devices (**C-J**). The guest/host layer is obtained by thermal co-evaporation of the two materials and the doping rate is controlled by tuning the evaporation rate of each material. The active area of the devices defined by the overlap between the ITO anode and the metallic cathode was 0.3 cm^2 . The current-voltage-luminance (I-V-L) characteristics of the devices were measured with a regulated power supply (Laboratory Power Supply EA-PS 3032-10B) combined with a multimeter and a 1 cm^2 area silicon calibrated photodiode (Hamamatsu). The spectral emission was recorded with a SpectraScan PR650 spectrophotometer. All the measurements were performed at room temperature and at ambient atmosphere, with no further encapsulation of devices.

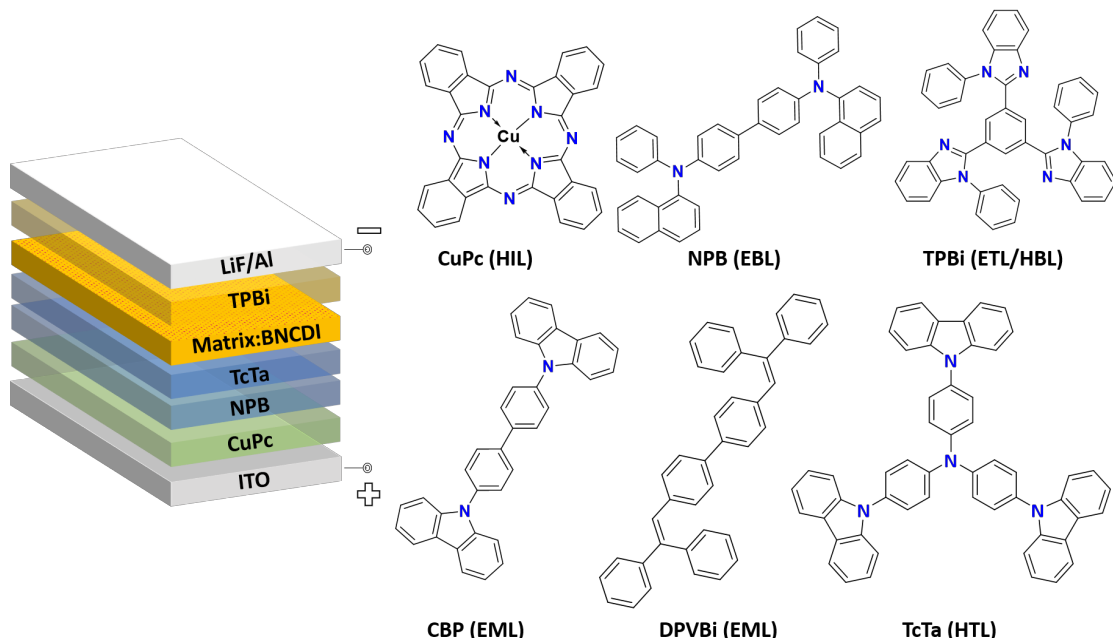


Fig. S151: Multistack OLED with its components.

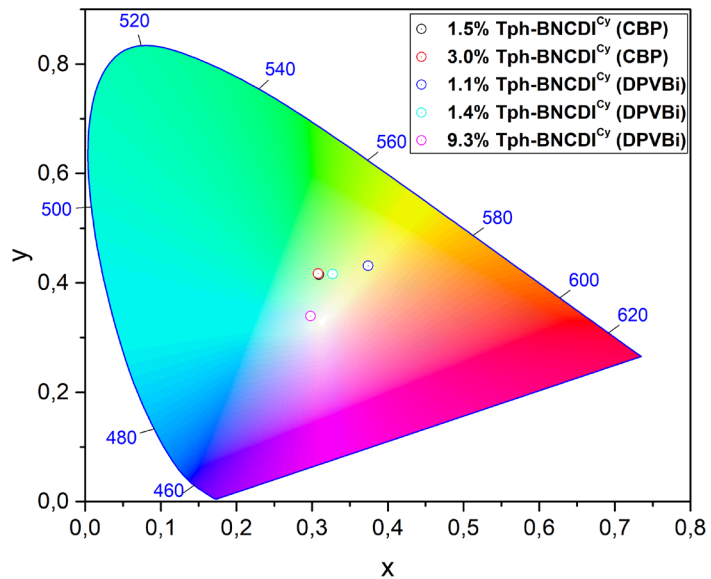


Fig. SI52: CIE chart of devices A-E.

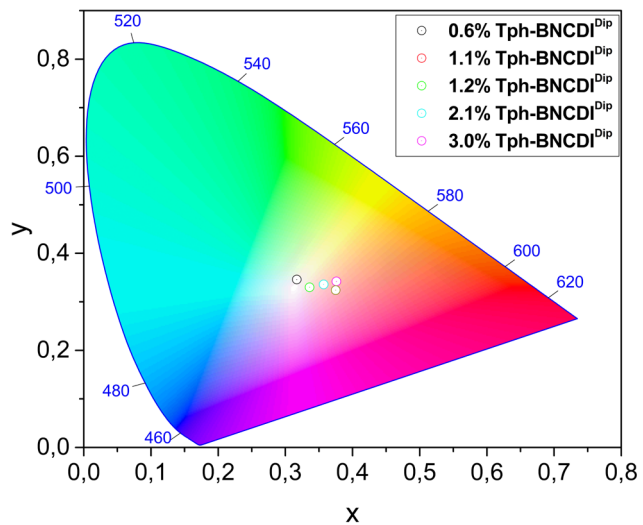


Fig. SI53: CIE chart of devices F-J.

Quantum Chemical Calculations

The equilibrium geometries were optimized with Gaussian 09¹² using B3LYP/6-31-G* level of theory with empirical dispersion correction (GD3), followed by a frequency calculation to ensure that the optimized structures were the true minima. The orbital energies of HOMO and LUMO and their energy differences were calculated for these optimized molecules.

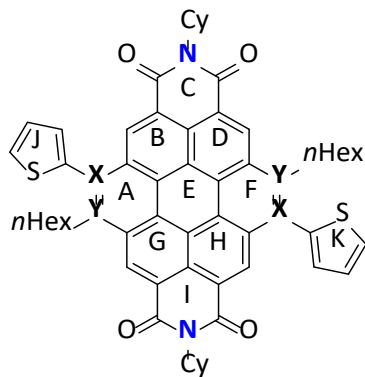
Results

Tab. 4 Overview of the calculation results.

compound	E _{LUMO} / eV	E _{HOMO} / eV	ΔE / eV
BNCDI^{Cy}	-3.06	-5.69	2.63
CDI^{Cy}	-2.91	-5.97	3.06
BNCDI^{Dip}	-3.15	-5.79	2.64
CDI^{Dip}	-2.99	-6.05	3.06

Nuclear independent chemical shift calculations

To compare the aromaticity of the **BNCDI^{Cy}** with its all carbon congener **CDI^{Cy}** were estimated by NICS¹³⁻¹⁵ calculations (CSGT-B3LYP/6-31-G*). The NICS values were determined 1 Å above the center of the respective ring and in plane (0 Å). In general the NICS(0) values correspond to the σ-π contribution to aromaticity and NICS(1) corresponds to the π-π contribution to aromaticity of respective system.



Tab. 5: NICS(0) and NICS(1) values of **BNCDI^{Cy}** and **CDI^{Cy}**.

ring	X,Y = C		X = B, Y = N	
	NICS(0)	NICS(1)	NICS(0)	NICS(1)
A	-8.68	-11.09	-3.25	-6.01
B	-9.89	-12.09	-9.53	-11.53
C	5.77	1.46	5.07	0.82
D	-9.89	-12.16	-8.24	-11.26
E	-1.18	-5.39	0.96	-3.34
F	-8.47	-10.95	-3.52	-6.26
G	-9.89	-12.09	-8.24	-13.23
H	-9.89	-12.09	-9.53	-11.53
I	5.77	1.46	5.07	0.82
J	-10.81	-8.21	-11.46	-9.08
K	-10.76	-8.94	-11.46	-9.16

BNCDI^{Cy}

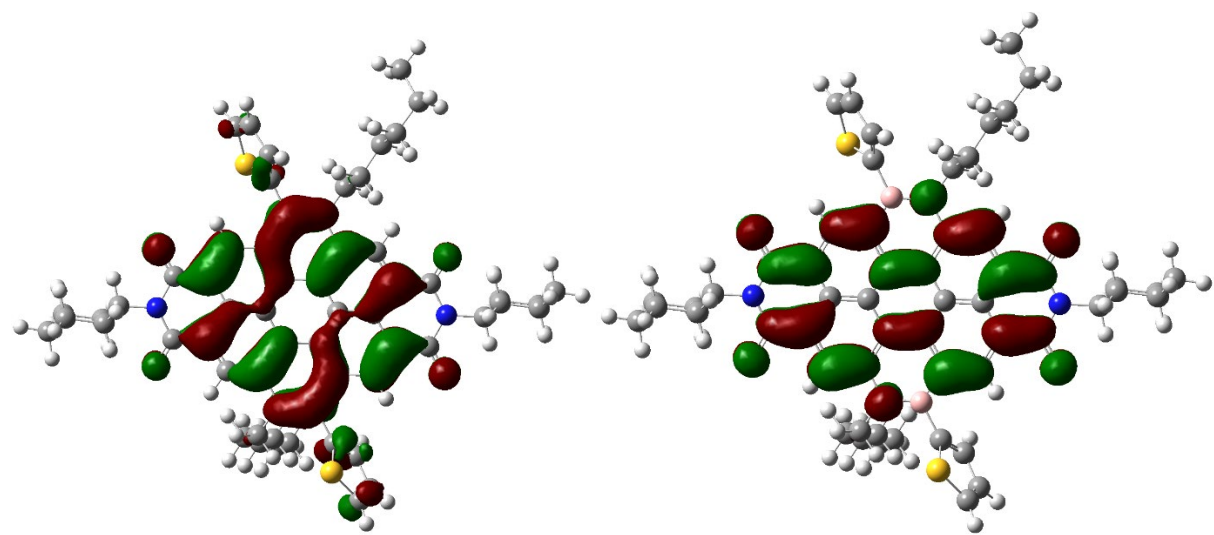


Fig. S154: Wave function for the HOMO (left) and LUMO (right) of BNCDI^{Cy} at a isovalue of 0.02.

Symmetry = C1

B3LYP/6-31G(d)

E=-3535.38972007 Ha

TAG	SYMBOL	X	Y	Z
1	C	-3.9244740	0.1120340	-0.5516430
2	C	-2.8859110	-0.8143410	-0.3226880
3	C	-1.5474210	-0.3506860	-0.2674060
4	C	-1.2615260	1.0369840	-0.4449610
5	C	-2.3265490	1.9552620	-0.6602160
6	C	-3.6486110	1.4537760	-0.7129000
7	C	-0.5071670	-1.3032120	-0.0251100
8	C	0.1066760	1.4740850	-0.4007280
9	C	1.1477090	0.5205100	-0.1663350
10	C	0.8602390	-0.8642420	0.0290130
11	C	2.4881940	0.9808280	-0.1317180
12	C	2.7889970	2.3488230	-0.3345140
13	C	1.7687700	3.2491360	-0.5705690
14	C	0.4152160	2.8397600	-0.6003460
15	B	-0.7306300	3.8363690	-0.8421290
16	N	-2.0688880	3.3203630	-0.8242700
17	C	-5.3420290	-0.3346240	-0.6197600
18	H	-4.4962800	2.1006550	-0.8863530
19	C	4.1925910	2.8253560	-0.2953770
20	H	2.0234550	4.2903670	-0.7328450
21	C	-3.1839840	-2.1883740	-0.1588790
22	C	-2.1638750	-3.0901830	0.0711330
23	C	-0.8150310	-2.6720890	0.1550120
24	C	-4.5843510	-2.6700540	-0.2370420
25	H	-2.4175770	-4.1379580	0.1859200

26	B	0.3272400	-3.6614670	0.4293000
27	N	1.6589760	-3.1329180	0.4866850
28	C	1.9238830	-1.7778240	0.2705220
29	C	3.5268810	0.0553190	0.1005110
30	C	4.9470400	0.4967360	0.1329150
31	C	3.2485290	-1.2812730	0.2966710
32	H	4.0970650	-1.9287080	0.4638920
33	N	5.1996010	1.8603620	-0.0563310
34	N	-5.5916850	-1.7032520	-0.4664280
35	C	2.7965660	-4.0275960	0.7938920
36	C	-3.2285640	4.2439750	-0.8432120
37	O	5.8557380	-0.3055980	0.3204120
38	O	4.4750520	4.0047660	-0.4584540
39	O	-6.2509190	0.4680760	-0.8035130
40	O	-4.8636870	-3.8542910	-0.1086910
41	C	-3.8626750	4.4458170	0.5426250
42	H	-3.9675180	3.8926220	-1.5692350
43	H	-2.8680260	5.2030310	-1.2086050
44	C	-2.8894480	5.0084590	1.5845000
45	H	-4.2881190	3.5047630	0.9121160
46	H	-4.7069590	5.1367100	0.4135490
47	C	-3.5485750	5.2608110	2.9443240
48	H	-2.4470540	5.9403720	1.2073840
49	H	-2.0531110	4.3079000	1.7158820
50	C	-2.5704680	5.8009350	3.9944370
51	H	-3.9978780	4.3264500	3.3126430
52	H	-4.3801620	5.9706810	2.8223910
53	C	-3.2311840	6.0559990	5.3525960
54	H	-2.1195510	6.7319650	3.6223450
55	H	-1.7420610	5.0882670	4.1155660
56	H	-4.0405500	6.7913460	5.2651870
57	H	-3.6652590	5.1339190	5.7586810
58	C	3.5710690	-4.4855540	-0.4463520
59	H	2.3851970	-4.9011380	1.3000260
60	H	3.4607810	-3.5333350	1.5097520
61	C	4.7238440	-5.4250480	-0.0762930
62	H	3.9559650	-3.6207270	-1.0006220
63	H	2.8747920	-4.9988610	-1.1210360
64	C	5.4983580	-5.9284860	-1.3010560
65	H	4.3200540	-6.2756390	0.4890340
66	H	5.4171500	-4.9041830	0.6009280
67	C	6.7058830	-6.8167290	-0.9614390
68	H	5.8438920	-5.0613940	-1.8813770
69	H	4.8127320	-6.4846220	-1.9579190
70	C	6.3375600	-8.1388830	-0.2774970
71	H	7.3988020	-6.2526240	-0.3210020
72	H	7.2540060	-7.0329230	-1.8881000
73	H	5.8725540	-7.9754790	0.7009930
74	H	7.2249990	-8.7620540	-0.1194810
75	H	5.6302970	-8.7133250	-0.8893050
76	C	6.6054400	2.3534120	-0.0070130
77	C	7.2486350	2.1458820	1.3740760

78	C	7.4682310	1.7850680	-1.1458340
79	H	6.5083760	3.4279840	-0.1695110
80	C	8.6520420	2.7733890	1.3965320
81	H	7.3189650	1.0764180	1.5915330
82	H	6.6110840	2.6009840	2.1424660
83	C	8.8706350	2.4145850	-1.1024690
84	H	7.5455020	0.6990160	-1.0421100
85	H	6.9818890	1.9941820	-2.1068920
86	C	9.5316280	2.2108190	0.2692730
87	H	9.1207590	2.5977290	2.3727320
88	H	8.5678960	3.8639210	1.2788990
89	H	9.4940000	1.9851420	-1.8964670
90	H	8.7941210	3.4922510	-1.3095980
91	H	10.5217390	2.6834970	0.2878310
92	H	9.6889560	1.1354850	0.4373920
93	C	-6.9950190	-2.1999110	-0.5429270
94	C	-7.8720490	-1.6592750	0.5985200
95	C	-7.6245070	-1.9646570	-1.9259200
96	H	-6.8956970	-3.2774090	-0.4027460
97	C	-9.2710910	-2.2934450	0.5268720
98	H	-7.9529840	-0.5715750	0.5170850
99	H	-7.3951000	-1.8868750	1.5601110
100	C	-9.0248400	-2.5973720	-1.9767860
101	H	-7.6967710	-0.8909270	-2.1206070
102	H	-6.9770000	-2.4003320	-2.6971860
103	C	-9.9188010	-2.0631350	-0.8470760
104	H	-9.9046100	-1.8837010	1.3232670
105	H	-9.1920700	-3.3749790	0.7117290
106	H	-9.4839490	-2.4026090	-2.9538970
107	H	-8.9369450	-3.6898110	-1.8818170
108	H	-10.9064110	-2.5397990	-0.8860220
109	H	-10.0795010	-0.9851660	-0.9936930
110	C	0.0647060	-5.1914840	0.6628350
111	C	0.3774950	-6.2759570	-0.1269540
112	S	-0.7882750	-5.7429400	2.0909940
113	C	-0.0517140	-7.5312800	0.4002620
114	H	0.8922020	-6.1766730	-1.0771280
115	C	-0.6927000	-7.4034880	1.6017450
116	H	0.1084260	-8.4827660	-0.0955030
117	H	-1.1115150	-8.1832220	2.2244980
118	C	-0.4223840	5.3569730	-1.0813130
119	C	0.1769840	6.2461490	-0.2171450
120	S	-0.7073600	6.1490710	-2.6195880
121	C	0.3897530	7.5481900	-0.7642440
122	H	0.4567380	5.9713580	0.7950490
123	C	-0.0354680	7.6476950	-2.0597130
124	H	0.8453350	8.3671920	-0.2181990
125	H	0.0183530	8.5037550	-2.7196380
126	H	-2.5106410	6.4373290	6.0850460

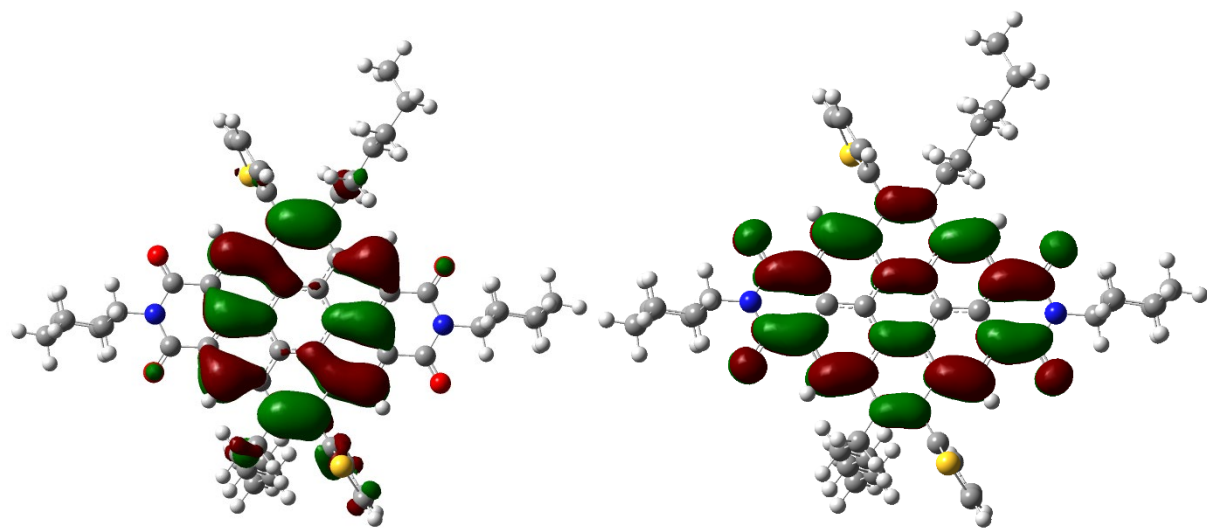
CDI^{Cy}

Fig. S155: Wave function for the HOMO (left) and LUMO (right) of **CDI^{Cy}** at an isovalue of 0.02.

Symmetry = C1

B3LYP/6-31G(d)

E=-3528.49902578 Ha

TAG	SYMBOL	X	Y	Z
1	C	3.8685890	-0.1350270	-0.5566390
2	C	2.8375820	0.7954330	-0.2850010
3	C	1.4992210	0.3504740	-0.2161210
4	C	1.2037390	-1.0305680	-0.4171330
5	C	2.2478860	-1.9642530	-0.6749750
6	C	3.5783580	-1.4702160	-0.7460880
7	C	0.4616940	1.2910870	0.0528890
8	C	-0.1483080	-1.4660370	-0.3622020
9	C	-1.1870990	-0.5229740	-0.1054890
10	C	-0.8899650	0.8550930	0.1103740
11	C	-2.5291840	-0.9607370	-0.0689730
12	C	-2.8290090	-2.3280590	-0.2851180
13	C	-1.8210310	-3.2373570	-0.5319980
14	C	-0.4596810	-2.8360460	-0.5745810
15	C	5.2836430	0.3157020	-0.6392950
16	H	4.4100380	-2.1295330	-0.9572400
17	C	-4.2372330	-2.7999800	-0.2429550
18	H	-2.0892400	-4.2750700	-0.6888880
19	C	3.1353640	2.1672910	-0.0934360
20	C	2.1290370	3.0737110	0.1690840
21	C	0.7729150	2.6627630	0.2563040
22	C	4.5390200	2.6464540	-0.1804210
23	H	2.3937250	4.1159190	0.3017270
24	C	-1.9342610	1.7872780	0.3741890
25	C	-3.5629170	-0.0260060	0.1795930
26	C	-4.9825410	-0.4682530	0.2104810
27	C	-3.2701510	1.3045740	0.3953360

28	H	-4.1029420	1.9718980	0.5776380
29	N	-5.2370040	-1.8338010	0.0097950
30	N	5.5366010	1.6835840	-0.4528450
31	C	-2.7168950	4.1665420	0.8871240
32	C	3.0609380	-4.3522570	-1.0617250
33	O	-5.8925210	0.3286090	0.4066950
34	O	-4.5222250	-3.9769900	-0.4169980
35	O	6.1914700	-0.4768050	-0.8608820
36	O	4.8218840	3.8264320	-0.0239490
37	C	3.8545480	-4.6570910	0.2315830
38	H	3.7516580	-3.9751880	-1.8253940
39	H	2.6590660	-5.2904000	-1.4509700
40	C	3.0274420	-5.3462760	1.3208310
41	H	4.2812830	-3.7309870	0.6369130
42	H	4.7061090	-5.2963660	-0.0378080
43	C	3.8300120	-5.6301640	2.5944340
44	H	2.6176050	-6.2859070	0.9262410
45	H	2.1605150	-4.7187270	1.5718300
46	C	3.0045840	-6.3231800	3.6849740
47	H	4.2349740	-4.6865350	2.9894890
48	H	4.7017140	-6.2544270	2.3471110
49	C	3.8086240	-6.6035300	4.9581900
50	H	2.6014680	-7.2660310	3.2880620
51	H	2.1333120	-5.6985130	3.9299160
52	H	4.6683630	-7.2513970	4.7466230
53	H	4.1954260	-5.6732570	5.3922680
54	C	-3.3848330	4.6884770	-0.4005440
55	H	-2.3092300	5.0188690	1.4374020
56	H	-3.4777910	3.7190620	1.5367330
57	C	-4.4881750	5.7110960	-0.1129190
58	H	-3.7949800	3.8467840	-0.9747030
59	H	-2.6127870	5.1468320	-1.0324740
60	C	-5.1327290	6.2672010	-1.3892220
61	H	-4.0625570	6.5306590	0.4814700
62	H	-5.2641010	5.2460510	0.5135140
63	C	-6.2932360	7.2434090	-1.1392110
64	H	-5.4982010	5.4267280	-1.9962600
65	H	-4.3611980	6.7683990	-1.9929470
66	C	-5.8831210	8.5329550	-0.4179170
67	H	-7.0750800	6.7322750	-0.5593580
68	H	-6.7491660	7.5019750	-2.1043510
69	H	-5.5149360	8.3327250	0.5943370
70	H	-6.7303000	9.2225050	-0.3294200
71	H	-5.0851370	9.0516880	-0.9645480
72	C	-6.6445970	-2.3237100	0.0603140
73	C	-7.2835850	-2.1249350	1.4446570
74	C	-7.5095280	-1.7461660	-1.0722360
75	H	-6.5511710	-3.3973750	-0.1097470
76	C	-8.6874650	-2.7515570	1.4662220
77	H	-7.3526220	-1.0571090	1.6699070
78	H	-6.6444390	-2.5859880	2.2081720
79	C	-8.9123600	-2.3748350	-1.0296520

80	H	-7.5854800	-0.6608800	-0.9605970
81	H	-7.0258960	-1.9489230	-2.0360460
82	C	-9.5695250	-2.1802780	0.3452690
83	H	-9.1534440	-2.5823370	2.4448480
84	H	-8.6046100	-3.8413290	1.3407030
85	H	-9.5374110	-1.9391630	-1.8188980
86	H	-8.8373260	-3.4510950	-1.2446390
87	H	-10.5599690	-2.6522890	0.3630950
88	H	-9.7254910	-1.1060650	0.5214060
89	C	6.9404960	2.1792550	-0.5364510
90	C	7.8313960	1.6086190	0.5792930
91	C	7.5521850	1.9790960	-1.9329500
92	H	6.8460100	3.2530240	-0.3676560
93	C	9.2293910	2.2450140	0.5067990
94	H	7.9111560	0.5235210	0.4680150
95	H	7.3666030	1.8106040	1.5525010
96	C	8.9519150	2.6133830	-1.9848940
97	H	7.6222100	0.9108640	-2.1559130
98	H	6.8951880	2.4341310	-2.6848160
99	C	9.8599840	2.0505110	-0.8805860
100	H	9.8727370	1.8151630	1.2844590
101	H	9.1523920	3.3214250	0.7203320
102	H	9.3986630	2.4438940	-2.9723770
103	H	8.8654360	3.7030180	-1.8606890
104	H	10.8469480	2.5284930	-0.9195680
105	H	10.0189610	0.9767740	-1.0569000
106	C	0.0567410	5.0156100	0.7518890
107	C	0.0708860	6.0374140	-0.1620280
108	S	0.5527890	5.5962590	2.3286380
109	C	0.4710330	7.2922420	0.3929970
110	H	-0.1909290	5.8889500	-1.2039740
111	C	0.7610070	7.2113820	1.7260870
112	H	0.5419580	8.2102870	-0.1799110
113	H	1.0878650	8.0012560	2.3895700
114	C	0.2348450	-5.1901890	-1.0524300
115	C	-0.0537430	-6.1642620	-0.1319410
116	S	0.0164300	-5.8018320	-2.6795580
117	C	-0.4334560	-7.4098440	-0.7204770
118	H	0.0085910	-5.9909300	0.9362730
119	C	-0.4398790	-7.3685830	-2.0866700
120	H	-0.6919050	-8.2935170	-0.1474420
121	H	-0.6872560	-8.1618770	-2.7798010
122	H	3.1961890	-7.0988250	5.7203090
123	C	0.6075480	-3.7724240	-0.8220860
124	C	1.9323960	-3.3591850	-0.8639870
125	C	-1.6117300	3.1713890	0.6093100
126	C	-0.2908000	3.5900190	0.5367330

BNCDI^{Dip}

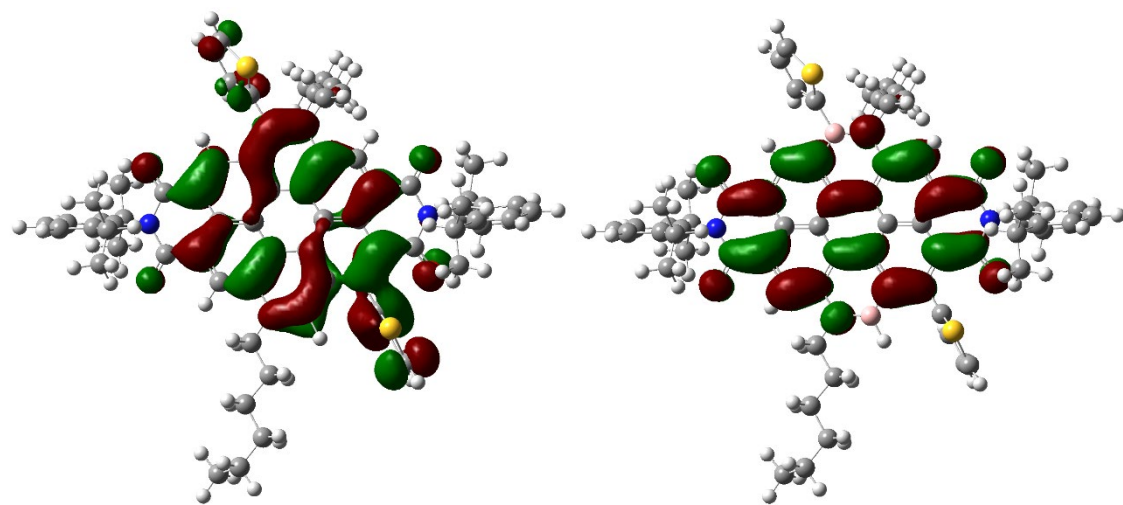


Fig. SI56: Wave function for the HOMO (left) and LUMO (right) of BNCDI^{Dip} at an isovalue of 0.02.

Symmetry = C1

B3LYP/6-31G(d)

E=-3999.90527690 Ha

TAG	SYMBOL	X	Y	Z
1	C	-3.3661990	1.4064180	-0.5184590
2	C	-2.7321480	0.1661210	-0.2648850
3	C	-1.3122530	0.1323480	-0.2665020
4	C	-0.5539860	1.3271870	-0.4723920
5	C	-1.2239320	2.5630240	-0.6843040
6	C	-2.6350820	2.5560810	-0.7221990
7	C	-0.6664540	-1.1258330	-0.0542160
8	C	0.8817890	1.2559800	-0.4537650
9	C	1.5272520	-0.0033950	-0.2391740
10	C	0.7732680	-1.2010410	-0.0513300
11	C	2.9463390	-0.0407980	-0.2240370
12	C	3.7009830	1.1428070	-0.4243570
13	C	3.0559840	2.3415790	-0.6470550
14	C	1.6448370	2.4288910	-0.6605870
15	B	0.9230310	3.7662630	-0.8916890
16	N	-0.5099390	3.7509320	-0.8616040
17	C	-4.8429580	1.5172340	-0.5859280
18	H	-3.2046180	3.4532740	-0.9160920
19	C	5.1815250	1.1049410	-0.3985240
20	H	3.6564050	3.2293110	-0.8112910
21	C	-3.5010660	-1.0083920	-0.0194050
22	C	-2.8545550	-2.2288290	0.1846220
23	C	-1.4268030	-2.2973780	0.1493460
24	C	-4.9869720	-0.8953040	0.0533100
25	B	-0.6838300	-3.6323640	0.3012020
26	N	0.7387850	-3.6269390	0.2790700

27	C	1.4556870	-2.4369140	0.1310320
28	C	3.5966220	-1.2763780	-0.0148790
29	C	5.0791670	-1.3574130	0.0246380
30	C	2.8698160	-2.4359800	0.1537900
31	H	3.4392650	-3.3417560	0.3048840
32	N	5.7738370	-0.1523740	-0.1595960
33	N	-5.5530330	0.3488260	-0.3081760
34	C	1.5388970	-4.8720550	0.4010990
35	C	-1.2742330	5.0217630	-0.8732690
36	O	5.6786270	-2.4078590	0.2061790
37	O	5.8776850	2.0955510	-0.5617370
38	O	-5.4177840	2.5639280	-0.8539470
39	O	-5.7290940	-1.8016030	0.3910360
40	C	-1.7864850	5.4314080	0.5171690
41	H	-2.0946450	4.9529510	-1.5933720
42	H	-0.6029100	5.7937430	-1.2427620
43	C	-0.6706220	5.6034150	1.5537310
44	H	-2.5204730	4.7053800	0.8879470
45	H	-2.3268120	6.3798820	0.3941740
46	C	-1.1866910	6.0823860	2.9145460
47	H	0.0789420	6.3092170	1.1713360
48	H	-0.1454420	4.6470610	1.6860340
49	C	-0.0728200	6.2374030	3.9567740
50	H	-1.9411360	5.3751740	3.2903740
51	H	-1.7064810	7.0440850	2.7913550
52	C	-0.5881200	6.7198980	5.3161520
53	H	0.6813220	6.9410220	3.5762870
54	H	0.4433700	5.2743010	4.0787010
55	H	-1.0800790	7.6963460	5.2269300
56	H	0.2264150	6.8207810	6.0423470
57	H	-1.3216040	6.0174910	5.7310510
58	C	0.7569430	-6.1804270	0.4908480
59	H	2.1762690	-4.7838650	1.2901320
60	H	2.2086780	-4.9281840	-0.4660150
61	C	1.7154770	-7.3777240	0.5634770
62	H	0.0998540	-6.2890190	-0.3797240
63	H	0.1074360	-6.1765770	1.3737220
64	C	0.9691550	-8.7132280	0.6829700
65	H	2.3944270	-7.2511060	1.4176470
66	H	2.3514510	-7.3974040	-0.3340970
67	C	1.8790190	-9.9511160	0.6551440
68	H	0.2422420	-8.7859470	-0.1382420
69	H	0.3808310	-8.7151090	1.6125430
70	C	2.8504130	-10.0427210	1.8383070
71	H	2.4466330	-9.9602160	-0.2864360
72	H	1.2476000	-10.8494410	0.6394660
73	H	3.5700260	-9.2164130	1.8392530
74	H	3.4231770	-10.9764270	1.8073250
75	H	2.3097150	-10.0136920	2.7929000
76	C	7.2207670	-0.2032660	-0.1033860
77	C	7.9295860	-0.5223040	-1.2706950
78	C	7.8541860	0.0722610	1.1177610

79	C	9.3256310	-0.5690410	-1.1893710
80	C	9.2519530	0.0228050	1.1488700
81	C	9.9827410	-0.2977810	0.0077450
82	H	9.9031700	-0.8185960	-2.0749600
83	H	9.7728030	0.2392890	2.0772660
84	H	11.0681550	-0.3346180	0.0512840
85	C	-7.0003560	0.4201360	-0.3445530
86	C	-7.6610290	-0.0107250	-1.5053450
87	C	-7.6817620	0.9074330	0.7800980
88	C	-9.0582790	0.0597940	-1.5190960
89	C	-9.0778120	0.9716600	0.7150770
90	C	-9.7618230	0.5505290	-0.4222040
91	H	-9.6002240	-0.2763000	-2.3984130
92	H	-9.6341510	1.3530160	1.5667770
93	H	-10.8470860	0.6022180	-0.4528390
94	C	-6.9076280	-0.5754090	-2.7018720
95	H	-5.8375400	-0.4092590	-2.5395800
96	C	-6.9506000	1.3635010	2.0343870
97	H	-5.8837170	1.1571970	1.9016900
98	C	-7.4056040	0.5695520	3.2715180
99	H	-8.4630760	0.7479200	3.4982060
100	H	-7.2698010	-0.5054800	3.1117870
101	H	-6.8227630	0.8673090	4.1514180
102	C	-7.1005250	2.8825990	2.2337680
103	H	-6.7342970	3.4199320	1.3533190
104	H	-8.1502540	3.1578920	2.3907770
105	H	-6.5316760	3.2140460	3.1111390
106	C	-7.2775700	0.1452020	-4.0096640
107	H	-8.3285390	-0.0143130	-4.2767700
108	H	-7.1113890	1.2244160	-3.9224710
109	H	-6.6663560	-0.2337040	-4.8372470
110	C	-7.1242940	-2.0974060	-2.8061520
111	H	-6.8141130	-2.5964270	-1.8830390
112	H	-8.1816710	-2.3288990	-2.9829740
113	H	-6.5434720	-2.5121940	-3.6390100
114	C	7.0707050	0.4410140	2.3694440
115	H	6.0045760	0.3209810	2.1518130
116	C	7.2268370	-0.8185710	-2.5873600
117	H	6.1523290	-0.6691690	-2.4415920
118	C	7.4294620	-2.2881160	-2.9991390
119	H	8.4887810	-2.5059300	-3.1802260
120	H	7.0735290	-2.9589770	-2.2105220
121	H	6.8793580	-2.5081430	-3.9221210
122	C	7.6685410	0.1575800	-3.6918820
123	H	7.4940850	1.1939700	-3.3836400
124	H	8.7344440	0.0474710	-3.9230250
125	H	7.1067590	-0.0299010	-4.6147050
126	C	7.2976690	1.9199070	2.7348190
127	H	8.3497130	2.1061560	2.9820310
128	H	7.0251310	2.5680540	1.8958560
129	H	6.6927640	2.1987140	3.6063220
130	C	7.3953710	-0.4975750	3.5444160

131	H	7.2152570	-1.5422270	3.2686320
132	H	8.4417090	-0.4060240	3.8580230
133	H	6.7683460	-0.2541950	4.4104140
134	H	-1.2531840	-4.6589560	0.4211410
135	C	-3.6036490	-3.4870110	0.4179270
136	C	-3.8391900	-4.1229820	1.6054350
137	S	-4.2335160	-4.4120600	-0.9209960
138	C	-4.5485050	-5.3536500	1.4530810
139	H	-3.5246780	-3.7145320	2.5594840
140	C	-4.8289590	-5.6452150	0.1479020
141	H	-4.8351640	-5.9911840	2.2825370
142	H	-5.3472960	-6.5067860	-0.2517730
143	C	1.7442750	5.0824830	-1.1282870
144	C	2.6221030	5.6967630	-0.2627640
145	S	1.7506460	5.9354360	-2.6602860
146	C	3.2779340	6.8441420	-0.8038540
147	H	2.7910120	5.3331720	0.7460300
148	C	2.9098480	7.0965880	-2.0960630
149	H	3.9953140	7.4458330	-0.2563810
150	H	3.2593570	7.8834870	-2.7516930

CDI^{Dip}

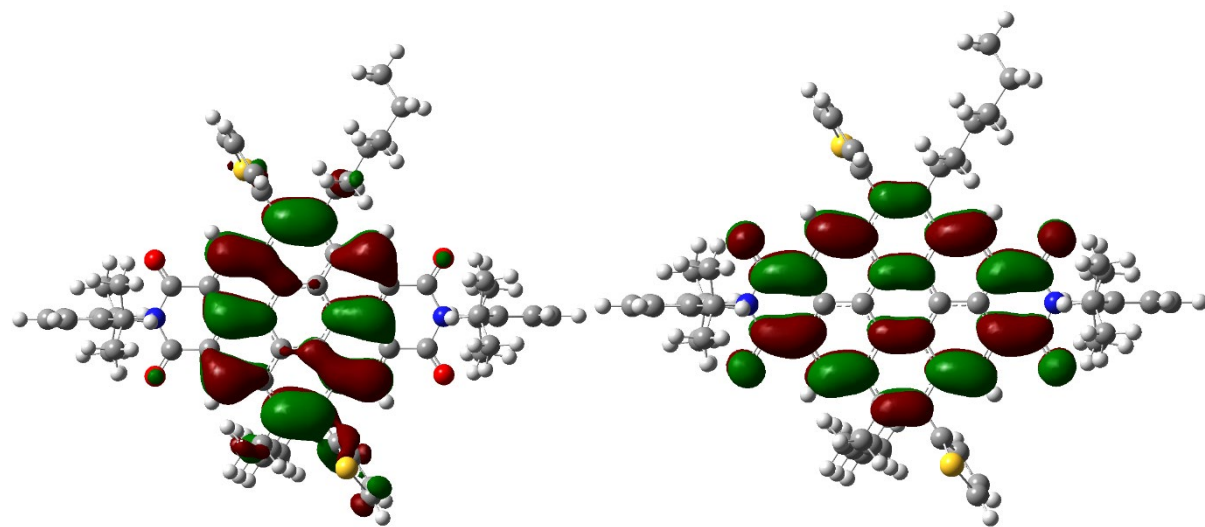


Fig. SI57: Wave function for the HOMO (left) and LUMO (right) of **CDI^{Dip}** at an isovalue of 0.02.

Symmetry = C1

B3LYP/6-31G(d)

E=-3993.04202776 Ha

TAG	SYMBOL	X	Y	Z
1	C	3.6923630	-1.0988380	-0.5678910
2	C	2.9407060	0.0575710	-0.2402860
3	C	1.5320690	-0.0298100	-0.1713850
4	C	0.8879220	-1.2773420	-0.4273220
5	C	1.6531920	-2.4385520	-0.7365310
6	C	3.0654660	-2.3032100	-0.8074270
7	C	0.7719370	1.1336900	0.1518340
8	C	-0.5311540	-1.3507120	-0.3755890
9	C	-1.2918540	-0.1844040	-0.0628190
10	C	-0.6467310	1.0583180	0.2113920
11	C	-2.7024450	-0.2613140	-0.0306600
12	C	-3.3427460	-1.4939740	-0.3190760
13	C	-2.6034510	-2.6186420	-0.6187370
14	C	-1.1846830	-2.5830020	-0.6474740
15	C	5.1723820	-1.0277150	-0.6563310
16	H	3.6977690	-3.1449500	-1.0588600
17	C	-4.8241160	-1.5858600	-0.3033510
18	H	-3.1321340	-3.5404880	-0.8292280
19	C	3.5796180	1.3004580	0.0067800
20	C	2.8409600	2.4220950	0.3186290
21	C	1.4253220	2.3700070	0.4065140
22	C	5.0578980	1.4074340	-0.0743530
23	C	-1.4123370	2.2162570	0.5323350
24	C	-3.4556210	0.8980430	0.2847270
25	C	-4.9384000	0.8396800	0.3173070
26	C	-2.8269030	2.0937710	0.5599430
27	H	-3.4583890	2.9422560	0.7917160

28	N	-5.5224080	-0.4046560	0.0175190
29	N	5.7546260	0.2277430	-0.4029380
30	C	-1.5577880	4.6948400	1.1367140
31	C	1.8234270	-4.9423490	-1.2004320
32	O	-5.6343930	1.8089870	0.5812850
33	O	-5.4285670	-2.6184620	-0.5483820
34	O	5.8679160	-1.9949340	-0.9285330
35	O	5.6606310	2.4507500	0.1252690
36	C	2.4984870	-5.4773810	0.0855350
37	H	2.5950450	-4.7377660	-1.9521570
38	H	1.1948720	-5.7326610	-1.6167020
39	C	1.5093390	-5.9297390	1.1641770
40	H	3.1636110	-4.7125610	0.5061960
41	H	3.1407130	-6.3221760	-0.1973040
42	C	2.1972820	-6.4605440	2.4257910
43	H	0.8494870	-6.7042970	0.7504850
44	H	0.8559900	-5.0885210	1.4356670
45	C	1.2068890	-6.9039340	3.5092090
46	H	2.8604490	-5.6839020	2.8353570
47	H	2.8486840	-7.3063460	2.1599450
48	C	1.8951780	-7.4355440	4.7700630
49	H	0.5436750	-7.6777990	3.0968690
50	H	0.5581880	-6.0561370	3.7732010
51	H	2.5240170	-8.3041690	4.5388790
52	H	1.1654800	-7.7429020	5.5278480
53	H	2.5412070	-6.6704690	5.2182470
54	C	-2.1012050	5.3950840	-0.1249930
55	H	-0.9382440	5.4051680	1.6904860
56	H	-2.3920990	4.4359950	1.7989490
57	C	-2.9224340	6.6446980	0.2062280
58	H	-2.7115210	4.6913970	-0.7070140
59	H	-1.2523230	5.6695430	-0.7653110
60	C	-3.4578190	7.3535760	-1.0443630
61	H	-2.2985520	7.3329030	0.7921960
62	H	-3.7665690	6.3653940	0.8544330
63	C	-4.3385970	8.5781720	-0.7495480
64	H	-4.0373130	6.6322500	-1.6378060
65	H	-2.6107910	7.6603290	-1.6765480
66	C	-3.5972610	9.7333990	-0.0658270
67	H	-5.1894020	8.2679310	-0.1263060
68	H	-4.7678260	8.9383170	-1.6941240
69	H	-3.2258190	9.4496080	0.9251460
70	H	-4.2536940	10.6011350	0.0653100
71	H	-2.7347370	10.0542780	-0.6639770
72	C	-6.9701000	-0.4749000	0.0311680
73	C	-7.6707240	-0.1089860	-1.1278320
74	C	-7.6122160	-0.9040600	1.2023560
75	C	-9.0676190	-0.1773910	-1.0898880
76	C	-9.0097360	-0.9688120	1.1890220
77	C	-9.7328450	-0.6059710	0.0557570
78	H	-9.6394010	0.1083170	-1.9682150
79	H	-9.5361430	-1.3080600	2.0765930

80	H	-10.8184860	-0.6576110	0.0653880
81	C	7.1990260	0.3130480	-0.4842690
82	C	7.7816800	0.7120180	-1.6965170
83	C	7.9558440	-0.0088030	0.6520090
84	C	9.1774970	0.7908650	-1.7499310
85	C	9.3486800	0.0733990	0.5478560
86	C	9.9557160	0.4717520	-0.6402250
87	H	9.6589850	1.1068110	-2.6710220
88	H	9.9637140	-0.1771790	1.4075420
89	H	11.0391080	0.5342020	-0.7013790
90	C	6.9438660	1.0803530	-2.9124650
91	H	5.8990760	0.8371180	-2.6937920
92	C	7.3078930	-0.4533010	1.9554930
93	H	6.2224660	-0.3627430	1.8453820
94	C	7.7144170	0.4537670	3.1298960
95	H	8.7897680	0.3922780	3.3334310
96	H	7.4694410	1.4994340	2.9148570
97	H	7.1865220	0.1541200	4.0430190
98	C	7.6155440	-1.9353600	2.2385230
99	H	7.2860970	-2.5616490	1.4032630
100	H	8.6914130	-2.0934510	2.3798950
101	H	7.1040910	-2.2677270	3.1500940
102	C	7.3411540	0.2620120	-4.1530000
103	H	8.3666380	0.4815160	-4.4716070
104	H	7.2724290	-0.8118990	-3.9487000
105	H	6.6768300	0.4986370	-4.9925810
106	C	7.0144750	2.5963590	-3.1755900
107	H	6.6933010	3.1535400	-2.2897870
108	H	8.0384160	2.9040230	-3.4196100
109	H	6.3695350	2.8723180	-4.0187930
110	C	-6.8355740	-1.3182790	2.4439590
111	H	-5.7801640	-1.0758930	2.2823520
112	C	-6.9595750	0.3694360	-2.3857230
113	H	-5.8816890	0.2536670	-2.2333180
114	C	-7.2288280	1.8666290	-2.6255490
115	H	-8.2948870	2.0497090	-2.8059140
116	H	-6.9246390	2.4548570	-1.7538900
117	H	-6.6732780	2.2224010	-3.5017980
118	C	-7.3311210	-0.4852290	-3.6099820
119	H	-7.1142700	-1.5428430	-3.4253060
120	H	-8.3953110	-0.3956400	-3.8568650
121	H	-6.7591150	-0.1617080	-4.4876870
122	C	-6.9289200	-2.8412100	2.6543500
123	H	-7.9657160	-3.1477840	2.8378670
124	H	-6.5684470	-3.3722970	1.7677570
125	H	-6.3281960	-3.1490470	3.5189440
126	C	-7.2856410	-0.5368980	3.6903620
127	H	-7.2015820	0.5424680	3.5240930
128	H	-8.3260740	-0.7589380	3.9539850
129	H	-6.6625220	-0.8047130	4.5518840
130	C	-1.1260260	-5.0177970	-1.2104190
131	C	-1.6831870	-5.8950560	-0.3160620

132	S	-1.4702500	-5.5178850	-2.8536040
133	C	-2.3722980	-6.9815080	-0.9376120
134	H	-1.5985350	-5.7627890	0.7564770
135	C	-2.3419840	-6.9144960	-2.3024830
136	H	-2.8694350	-7.7734770	-0.3884260
137	H	-2.7805000	-7.5988360	-3.0168360
138	C	0.6388240	3.5288960	0.7349880
139	C	-0.7444180	3.4612100	0.8124740
140	C	0.9893710	-3.6968070	-0.9729630
141	C	-0.3971070	-3.7542940	-0.9381000
142	H	3.3666200	3.3539610	0.4904690
143	C	1.3435750	4.8089130	0.9882770
144	C	1.6115980	5.8218580	0.1040640
145	S	1.9893000	5.1898870	2.5716940
146	C	2.3293020	6.9114400	0.6873490
147	H	1.3096320	5.7806110	-0.9367720
148	C	2.6028190	6.7146130	2.0117910
149	H	2.6297630	7.7981090	0.1400310
150	H	3.1302320	7.3708450	2.6915830

Calculated Absorption Spectra

The UV/Vis spectra were calculated at the level of time-dependent density functional theory (TD-DFT) with the B3LYP/6-31-G*-level of theory with empirical dispersion correction (GD3) and TD = 40 states.

Tab. 6 Overview of the calculation results for the TD-DFT calculations.

compound	λ_{max}	Oscillator strength (f)	orbitals
BNCDI^{Cy}	514 nm	0.4354	HOMO->LUMO
	420 nm	0.0737	HOMO-4->LUMO HOMO-3->LUMO
	406 nm	0.1102	HOMO-4->LUMO HOMO-3->LUMO HOMO->LUMO+1 HOMO>LUMO+2
	327 nm	0.5860	HOMO-10->LUMO HOMO-9->LUMO HOMO-3->LUMO HOMO->LUMO+1 HOMO>LUMO+2
CDI^{Cy}	478 nm	0.1490	HOMO-1->LUMO+1 HOMO->LUMO
	427 nm	0.2886	HOMO-1->LUMO HOMO->LUMO+1
	337 nm	0.5419	HOMO-9->LUMO HOMO-6->LUMO HOMO-4->LUMO HOMO-3->LUMO+1 HOMO-1->LUMO+1 HOMO->LUMO+1
	335 nm	0.3028	HOMO-9->LUMO HOMO-1->LUMO HOMO-1->LUMO+1 HOMO->LUMO HOMO-3->LUMO+1 HOMO-1->LUMO+1 HOMO>LUMO+1

Literature

1. J. Buchenska, *J. Appl. Polym. Sci.*, **2001**, *80*, 1914-1919.
2. Z. J. Chen, L. M. Wang, G. Zou, L. Zhang, G. J. Zhang, X. F. Cai, M. S. Teng, *Dyes Pigm.*, **2012**, *94*, 410-415.
3. H. Langhals, O. Krotz, K. Polborn, P. Mayer, *Angew. Chem. Int. Ed. Engl.*, **2005**, *44*, 2427-2428.
4. I. Ghosh, T. Ghosh, J. I. Bardagi, B. Konig, *Science*, **2014**, *346*, 725-728.
5. X. Mo, H.-Z. Chen, M.-M. Shi, M. Wang, *Chem. Phys. Lett.*, **2006**, *417*, 457-460.
6. R. K. Gupta, A. S. Achalkumar, *J. Org. Chem.*, **2018**, *83*, 6290-6300.
7. S. Sengupta, R. K. Dubey, R. W. Hoek, S. P. van Eeden, D. D. Gunbas, F. C. Grozema, E. J. Sudholter, W. F. Jager, *J. Org. Chem.*, **2014**, *79*, 6655-6662.
8. F. Wurthner, V. Stepanenko, Z. Chen, C. R. Saha-Moller, N. Kocher, D. Stalke, *J. Org. Chem.*, **2004**, *69*, 7933-7939.
9. A. Lik, L. Fritze, L. Muller, H. Heitzen, *J. Am. Chem. Soc.*, **2017**, *139*, 5692-5695.
10. B. Wrackmeyer, *Z. Naturforsch. B.*, **2015**, *70*, 421-424.
11. J. L. Bredas, R. Silbey, D. S. Boudreux, R. R. Chance, *J. Am. Chem. Soc.*, **1983**, *105*, 6555-6559.
12. M. J. Frisch, G. W. Trucks, H. B. Schlegel, G. E. Scuseria, M. A. Robb, J. R. Cheeseman, G. Scalmani, V. Barone, G. A. Petersson, H. Nakatsuji, X. Li, M. Caricato, A. V. Marenich, J. Bloino, B. G. Janesko, R. Gomperts, B. Mennucci, H. P. Hratchian, J. V. Ortiz, A. F. Izmaylov, J. L. Sonnenberg, Williams, F. Ding, F. Lipparini, F. Egidi, J. Goings, B. Peng, A. Petrone, T. Henderson, D. Ranasinghe, V. G. Zakrzewski, J. Gao, N. Rega, G. Zheng, W. Liang, M. Hada, M. Ehara, K. Toyota, R. Fukuda, J. Hasegawa, M. Ishida, T. Nakajima, Y. Honda, O. Kitao, H. Nakai, T. Vreven, K. Throssell, J. A. Montgomery Jr., J. E. Peralta, F. Ogliaro, M. J. Bearpark, J. J. Heyd, E. N. Brothers, K. N. Kudin, V. N. Staroverov, T. A. Keith, R. Kobayashi, J. Normand, K. Raghavachari, A. P. Rendell, J. C. Burant, S. S. Iyengar, J. Tomasi, M. Cossi, J. M. Millam, M. Klene, C. Adamo, R. Cammi, J. W. Ochterski, R. L. Martin, K. Morokuma, O. Farkas, J. B. Foresman, D. J. Fox, Gaussian 16 Rev. C.01, **2016**.
13. B. Goldfuss, P. v. R. Schleyer, *Organometallics*, **1997**, *16*, 1543-1552.
14. P. V. R. Schleyer, C. Maerker, A. Dransfeld, H. Jiao, N. J. R. van Eikema Hommes, *J. Am. Chem. Soc.*, **1996**, *118*, 6317-6318.
15. P. V. R. Schleyer, M. Manoharan, Z. X. Wang, B. Kiran, H. Jiao, R. Puchta, N. J. R. van Eikema Hommes, *Org. Lett.*, **2001**, *3*, 2465-2468.